# ANTENNAS FOR UBIQUITOUS RADIO SERVICES IN A WIRELESS INFORMATION SOCIETY

## Proceedings of the End Symposium Concluding the Wide Band Sparse Element Array Antennas - WiSE Project

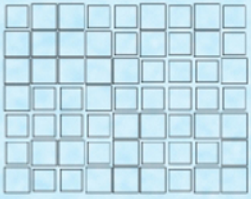

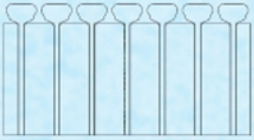

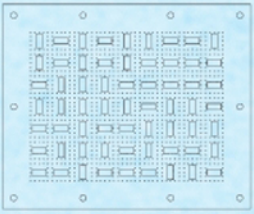

Edited by
Ioan E. Lager and
Massimiliano Simeoni

# Antennas for ubiquitous radio services in a wireless information society


stw
Technologiestichting STW


TU Delft
Delft University of Technology


IRCTR
International Research Centre for
Telecommunications and Radar

# Antennas for ubiquitous radio services in a wireless information society

Proceedings of the Symposium concluding the
Wide Band Sparse Element Array Antennas – **WiSE** project

March 4, 2010, Wassenaar, the Netherlands

edited by

**Ioan E. Lager** and **Massimiliano Simeoni**

International Research Centre for Telecommunications and Radar – IRCTR
Delft University of Technology, Delft, the Netherlands

**2010**
**IOS Press**

ISBN 978-1-60750-486-3 (print)
ISBN 978-1-60750-487-0 (online)

Published by IOS Press BV under the imprint Delft University Press

IOS Press BV
Nieuwe Hemweg 6b
1013 BG Amsterdam
The Netherlands
tel: +31−20−688 3355
fax: +31−20−687 0019
email: info@iospress.nl
www.iospress.nl



PRINTED IN THE NETHERLANDS

*This publication is supported by:*
International Research Centre for Telecommunications and Radar – IRCTR
Faculty of Electrical Engineering, Mathematics and Computer Science,
Delft University of Technology,
Mekelweg 4, 2628 CD Delft, the Netherlands
tel: +31−15−27 81034
fax: +31−15−27 84046
www.irctr.tudelft.nl

# Preface

Wireless applications have pervasively penetrated the everyday life. They visibly manifest themselves in the omnipresent (mobile) communication devices that are deeply rooted in the present day lifestyle (see the multitude of sound, image and data carrying systems surrounding us). They manifest themselves less visibly, but equally ubiquitously, in weather and traffic monitoring systems, in defence and security technology, etc. They are praised for supporting and facilitating our daily routine and are (in fact, unjustly) blamed for thoroughly invading our privacy. They are instrumental for locating endangered people and for effectively treating diseases and, at the same time, are often cited among the perilous health-hazards.

The present day societal needs exert a lot of pressure on wireless systems for providing increased performance, with a twofold direction presenting the most challenging requirements: on the one hand, the constantly higher channel transmission capacity driven by the (multimedia) wireless data-link systems and, on the other hand, the pattern shaping, often complemented by beam agility, demanded by the high-end radar and space-borne telecommunication application.

The completion of these tasks is extremely complex, with the design of adequate antenna (systems) playing a pivotal role. Although antenna engineering has a long history of achievements, the magnitude of the present demands necessitates, and will still do so in the future, a continuous and sustained effort. The success in this area is indissolubly connected to mastering a broad knowledge arch, having as main pillars the in depth understanding of the pertaining (physical) phenomena and the needed manufacturing and measurement technological utensils.

Recognising these commandments, the International Research Centre for Telecommunications and Radar (IRCTR) has initiated in early 2004 the Wide Band Sparse Element Array Antennas (**WiSE**) project, a scientific endeavour having a twofold objective: the assembling of a catalogue of (ultra) wide-band radiators that are, preferably, amenable to being incorporated in array antennas and the exploration of the functional possibilities arising from accommodating various radiators on a common aperture, an approach termed as the 'shared aperture concept'.

Investigations performed over a period of almost 6 years have confirmed *some* of the initial expectations, while opening new, challenging directions to

be pursued. The undertaken research resulted into a multitude of theoretical aspects being elucidated, with solutions concerning the physical implementation of these concepts being also put forward. The performed activities materialised themselves in a sizeable published scientific output and, also, in several concept demonstrators with practical applicability. At the end of this route, IRCTR is firmly anchored on the map of European antenna research and development, with a well established international recognition in the field of non-uniform and/or interleaved array antennas.

The present work offers a retrospect of the project's main achievements, while also assessing their relevance within a wider antenna engineering perspective. The volume touches upon a broad selection of topics, spanning from fundamental electromagnetics up to accounts on the state-of-the-art manufacturing technologies. The included contributions are authored by the **WiSE** project participants, by the members of the Users' Committee and by representatives of leading European institutes involved in the complex and fascinating antenna research area.

Ioan E. Lager
Massimiliano Simeoni.

Delft, December 22, 2009.

# Contents

# The Wide Band Sparse Element Array Antennas – WiSE project: an overview

**Ioan E. Lager**, **Leo P. Ligthart** and **Piet van Genderen**
*International Research Centre for Telecommunications and Radar (IRCTR), Faculty of Electrical Engineering, Mathematics and Computer Science, Delft University of Technology, 2628 CD, Delft, the Netherlands (i.e.lager@tudelft.nl)*

**Abstract**

A review on the Wide Band Sparse Element Array Antennas (**WiSE**) project is provided. After describing the general structure of the project and its initial goals, the activities undertaken in the two principal, and the various spin-off and supporting lines of research will be outlined. The most prominent theoretical and applicative achievements will be enumerated, by insisting on the delivered concept demonstrators and scientific output and, at the same time, on the societal impact of the obtained results.

## 1 Introduction

The rapid increase of the use of radio-waves for telecommunication and radar has lead to new requirements on the antenna systems supporting the implemented services. These requirements have as a common feature the fact that they make reference to a large system bandwidth, sometimes expressed in a large instantaneous bandwidth, sometimes in a large spreading in frequency of many simultaneously transmitted, narrow-band signals. Moreover, the relevant signals must be directed or received in certain angular directions, this translating in a need for the antenna system to provide spatial filtering, as well.

Addressing these challenging demands imperatively calls for the use of antenna arrays. While many solutions employing fully populated, uniform arrays are available in the literature (a comprehensive overview being given in the Introduction of [1]), the inherent complexity of such systems, especially when modularity and combined transmit-receive capabilities are required at element level, results in prohibitive costs if not rendering the problem technologically unfeasible. A solution may then be found by resorting to non-periodic arrays that, due to their implicitly reduced number of elements, may significantly reduce the cost of the arrays. Moreover, the sparsity of the

Antennas for Ubiquitous Radio Services in a Wireless Information Society
I.E. Lager and M. Simeoni (Eds.). 
doi:10.3233/978-1-60750-487-0-1

architecture creates room for deploying sub-arrays in the resulting unused areas, a feature that can be expediently employed for embedding multi-functionality in the system.

These ideas provided the International Research Centre for Telecommunications and Radar (IRCTR) with the incentive for initiating in 2004 the **Wide Band Sparse Element Array Antennas (WiSE)** project. This complex scientific endeavour was supported by the Technologiestichting STW (Dutch Technology Foundation) and was co-financed by industrial and governmental organisations, namely by THALES Nederland BV (TNL) and by the Dutch Ministry of Defence.

After about 6 years of focused efforts, **WiSE** is coming now to a conclusion, with this work cataloguing the project's most significant achievements. The account now proceeds by discussing the general functional structure, insisting on the strategies that were adopted for streamlining the research activities. The work will then progress by outlining the main research lines and the ancillary activities that unfolded during the span of the project. A summary of the most relevant outcomes of the undertaken research will then be made. The account will be concluded by drawing some conclusions and by acknowledging the contribution of the organisations and individuals who have ensured the success of this scientific endeavour.

# 2 General information

## 2.1 The functional structure of the project

The **WiSE** project was devised by having in view a broad, international cooperation (see Fig. 1), in which IRCTR, acting on behalf of the Delft University of Technology (DUT), had the role of project leader and coordinator while, at the same time, making optimum use of its internal research potential. According to the project proposal, the tasks were ascribed among the partner organisations as follows:

- IRCTR: the study of moderately and ultra wide-band radiators, their integration in sparse array configurations, the assembling of shared aperture antennas by interleaving sparse arrays, etc;

- the Romanian Military Equipment and Technologies Research Agency (METRA), Romania: the study of (conformal) integrated antenna systems and their implementation in devices to be employed for military communication and positioning applications;

- the Middle East Technical University (METU) of Ankara, Turkey: the design of (ultra) wide-band and multiple resonance radiators and the investigation of the (ultra) wide-band radiation mechanism.

This initial distribution of objectives was adjusted in the course of the project, with the investigations on ultra wide-band (UWB) radiators being concentrated almost completely at IRCTR.

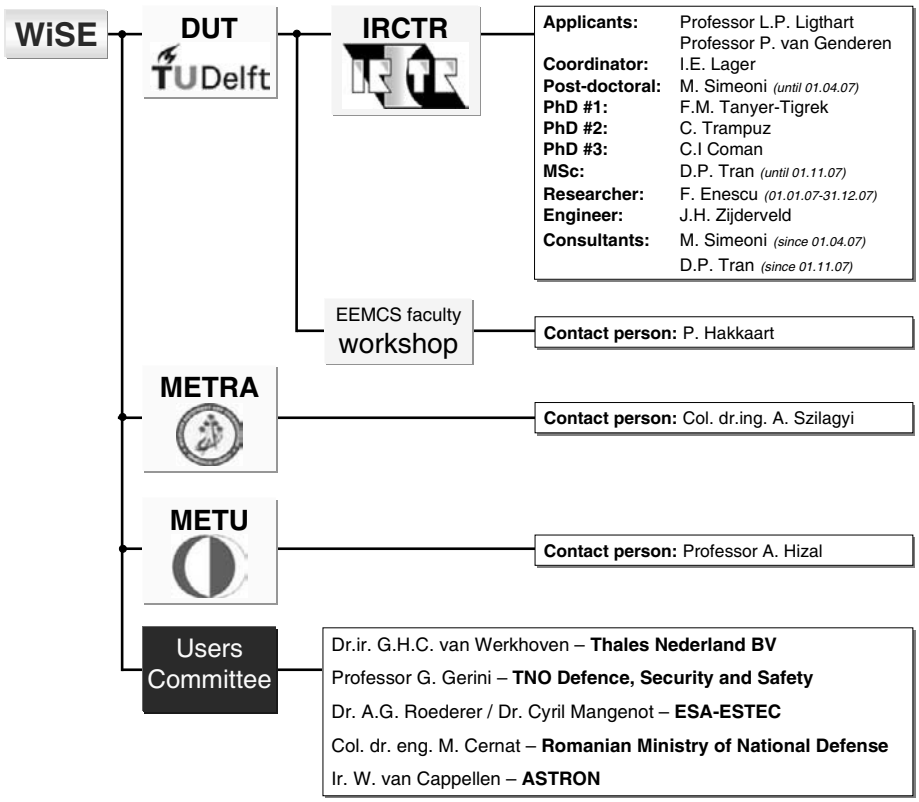


Figure 1: The overall structure of the **WiSE** project.

## 2.2 The personnel involvement in the project

The overall personnel structure of the **WiSE** project is presented in Fig. 1. The two applicants and the coordinator formed the management team – the project's acting decision body. The three PhD students have joined IRCTR at various stages, with the PhD #3 (a positioned financed by the Dutch Ministry of Defence, via the 'Partnership for Peace' programme) starting 3 years before the official kick-off of **WiSE** and the PhD #1 and # 2 starting in 2006 and 2007, respectively. The bridge between the specific research

activities undertaken by the PhD students was ensured by the work of the post-doctoral, the MSc and the coordinator. The first two have pursued their contributions to **WiSE** as consultants, positions not mentioned in the initial proposal that represented a direct contribution of DUT. The project benefited throughout its entire span from the experience of the engineer, who assisted the **WiSE** team in performing the various measurements. To conclude with, a one year position was created for a METRA researcher that carried out at IRCTR some targeted activities of mutual interest.

### 2.3 The management of the project

The current decisional body of the project was represented by the management team (MT), with the daily supervision being the task of the coordinator. The activity was monitored by means of project meetings attended by the researchers and MT meetings that were organised when appropriate.

The progress in **WiSE** was assessed by a group of industrial and governmental institutions that constituted the Users' Committee (UC). This body convened twice a year, on which occasions the progress was reported, the strategic decisions concerning the activities to be performed were taken and the deliverables to be produced were decided upon.

## 3 Performed research activities

As indicated in the project proposal, the activity in **WiSE** was divided, in a broad sense, into two research aims. These main lines were complemented by other activities, one of them being already stipulated in the proposal and some other expanding intermediate research results. Although not defined originally, a decision was made in the course of the project for four concept demonstrators that were deemed representative for the type of research undertaken by the team.

### 3.1 The research aim #1: compiling a catalogue of (ultra) wide-band radiators

This research aim focused on assembling a catalogue of (ultra) wide-band radiators that, preferably, are amenable to integration in planar arrays. This activity came as a continuation of preexisting preoccupations in the field of wide-band radiators at both IRCTR [2, 3, 4] and METU [5, 6].

Within the scope of the project, the investigation of this topic was initiated by the PhD #3 who firstly focused on dielectric filled type of radiators.

Nevertheless, in view of the technological difficulties and the high manufacturing costs that characterise this type of radiators, the printed laminate procedure was selected as technology of choice [7, 8]. Several moderate bandwidth microstrip patch (type of) antennas were produced in this manner, these radiators being excellently suited for integration in planar arrays. Some representative examples in this category are reported in [9, 10, 11].

In view of largely extending the operational bandwidth of the produced radiators, attention has shifted in the second half of the project to coplanar waveguide (CPW) fed antennas of the dipole and loop variety. These antennas, collected within the generic DEMO$_3$[1] demonstrator, were shown to be characterised by unprecedented impedance bandwidths (in excess of 150% relative bandwidth) as indicated in [12, 13, 14, 15]. The operation of these radiators was also demonstrated in linear array environments [16]. Despite of some preliminary studies being carried out, their suitability for planar arrays is still an open question.

A particularly interesting result was obtained in the field of wide-band radiators possessing controllable filtering properties. These recent results are circumscribed to the DEMO$_4$[2] and will form the object of future publications.

### 3.2 The research aim #2: the investigation of non-periodic and interleaved array antennas

This research aim was structured around the investigation of the array antenna architectures accommodating various types of radiators on a common aperture, an approach termed as the 'shared aperture concept' (a detailed presentation of this concept being discussed in [1]). The initial expectations were focused on reusing the empty space available in non-periodic arrays for deploying individual elements or sub-arrays supporting alternative services. As the project progressed, array interleaving became a topic of investigation in itself, demonstrating the versatility of this technique with clear ramifications in implementing multi-functionality.

A first application was the interleaving of balanced sub-arrays operating at different, but contiguous, bandwidths. The validity of this strategy was demonstrated in [1, 9]. In the process of devising these type of antennas, the high relevance of the deterministic element placement, especially in conjunction with a complementary division of a full aperture, was attested.

[1] DEMO$_3$ demonstrator: a collection of elementary radiators and small arrays providing at least 50% operational bandwidth.

[2] DEMO$_4$ demonstrator: a complex, wearable receive antenna system for a METRA defined application.

This experiment opened the way for a productive line of research concerning the application of the complementary division to the implementation of multi-functionality, an approach whose resources were firstly outlined in [17]. This line of thinking received its concrete instantiation in two **WiSE** concept demonstrators, namely:

- the $\mathsf{DEMO}_1$ demonstrator: an array antenna for a system for in-flight, airplane-satellite communication requiring polarisation agility; the solution to this objective was anticipated in [18] and later proven in [19];
- the $\mathsf{DEMO}_2$ demonstrator: an interleaved antenna combining on a single aperture the transmit and receive units of a Frequency Modulated – Continuous Wave (FM-CW) radar system; the steps towards establishing this approach as a viable alternative to the classic design employing separate antennas are outlined in the publications [20, 21, 22].

A number of supporting activities addressed specific aspects that intervene in the extremely complex design of non-periodic array architectures. For example, [23] examined the evaluation of the mutual coupling in non-periodic array antennas consisting of aperture type radiators while [24, 25] focused on some of the applicable features of non-periodic, linear arrays.

### 3.3 Complementary and spin-of activities

The two research aims in **WiSE** were complemented by a significant number of research activities circumscribed to parallel or spin-off projects.

Some of the parallel activities were functionally integrated in **WiSE**. A first such project was **Scan Optimisation for Wide Band Radar** that unfolded between 2003 and 2005 in cooperation with TNL. Secondly, **WiSE** took advantage in the period 2006 – 2008 from a collaboration with the Institute of Radio-physics and Electronics (IRE), Kharkov, Ukraine, an organisation functioning under the umbrella of the National Academy of Sciences of Ukraine. Based on a bilateral agreement between IRCTR and IRE, the generated knowledge was integrated in the **WiSE** research aim #1 collection of results. To conclude with, a project entitled **Communication System Integrated in the Protection Equipment** was carried out at METRA, its results being a part of the $\mathsf{DEMO}_4$ demonstrator.

Upon turning to spin-off activities, a cooperation between IRCTR and the European Space Agency – European Space Research and Technology Centre (ESA-ESTEC) is in progress since 2007 within the frame of the **Innovative array antenna architectures** project. This undertaking explores the non-periodic placement strategies for ensuring very narrow beams, low

side-lobes levels and preventing the onset of grating lobes in the case of very large array antennas for space applications. The most notable results obtained thus far in the project concern the so-called 'sun flower' configuration, a pseudo-random, deterministic array architecture design method [26, 27]. Furthermore, the preoccupations related to UWB radiators motivated the initiation of a collaborative effort with the Laboratory of Electromagnetic Research, DUT, having as objective the investigation of pulsed-field antenna models. A first concrete achievement is the pulsed-field multi-port antenna system reciprocity relation study, reported in [28].

# 4 Outcomes of the **WiSE** project

## 4.1 Promoted concepts

The research activities in **WiSE** promoted and proved a series of concepts that demonstrated their relevance in the field of (array) antenna design. The most notable example in this category is the 'shared aperture antenna' concept, a strategy that has shown its effectiveness for implementing multi-functionality in radio front-ends. Another concept that, among others, had a determining effect on the amount and quality of concept demonstrators that could be generated by the project is the 'technology driven antenna design' an approach that accounts for the potentialities *and* limitations of the employed technology already in the initial phases of the design.

## 4.2 Concept demonstrators

The project offered the adequate frame for developing, manufacturing and physically validating a large number of demonstrators. In the initial phase, a number of (stacked) patch, cavity backed radiators were produced. These elements were subsequently integrated in an interleaved array antenna that was elaborately examined in [1] and in several linear arrays examined in [8, 11, 24, 25]. In the second phase of the project, four concept demonstrators were agreed upon with the members of the UC, namely:

- the **DEMO**$_1$ demonstrator: an array antenna for a system for in-flight, airplane-satellite communication requiring polarisation agility;

- the **DEMO**$_2$ demonstrator: an interleaved antenna combining on a single aperture the transmit and receive units of a Frequency Modulated – Continuous Wave (FM-CW) radar system;

- the $\mathsf{DEMO}_3$ demonstrator: a collection of elementary radiators and small arrays providing at least 50% operational bandwidth;
- the $\mathsf{DEMO}_4$ demonstrator: a complex, wearable receive antenna system for a METRA defined application.

All demonstrators were brought to a physical implementation, with extensive measurement campaigns being effectuated for their full characterisation. The produced devices are amenable to being directly used in future research activities undertaken at IRCTR or at the partner organisations.

### 4.3 Scientific output

Table 1: Aggregate scientific output of the **WiSE** project, as of March 4, 2010.

| | Publication type | Phase | |
|---|---|---|---|
| | | Preparatory period | **WiSE** project span |
| The **WiSE** project | Dissertations, books | | 3 |
| | Journal contributions | 2 | 8 |
| | Conference contributions | 2 | 33 |
| | Scientific reports (not issued as refereed contributions) | 1 | 13 |
| Spin-off activities | Journal contributions | | 2 |
| | Conference contributions | | 9 |

The scientific output of the project consists of three books: two PhD dissertations (a third being in preparation) and a volume containing the proceedings of the **WiSE** End Symposium, and of a sizeable number of journal and conference contributions. Table 1 offers a complete overview of the generated output, subdivided into publications pertaining to the **WiSE** activities and to the spin-off research lines. Note that a 1:4 ratio of journal to conference contributions was ensured, this reflecting a deliberate editorial policy oriented on journal, rather than conference, publications.

### 4.4 WiSE – an instrumental tool for improving the effectiveness of the IRCTR investigation capabilities

The project was instrumental for improving the effectiveness of the research endowment at IRCTR. To begin with, the IRCTR measurement facilities centred around the Delft University Chamber for Antenna Tests (DUCAT) were significantly upgraded by the addition of a powerful vector network analyzer and of a full 2×24 crossbar mechanical switch test-set. The measurement setup in Fig. 2 is illustrative for the type of array measurements that were greatly facilitated by the investments made in the project.

Figure 2: Array antenna measurement environment consisting of an Agilent Technologies E8364B vector network analyzer, an Agilent Technologies 87050-K24 – full 2×24 crossbar mechanical switch test-set and calibrated cables. The device under test at the very left side of the image is a linear array consisting of 15 'Eared' type, UWB radiators (device circumscribed to the $\mathsf{DEMO}_3$ demonstrator).

**WiSE** also allowed assembling an effective and versatile software platform consisting of the CST Microwave Studio package (employed primarily for the simulation of complex radiators and array environments) and of the Agilent's Advanced Design System – ADS package (employed for both radiator simulations and system integration). Additionally, IRCTR was granted a number of licenses for the EMPIRE XCcel electromagnetic simulator by the IMST GmbH, Kamp-Lintfort, as part of a bilateral cooperation, this donation being hereby acknowledged. This tool was employed for simulating large, non-periodic array antenna structures.

### 4.5 Societal impact of the project

The project contributed in a substantial manner to the international recognition of IRCTR as an established antenna research centre. The institute's visibility was further enhanced by its active presence in the **COST Action IC0603 – Antenna Systems & Sensors for Information Society Technologies (ASSIST)**, presently the largest European network in the area of antenna research and development. In it, IRCTR acts, since 2008, as Grant-holder and the **WiSE** coordinator as Secretary. The results of the project, the experienced gained in the field of non-periodic and interleaved array antennas in the first place, receive a constant attention on behalf of the participants in this Action.

## 5 Conclusions and prospects

Wide Band Sparse Element Array Antennas (**WiSE**), the largest project effectuated by IRCTR in the field of antenna research, represents a clear success. Unfolding over a period of about 6 years, the explorations resulted in promoting some concepts that have a demonstrated applicability, with the shared aperture antenna concept being the most prominent one. The research activities generated a sizeable amount of concept demonstrators that were extensively validated by means of physical experiments. The results generated by the project are at the origin of a large scientific output. The experience thus accumulated is at the origin of a broad spectrum of spin-off activities that already emerged or that are expected to be initiated in the (near) future. The **WiSE** outcomes contributed decisively to IRCTR acquiring a well established international recognition, with the institute now firmly anchored on the map of European antenna research and development.

Based on the conclusions of the last **WiSE** UC meeting, it can be affirmed that the non-periodic (sparse) array antenna concept has still a significant scientific and applicative potential, especially in the field of telecommunications. This concept is expected to receive increased attention in view of the manifest trend towards increasing the integration of the antennas into the radio frequency (RF) systems. This approach is accompanied by a substantial complication of the engineering aspects, the sparse array architectures being deemed to provide handles to alleviating the demanding implementation requirements. The future research in this area should also account for the management of the various resources of the RF systems supporting both radar and telecommunication applications, the antenna research playing, again, an instrumental role.

## 6 Acknowledgement

The achievements of the project could not have been obtained without the instrumental contribution of a large number of organisations and individuals. A first word of gratitude is due to the direct participants in the project: PhD students, post-doctorals, engineers and technicians who, through their talent and devotion, generated the excellent results that can be now catalogued. Secondly, the support received from the Technologiestichting STW, the main financial supporter of the project, and from THALES Nederland BV, and the Dutch Ministry of Defence, the two co-financing organisations is hereby acknowledged. A special thank is due to the members of the Users' Committee for their professional counseling and active support of the undertaken research activities. The efforts spent by the organisations that assisted the **WiSE** team in the development and assessment of the demonstrators, the Delft University of Technology workshop in the first place, is greatly acknowledged. To conclude with, recognition is expressed towards the entire scientific and supporting IRCTR personnel who effectively and collegially contributed to the success of this scientific undertaking.

## Bibliography

[1] C. I. Coman, *Shared Aperture Array Antennas Composed of Differently Sized Elements Arranged in Sparse Sub-arrays*, dissertation, Delft University of Technology, January, 2006.

[2] M. Tian, *Characterization of Miniature Dielectric-filled Open-ended Waveguide Antennas*, dissertation, Delft University of Technology, October, 1995.

[3] A. Moumen, *Analysis and Synthesis of Compact Feeds for Large Multiple-Beam Reflector Antennas*, dissertation, Delft University of Technology, March, 2001.

[4] A. A. Lestari, *Antennas for Improved Ground Penetrating Radar*, dissertation, Delft University of Technology, June, 2003.

[5] O. A. Civi, A. Hizal, "Microstrip patch antenna on magnetized cylindrical ferrite substrate," in *IEEE Antennas Propagat. Symp. Dig.*, pp. 1516–1519, Montreal, Canada, July 1997.

[6] A. Hizal, C. Yardim, and E. Halavut, "Wideband tapered rolling strip antenna," in *Proc. IEEE AP2000 Millennium Conference on Antennas & Propagation*, Davos, Switzerland, April, 2000.

[7] I. E. Lager, M. Simeoni, and L. P. Ligthart, "Technological antenna design – an instrument for the mass-production of antenna systems," in *Proc.* $11^{th}$ *Int. Symp. on Antenna Technology and Applied Electromagnetics*, pp. 44–45, Saint-Malo, France, June 2005.

[8] M. Simeoni, C. I. Coman, and I. E. Lager, "Cost-effective array antennas for narrow-beam, wide-angle scanning applications," in *Proc. 36$^{th}$ European Microwave Conference – EuMC*, pp. 1790–1793, Manchester, UK, Sept. 2006.

[9] C. I. Coman, I. E. Lager, and L. P. Ligthart, "The design of shared aperture antennas consisting of differently sized elements," *IEEE Trans. Antennas Propag.*, vol. 54, no. 2, pp. 376–383, Feb. 2006.

[10] M. Simeoni, C. I. Coman, and I. E. Lager, "Patch end-launchers – a family of compact colinear coaxial-to-rectangular waveguide transitions," *IEEE Trans. Microw. Theory Tech.*, vol. 54, no. 4, pp. 1503–1511, April 2006.

[11] I. E. Lager, M. Simeoni, "Experimental investigation of the mutual coupling reduction by means of cavity enclosure of patch antennas," in *Proc. 1$^{st}$ European Conference on Antennas and Propagation – EuCAP*, Nice, France, November 2006.

[12] F. M. Tanyer-Tigrek, D. P. Tran, I. E. Lager, L. P. Ligthart, "Over 150% Bandwidth, Quasi-Magnetic, Printed Antenna," in *IEEE Antennas Propagat. Symp. Dig.*, San Diego, CA, July 2008.

[13] D. P. Tran, F. M. Tanyer-Tigrek, I. E. Lager, and L. P. Ligthart, "A novel unidirectional, off-axis CPW-fed, matched by unbalanced fork-stub, UWB ring slot antenna printed on single layer PCB with back plane," in *IEEE Antennas Propagat. Symp. Dig.*, San Diego, CA, July 2008.

[14] F. M. Tanyer-Tigrek, D. P. Tran, I. E. Lager, and L. P. Ligthart, "Wide-band Tulip-Loop Antenna," in *Proc. 3$^{rd}$ European Conference on Antennas and Propagation – EuCAP*, pp. 1446–1449, Berlin, Germany, March 2009.

[15] F. M. Tanyer-Tigrek, D. P. Tran, I. E. Lager, and L. P. Ligthart, "CPW-Fed Quasi-Magnetic Printed Antenna for Ultra-Wideband Applications," *IEEE Antennas Propag. Mag.*, vol. 51, no. 2, pp. 61–70, April 2009.

[16] F. M. Tanyer-Tigrek, I. E. Lager, and L. P. Ligthart, "Efficient and accurate investigation of linear arrays consisting of UWB radiators," in *Proc. 39$^{th}$ European Microwave Conference – EuMC*, pp. 645–648, Rome, Italy, October 2009.

[17] C. I. Coman, I. E. Lager, and L. P. Ligthart, "Multifunction antennas – the interleaved sparse sub-arrays approach," in *Proc. 36$^{th}$ European Microwave Conference – EuMC*, pp. 1794–1797, Manchester, UK, Sept. 2006.

[18] M. Simeoni, I. E. Lager, and C. I. Coman, "Interleaving sparse arrays: a new way to polarization-agile array antennas?," in *IEEE Antennas Propagat. Symp. Dig.*, pp. 3145–3148, Honolulu, HI, June 2007.

[19] M. Simeoni, I. E. Lager, C. I. Coman, and A. G. Roederer, "Implementation of polarization agility in planar phased-array antennas by means of interleaved subarrays," *Radio Science*, vol. 44, RS5013, October 2009.

[20] C. Trampuz, M. Simeoni, I. E. Lager, L. P. Ligthart, "Complementarity based design of antenna systems for FMCW radar," in *Proc. 5$^{th}$ European Radar Conference – EuRAD*, pp. 216–219, Amsterdam, the Netherlands, October 2008.

[21] C. Trampuz, M. Simeoni, I. E. Lager, and L. P. Ligthart, "Low sidelobe interleaved transmit-receive antennas for FMCW radar applications," in *IEEE Antennas Propagat. Symp. Dig.*, Charleston, SC, June 2009.

[22] I. E. Lager, C. Trampuz, M. Simeoni, and L. P. Ligthart, "Interleaved array antennas for FMCW radar applications," *IEEE Trans. Antennas Propag.*, vol. 57, no. 8, pp. 2486–2490, Aug. 2009.

[23] M. J. Mehta, I. E. Lager, "Two-dimensional interpolation for the numerical estimation of the mutual coupling in large antenna arrays", in *Proc. 1st European Conference on Antennas and Propagation – EuCAP*, Nice, France, November 2005.

[24] J. H. Dickhof, C. I. Coman, I. E. Lager, and M. Simeoni, "Pattern synthesis of linear, sparse array antennas," in *Proc. 3rd European Radar Conference – EuRAD*, pp. 84–87, Manchester, UK, Sept. 2006.

[25] M. Simeoni, J. H. Dickhof, and I. E. Lager, "Investigation of the potential for reconfigurability of the non-uniform, linear array antennas," in *Proc. 29th ESA Antenna Workshop on Multiple Beams and Reconfigurable Antennas*, Noordwijk, the Netherlands, April 2007.

[26] M. C. Viganò, G. Toso, G. Caille, C. Mangenot, and I. E. Lager, "Spatial density tapered sunflower antenna array," in *Proc. 3rd European Conference on Antennas and Propagation – EuCAP*, pp. 778–782, Berlin, Germany, March 2009.

[27] M. C. Viganò, G. Toso, G. Caille, C. Mangenot, and I. E. Lager, "Sunflower array antenna with adjustable density taper," *Int. Journal of Antennas and Propagation, Hindawi Publ. Corp.*, vol. 2009, Article ID 624035.

[28] A. T. de Hoop, I. E. Lager, V. Tomassetti, "The pulsed-field multiport antenna system reciprocity relation – a time-domain approach," *IEEE Trans. Antennas Propag.*, vol. 57, no. 3, pp. 594–605, March 2009.

# The mathematics that models wavefield physics in engineering applications – A voyage through the landscape of fundamentals

**Adrianus T. de Hoop**
*Laboratory of Electromagnetic Research, Faculty of Electrical Engineering, Mathematics and Computer Science, Delft University of Technology, Mekelweg 4, 2628 CD Delft, the Netherlands*
*(a.t.dehoop@tudelft.nl / www.atdehoop.com)*

**Abstract**

The structural aspects of the mathematics that models wavefield physics in engineering applications are briefly, but rather completely, put in perspective.

## 1 Introduction

The structural aspects of the mathematics that models wavefield physics in engineering applications are briefly put in perspective. First, the system of wave field equations that governs electromagnetic, acoustic and elastodynamic wave motions is represented in its canonical form [1]. In a number of cases, this canonical form entails certain field compatibility relations that turn out to be essential ingredients in the numerical evaluation of the fields. The constitutive relations between the intensive and extensive field quantities are needed to make the number of equations equal to the number of unknown field components. These relations can include both instantaneous and relaxation behavior, subject to the condition of causality. The spatial operators in the systems of field equations entail a number of interface boundary conditions of the continuity type. In order to guarantee the uniqueness of the pertaining initial-value problem, again the condition of causality is to be invoked. A remarkable feature is that the corresponding uniqueness proofs cannot be constructed directly in the time domain, but have to take recourse to the time Laplace transformation of the field equations and the field quantities [2, 3]. Next, the computational aspects are addressed. These aspects involve first of all a geometrical discretization of the configuration at hand. From a topological point of view the simplex (tetrahedron in 3D) is the fundamental element. Based on this spatial

Antennas for Ubiquitous Radio Services in a Wireless Information Society
I.E. Lager and M. Simeoni (Eds.). 
doi:10.3233/978-1-60750-487-0-15

discretization, combined with linearly varying field components, and a corresponding linear time-domain interpolation, the space-time integrated field equations turn out to have the desired properties. The relevant field components are the ones that are in accordance with the continuity relations across interfaces where the constitutive coefficients show bounded jumps in values. In all practical situations the domain of computation has to be of bounded support and the outward radiation of the field across its boundary has to be modeled appropriately. For a rectangular domain of computation, the space-time coordinate stretching technique provides a perfectly matched embedding, whose termination causes spurious errors in the computed field values, the magnitudes of which can be made as small as desired by properly choosing the absorptive stretching parameters of the embedding [4].

TUDelft EM Research

**Synopsis:**

- System of wavefield equations in canonical form
- Field compatibility relations
- Constitutive relations in media with relaxation (absorption + dispersion)
- Spatial interface boundary conditions
- The principle of causality
- The initial-value problem and the time Laplace transformation
- Computational wavefield discretization
- The space-time integrated field equations + computational properties
- A simple application and benchmark problem

*Synopsis*

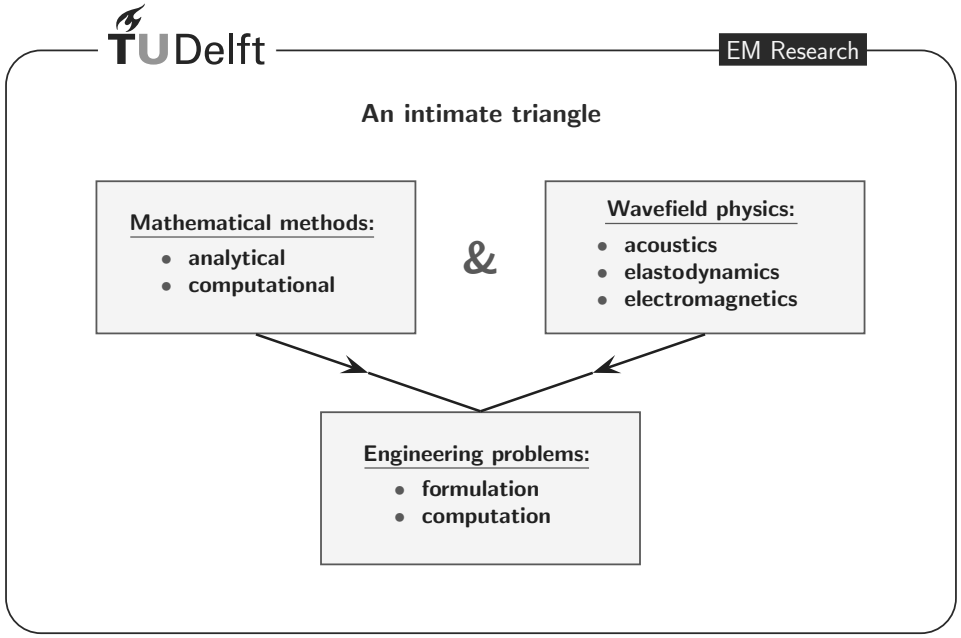


*Mathematics, (Wavefield) Physics, Engineering: An intimate triangle*

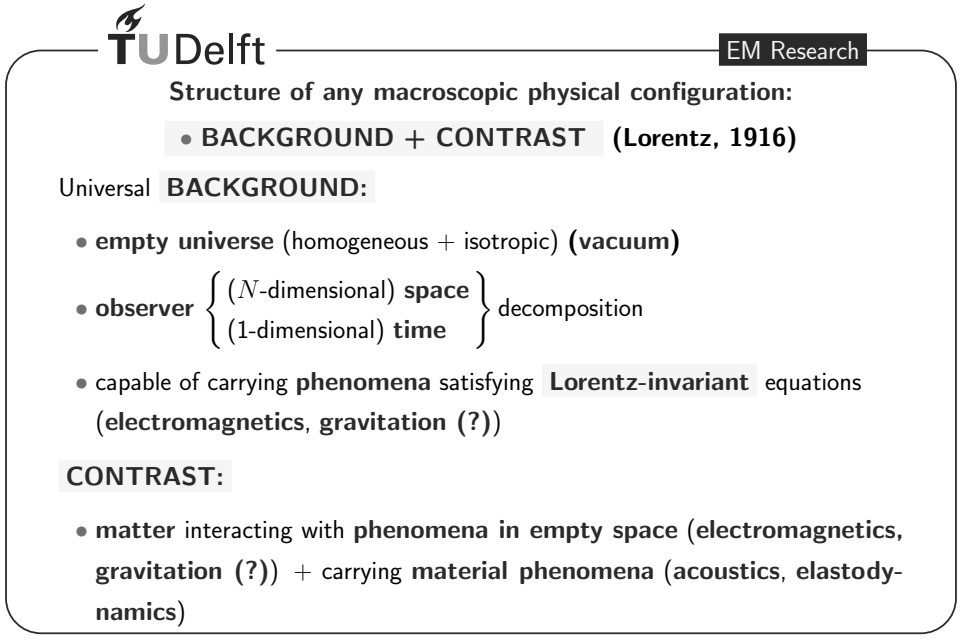


*Background and contrast in a macroscopic physical configuration*

TUDelft — EM Research

**Each (macroscopic) FIELD is represented by:**

**FOUR FIELD QUANTITIES (FLDQ's):**

- {**intensive FLDQ 1, intensive FLDQ 2**}
- {**extensive FLDQ 1**, **extensive FLDQ 2**}

**PROPERTIES:**

- **(intensive FLDQ 1) * (intensive FLDQ 2) =**
  - **area density of power flow**
- **(extensive FLDQ 1) * (extensive FLDQ 2) =**
  - **volume density of flow of momentum**

$\Longrightarrow$ **FLDQ = FLDQ**$(\boldsymbol{x}, t)$

with $\boldsymbol{x} = \{x_1, \ldots, x_N\} \in \mathbb{R}^N$ (**space**), $t \in \mathbb{R}$ (time)

*Intensive and extensive field quantities in space-time*

TUDelft — EM Research

**FIELD EQUATIONS**

**couple** • **RATES OF CHANGE IN SPACE ($\partial_{\boldsymbol{x}}$) of intensive FLDQ's**

**with** • **RATES OF CHANGE IN TIME ($\partial_t$) of extensive FLDQ's**

$\Longrightarrow$ **WAVE MOTION** $\Longleftarrow$

**CANONICAL (TENSOR) FORM:**

(Poincaré, 1905; Einstein, 1905; Minkowski, 1908)

- D($\boldsymbol{\partial_x}$) (**intensive FLDQ 1**) + $\partial_t$ (**extensive FLDQ 2**) = 0
- D($\boldsymbol{\partial_x}$) (**intensive FLDQ 2**) + $\partial_t$ (**extensive FLDQ 1**) = 0
- D: **array composed of unit tensors** (De Hoop, 1995, 2008)

• **COMPATIBILITY RELATIONS:** • $\partial_{x_1}\partial_{x_2}$ **(FLDQ)** = $\partial_{x_2}\partial_{x_1}$**(FLDQ)**

*Field equations in canonical (tensor) form + compatibility relations*

TUDelft EM Research

**CONSTITUTIVE RELATIONS:**

• **extensive FLDQ = CONSTITUTIVE OPERATOR (intensive FLDQ)**

**CONSTITUTIVE OPERATOR:**

- linear
- local $\Longrightarrow$ **SPATIAL DISPERSION** ($\Longrightarrow$ **infinite wavespeed**)
- time-invariant
- active (field-independent) part (= external sources) + passive (field-dependent) part (= medium response)
- medium response = **instantaneous response** + **(Boltzmann) relaxation** (absorption + dispersion)

*Constitutive relations in media with relaxation (absorption + dispersion)*

TUDelft EM Research

**CONSTITUTIVE RELATIONS:**

• **(extensive FLDQ 1,2)**$(\boldsymbol{x},t) =$

$$\underbrace{\textbf{(COEFF 1,2)}(\boldsymbol{x})}_{}*\underbrace{\textbf{(intensive FLDQ 1,2)}(\boldsymbol{x},t)}_{\textbf{instantaneous response}}+$$

$$\int_{\tau=0}^{\infty}\underbrace{\textbf{(RELAXF 1,2)}(\boldsymbol{x},\tau)}_{}*\underbrace{\textbf{(intensive FLDQ 1,2)}(\boldsymbol{x},t-\tau)}_{\textbf{Boltzmann relaxation}}\mathrm{d}\tau$$

• **BOLTZMANN RELAXATION** (Boltzmann, 1876) $\Longrightarrow$ **CAUSALITY**

*Constitutive relations (canonical form)*

TUDelft EM Research

**(PASSIVE) INTERFACE BOUNDARY CONDITIONS:**

- Across passive interface $\Sigma$ between two different media

**NO JUMPS ALLOWED in certain FLDQ's: WHICH ONES?**

- **DECOMPOSITION OF: $\boldsymbol{\partial_x}$ about $x \in \Sigma$:**

- $\boldsymbol{\partial_x} = \underbrace{\boldsymbol{\nu}(\boldsymbol{\nu}\cdot\boldsymbol{\partial_x})}_{\text{normal to } \Sigma} + \underbrace{[\boldsymbol{\partial_x} - \boldsymbol{\nu}(\boldsymbol{\nu}\cdot\boldsymbol{\partial_x})]}_{\text{tangential to } \Sigma}$

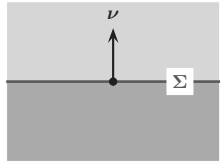


**CONTINUITY CONDITIONS:**

- D$(\boldsymbol{\nu})$**(intensive FLDQ 1,2)**$\big|_{-}^{+} = 0$

*Spatial interface boundary conditions*

TUDelft EM Research

**INITIAL-VALUE PROBLEM FIELD EQUATIONS:** $(t \in \mathbb{R}; t_0 \leq t < \infty)$

- **UNIQUENESS DATA:**

- **Field on bounded support** $\mathcal{D} \subset \mathbb{R}^N$

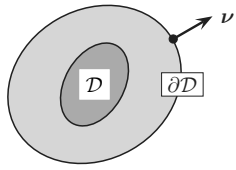


- **Initial field values: FLDQ's**$(\boldsymbol{x}, t_0)$ for $\boldsymbol{x} \in \mathcal{D}$
- **FIELD EQUATIONS** for $\boldsymbol{x} \in \mathcal{D};\ t_0 < t < \infty$
- **BOUNDARY VALUES:**
  - D$(\boldsymbol{\nu})$**(intensive FLDQ 1)**$(\boldsymbol{x}, t)$ for $\boldsymbol{x} \in \partial\mathcal{D},\ t_0 \leq t < \infty$ **OR**
  - D$(\boldsymbol{\nu})$**(intensive FLDQ 2)**$(\boldsymbol{x}, t)$ for $\boldsymbol{x} \in \partial\mathcal{D},\ t_0 \leq t < \infty$

*Time evolution of field (physics) = Initial-value problem field equations (mathematics) (1)*

TU Delft — EM Research

**INITIAL-VALUE PROBLEM FIELD EQUATIONS:** $(t \in \mathbb{R}; t_0 \leq t < \infty)$

- **UNIQUENESS DATA:**

- **Field on unbounded support** $\mathbb{R}^N$

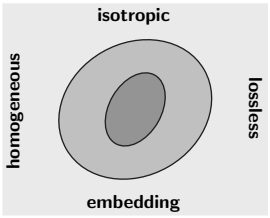


- **Initial field values: FLDQ's**$(\boldsymbol{x}, t_0)$ for $\boldsymbol{x} \in \mathbb{R}^N$
- **FIELD EQUATIONS** for $\boldsymbol{x} \in \mathbb{R}^N;\ t_0 < t < \infty$
- **OUTGOING WAVES in homogeneous, isotropic, lossless embedding**

*Time evolution of field (physics) = Initial-value problem field equations (mathematics) (2)*

TU Delft — EM Research

**INITIAL-VALUE PROBLEM FIELD EQUATIONS:** $(t \in \mathbb{R}; t_0 \leq t < \infty)$

- **MATHEMATICAL PROOF:**

- **Via shifted time Laplace transformation:** (De Hoop, 2003, 2004)

- $\widehat{\mathsf{FLDQ}}(\boldsymbol{x}, s) = \int_{t=\boldsymbol{t_0}}^{\infty} \exp(-st)\mathsf{FLDQ}(\boldsymbol{x}, t)\mathrm{d}t$
  for $s \in \mathbb{C}, \mathrm{Re}(s) > 0$
- $\partial_t \mathsf{FLDQ}(\boldsymbol{x}, t) \longmapsto s\,\widehat{\mathsf{FLDQ}}(\boldsymbol{x}, s) - \underbrace{\mathsf{FLDQ}(\boldsymbol{x}, \boldsymbol{t_0})}_{\text{initial value}}$

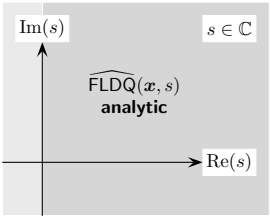


*Time evolution of field (physics) = Initial-value problem field equations (mathematics) (3)*

TUDelft EM Research

**INVERSE TIME LAPLACE TRANSFORMATION:** $(t \in \mathbb{R}; 0 \leq t < \infty)$

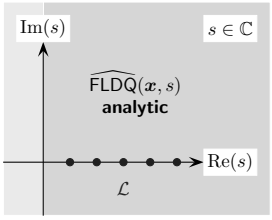


- **use of Lerch's uniqueness theorem:**
- $\{\widehat{\mathsf{FLDQ}}(\boldsymbol{x}, s)|_{s\in\mathcal{L}}\} \overset{\text{1-to-1}}{\longmapsto} \mathsf{FLDQ}(\boldsymbol{x}, t)H(t)$
- $\mathcal{L} = \{s \in \mathbb{C}; \mathrm{Im}(s) = 0, \mathrm{Re}(s) = \boldsymbol{s_0} + \boldsymbol{nh}, s_0 > 0, h > 0, n = 0, 1, 2, 3, \ldots\}$
- **via INSPECTION** (Tables of Laplace Transforms)
- **use of Schouten-Van der Pol theorem:** (Schouten, 1934; Van der Pol, 1934)
  - **For** $\exp[-\hat{\Phi}(\boldsymbol{x}, s)\tau] \longmapsto \Psi(\boldsymbol{x}, t, \tau)H(t)$
  - $\widehat{\mathsf{FLDQ}}[\boldsymbol{x}, \hat{\Phi}(\boldsymbol{x}, s)] \longmapsto \left[\int_{\tau=0}^{\infty} \Psi(\boldsymbol{x}, t, \tau)\mathsf{FLDQ}(\boldsymbol{x}, \tau)\mathrm{d}\tau\right] H(t)$

*Inverse time Laplace transformation*

TUDelft EM Research

**WAVEFIELD COMPUTATION**

- Select (bounded) **spatial domain of computation** $[\mathcal{D}] \subset \mathbb{R}^N$
- Select (bounded) **time window of computation** $[\mathcal{T}] \subset \mathbb{R}$
- Construct (unbounded) **Perfectly Matched Embedding (PME)** $[\mathcal{D}]^\infty = \mathbb{R}^N \backslash [\mathcal{D}]$ **via time-dependent orthogonal Cartesian coordinate stretching** (De Hoop, Remis, Van den Berg, 2007)
- **Terminate PME with periodic boundary conditions** (De Hoop, Remis, Van den Berg, 2007)
- **Discretize** $[\mathcal{D}]$ **into union of adjacent simplices**
- **Discretize** $[\mathcal{T}]$ **into union of successive intervals**

*Wavefield computation (1)*

TUDelft EM Research

## WAVEFIELD COMPUTATION

- **Discretize** FLDQ$(\boldsymbol{x}, t)$ **using:**
  - **piecewise linear interpolation on spatial grid**
  - **piecewise linear interpolation on temporal grid**
  - **nodal values of CONTINUOUS field components as (nodal, edge, face) expansion coefficients**
- **Substitute discretized field in space-time integrated field equations**
- **Compute integrations via simplicial ('trapezoidal') rule**
- **Discretize constitutive relations (piecewise constant in $[\mathcal{D}]$ )**
- **Solve system of equations in space-time expansion coefficients**

*Wavefield computation (2)*

TUDelft EM Research

## CONSTRUCTION OF PERFECTLY MATCHED EMBEDDING (PME)

- **Time Laplace-transform Cartesian coordinate stretching:**

$$\partial_{x_n} \longmapsto \partial_{\hat{X}_n} = \frac{1}{\hat{\chi}_n(x_n, s)} \partial_{x_n} \Longrightarrow \hat{X}_n(x_n, s) = \int_{\xi_n = a_n}^{x_n} \hat{\chi}_n(\xi_n, s) \mathrm{d}\xi_n \quad (n = 1, \ldots, N)$$

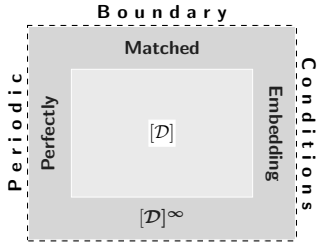


- $\{\hat{\chi}_n(x_n, s); n = 1, \ldots, N\}$ **analytic** for $s \in \mathbb{C}, \mathrm{Re}(s) > 0$, $\boldsymbol{x} \in [\mathcal{D}]^\infty$
- $\{\hat{\chi}_n(x_n, s); n = 1, \ldots, N\} > \mathbf{0}$ for $s \in \mathbb{C}, \mathrm{Re}(s) > 0, \mathrm{Im}(s) = 0$, $\boldsymbol{x} \in [\mathcal{D}]^\infty$
- $\{\hat{\chi}_n(x_n, s); n = 1, \ldots, N\} = \mathbf{1}$ for $\boldsymbol{x} \in [\mathcal{D}] \Longrightarrow$ **field unchanged in** $[\mathcal{D}]$

Boundary Conditions $\Longrightarrow$ spurious field (De Hoop, Remis, Van den Berg, 2007)

*Perfectly Matched Embedding*

TUDelft EM Research

**THE SPACE-TIME INTEGRATED FIELD EQUATIONS**

- **Apply operators**
  - $\int_{\boldsymbol{x}\in\mathcal{D}} \ldots \mathrm{d}V$ and - $\int_{t\in\mathcal{T}} \ldots \mathrm{d}t$ **to FIELD EQUATIONS**
- **Use**
- $\int_{\boldsymbol{x}\in\mathcal{D}} \mathsf{D}(\boldsymbol{\partial x})[\textbf{intensive FLDQ}(\boldsymbol{x},t)]\mathrm{d}V = \int_{\boldsymbol{x}\in\partial\mathcal{D}} \mathsf{D}(\boldsymbol{\nu})[\textbf{intensive FLDQ}(\boldsymbol{x},t)]\mathrm{d}A$ (Gauss in $\mathbb{R}^N$)
  - $\int_{t\in\mathcal{T}} \partial_t[\textbf{extensive FLDQ}(\boldsymbol{x},t)]\mathrm{d}t = [\textbf{extensive FLDQ}(\boldsymbol{x},t)]\Big|_{t\in\partial\mathcal{T}}$ (Gauss in $\mathbb{R}$)

$\Longrightarrow$ **In RHS's only continuous quantities occur**

*The space-time integrated field equations*

TUDelft EM Research

**THE SIMPLICIAL INTEGRATION RULE**

- **Simplicial integration rule in $\mathbb{R}^N$ (= trapezoidal rule in $\mathbb{R}$):**

**Let** $\Sigma^N \subset \mathbb{R}^N = N$**-simplex on vertices** $\{\boldsymbol{x}(0),\ldots,\boldsymbol{x}(N)\}$, then

- $\int_{\boldsymbol{x}\in\Sigma^N} [\textbf{discretized FLDQ}(\boldsymbol{x},t)]\mathrm{d}V \simeq \frac{V^N}{N+1}\Big[\mathsf{FLDQ}[(\boldsymbol{x}(0),t)] + \ldots + \mathsf{FLDQ}[(\boldsymbol{x}(N),t)]\Big]$
  - $V^N =$ **volume of** $\Sigma^N$

(De Hoop, 1995, 2008)

*Simplicial integration rule*

TUDelft EM Research

## UNIT TENSORS IN WAVEFIELD PHYSICS

**Symmetrical unit tensor of rank two: (Kronecker tensor)**

- $\delta_{i,p} = 1$ for $i = p,\ \delta_{i,p} = 0$ for $i \neq p$

**Unit tensors of rank four:**

- $\Delta_{i,j,p,q} = \delta_{i,p}\delta_{j,q}$ **(reproduction)**
- $\Delta^{-}_{i,j,p,q} = (1/2)(\Delta_{i,j,p,q} - \Delta_{i,j,q,p})$ **(electromagnetics)**
- $\Delta^{+}_{i,j,p,q} = (1/2)(\Delta_{i,j,p,q} + \Delta_{i,j,q,p})$ **(elastodynamics)**
- $\Delta^{\delta}_{i,j,p,q} = (1/N)\delta_{i,j}\delta_{p,q}$ **(acoustics)**
- $\Delta^{\Delta}_{i,j,p,q} = \Delta_{i,j,p,q} - \Delta^{\delta}_{i,j,p,q}$ **(elastodynamics)**
- $\Delta^{\Delta,+}_{i,j,p,q} = \Delta^{+}_{i,j,p,q} - \Delta^{\delta}_{i,j,p,q}$ **(elastodynamics)**

(De Hoop, 1995, 2008)

*Unit tensors in wavefield physics*

TUDelft EM Research

## TEST PULSES IN TIME FOR BENCHMARKING:

**The unipolar pulse:**

- $f(t) \geq 0$ for $t \geq 0$
- $\partial_t f(t)|_{t=t_\mathrm{r}} = 0 \Longrightarrow t_\mathrm{r}$ **(pulse rise time)**
- $A = f(t_\mathrm{r})$ **(pulse amplitude)**
- $t_\mathrm{w} = \dfrac{1}{A}\displaystyle\int_{t=0}^{\infty} f(t)\mathrm{d}t$ **(pulse time width)**

**The power exponential pulse:**

- $f(t) = A\left(\dfrac{t}{t_\mathrm{r}}\right)^{n} \exp\left[-n\left(\dfrac{t}{t_\mathrm{r}} - 1\right)\right] H(t)$ for $n = 1, 2, 3, \ldots$
- $t_\mathrm{w} = \dfrac{n!}{n^{n+1}} \exp(n) t_\mathrm{r}$
- $\hat{f}(s) = A \dfrac{n!}{(s + n/t_\mathrm{r})^{n+1}} \dfrac{\exp(n)}{t_\mathrm{r}^{n}}$ for $s \in \mathbb{C}, \mathrm{Re}(s) > 0$

*Test pulses in time for benchmarking*

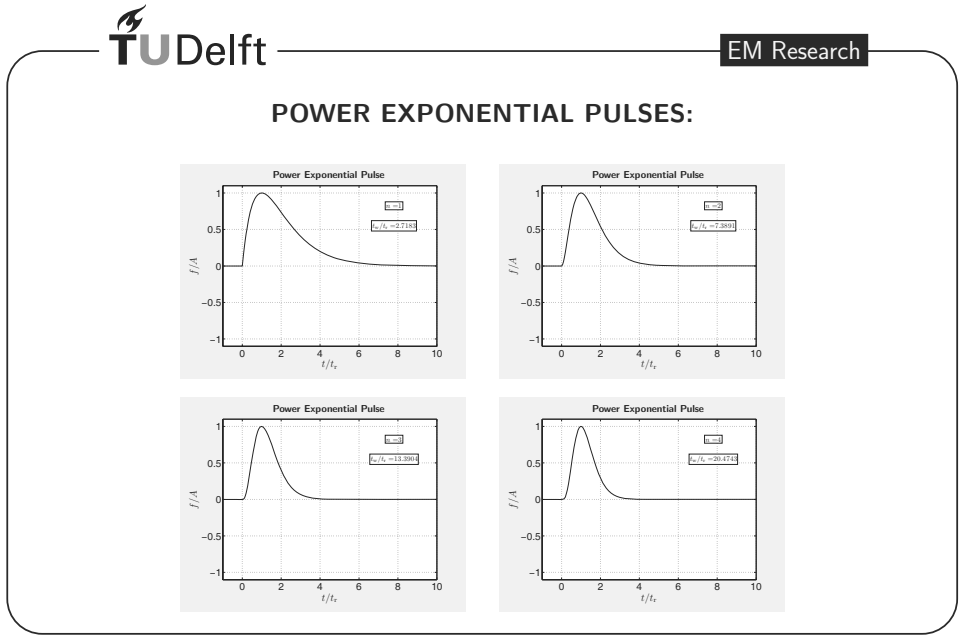


*Power Exponential pulses*

# Bibliography

[1] A. T. de Hoop, *Handbook of Radiation and Scattering of Waves*, London, Academic Press, 1995, xxx + 1083 pp. [Out of print. For freely downloadable www.image in .pdf format, www.atdehoop.com]

[2] A. T. de Hoop, "A time-domain uniqueness theorem for electromagnetic wavefield modeling in dispersive, anisotropic media," *The Radio Science Bulletin*, no. 305, pp. 17–21, June 2003.

[3] A. T. de Hoop, "A uniqueness theorem for the time-domain elastic-wave scattering in inhomogeneous, anisotropic solids with relaxation," *The Journal of the Acoustical Society of America*, vol. 115, no. 6, pp. 2711–2715, June 2004.

[4] A. T. de Hoop, R. F. Remis, P. M. van den Berg, "The 3D wave equation and its Cartesian coordinate stretched perfectly matched embedding – A time-domain Green's function performance analysis," *Journal of Computational Physics*, no. 221, pp. 88–105, 2007.

# Connected arrays of dipoles for telecom and radar applications: the solution for the common mode problem

**Giampiero Gerini**[†‡], **Daniele Cavallo**[†‡], **Andrea Neto**[†] and **Frank van den Bogaart**[†]

[†] *TNO Defence, Security and Safety, Oude Waalsdorperweg 63, 2597 AK, The Hague, The Netherlands, (e-mail: giampiero.gerini@tno.nl)*

[‡] *Eindhoven University of Technology, Den Dolech 2, 5600 MB, Eindhoven, The Netherlands.*

**Abstract**

The constantly increasing demand of advanced sensors and communications systems aboard of military platforms (ships, UAVs, aircraft, land vehicles, etc.) requires a high number of antennas, covering a very wide frequency spectrum. At the same time, the new platform concepts, dictated by an Integrated Topside Design approach, impose a very high level of structural integration of the antenna systems. The overall platform is designed keeping into account many different parameters including Radar Cross Section (RCS), Electromagnetic Interference (EMI), vulnerability etc. From an antenna system point of view, this translates into the necessity of developing antennas easy to be structurally integrated into different platforms and capable of combining more RF functions into the same aperture. In other words: wide-band active electronically scanned array antennas, preferably in planar printed technology which allows low weight, low profile and low costs. In this contribution, the development of a 6–9 GHz prototype array of dual-polarized connected dipoles is presented and discussed in detail. An analysis of spurious common-mode excitation is carried out and a novel design of a resonance-free connected array is presented.

## 1 Introduction

The realization of wide-band, wide-scanning angle, phased arrays with good polarization purity has been the object of many recent investigations. Although tapered slot antennas have very broad bandwidth, they are known to produce high cross-polarization components, especially in the diagonal cuts (45°), [1]. On the other hand, conventional phased array based on

Antennas for Ubiquitous Radio Services in a Wireless Information Society
I.E. Lager and M. Simeoni (Eds.). 
doi:10.3233/978-1-60750-487-0-27

printed radiating elements can achieve only moderate bandwidths ($\sim 25\%$), [2]–[4]. A novel trend in this field is the use of connected arrays, i.e. arrays of long dipoles or slots periodically fed (see Fig. 1), in order to approximate a Wheeler's continuous current sheet [5]. This concept was originally proposed by Hansen, [6], and further theoretically developed in [7], showing the ultra-wideband characteristic of such arrays. Thanks to the planarity of the radiators, the low cross-polarization level is among the most important features of such antenna solution.

The first practical demonstration of a planar connected array antenna was given in [8]. This consisted of a connected array of slots in the UHF band, with good performances observed for broadside radiation. In [9], the scanning performance of connected arrays was investigated for the first time and a theoretical design of a connected dipole array was presented (in the operational frequency band 6–9 GHz), with 40% relative bandwidth and wide scan capability, up to 45° in all the azimuth planes.

Preliminary measurements highlighted an unpredicted problem, associated with spurious common-mode resonances on the vertical feeding lines. The array element, in fact, is fed via balanced lines, which can support both differential (desired) and common (undesired) currents. From an analysis of the common-mode, it appears that the resonance condition depends on both the length of the lines and the periodicity of the array. It is important to highlight the fact that common-mode propagation might be not directly observable from the matching performance of the array, nevertheless, it is always visible in form of high level of cross polarization when scanning on the diagonal plane ($\varphi = 45°$). Due to the electrical connection of the elements, standard wideband baluns are not effective in connected arrays [10]. In this contribution, first the theoretical background of connected arrays is presented and then a novel type of Printed Circuit Board (PCB) transformers is proposed as a valid solution for the design of resonance-free connected dipole arrays.

## 2 Theoretical background

The theoretically ultra-wide bandwidth of connected arrays is always achieved at the cost of a 3 dBs loss in gain due to the fact that the antenna radiates equally in the upper and lower half-spaces. In reality, the design of connected arrays can be tuned to achieve almost any wanted impedance bandwidth and the compromise between the bandwidth and the efficiency of the system is typically the driving parameter. If a backing ground plane is used to improve the antenna efficiency, the bandwidth is limited to about

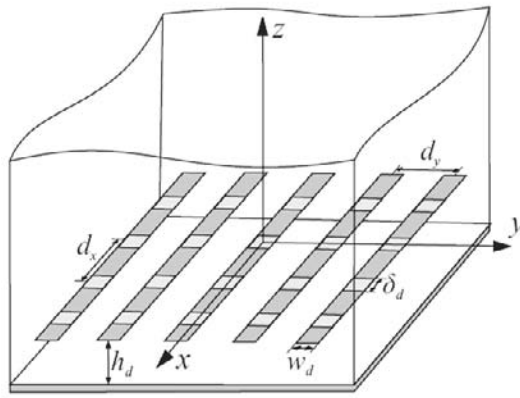


Figure 1: Geometry of 2-D connected arrays of dipoles with backing reflector.

50–60%. In alternative to a simple backing plane, other solutions characterized by wider bandwidths can be envisaged. For example, a bandwidth exceeding 10:1 is feasible at the expense of the efficiency ($1 \sim 2$ dB gain loss), by loading the array with a multi-layer dielectric structure and using absorbing materials in the backside of the antenna.

This configuration, in fact, guarantees that most of the power is radiated into the dielectric and the multiple matching layers realize the wide band matching to free space.

The GF of a periodic connected array of dipoles, with backing reflector as in Fig. 1, can be derived following an extension of the procedure given in [7]. The procedure leads to the following expression for the active input admittance at each feed:

$$Y = \frac{k_0 d_y}{\zeta_0 d_x} \sum_{m_x=-\infty}^{\infty} \frac{\operatorname{sinc}^2(k_{xm}\delta_d/2)}{\left(k_0^2 - k_{xm}^2\right) \displaystyle\sum_{m_y=-\infty}^{\infty} \frac{J_0(k_{ym} w_d/2)}{k_{zm}\left(1 - j\cot(k_{zm} h_d)\right)}} \tag{1}$$

where $J_0$ is the 0-th order Bessel function, $k_0$ and $\zeta_0$ are the free space propagation constant and characteristic impedance, respectively. Thus, the input admittance is a double summation of Floquet waves with $k_{xm} = k_0 \sin\theta\cos\varphi - 2\pi m_x/d_x$, $k_{ym} = k_0 \sin\theta \sin\varphi - 2\pi m_y/d_y$ and $k_{zm} = (k_0^2 - k_{xm}^2 - k_{ym}^2)^{1/2}$.

The behavior of the impedance as a function of the gap width $\delta_d$ is fairly elaborate. The real part of the admittance is associated, when the array is well sampled in terms of wavelength, with the fundamental mode ($m_x = m_y = 0$) only, while the imaginary part depends also on higher order Floquet modes. These latter constitute a lumped capacitance representing

the stored energy at the gap, which is in parallel to the resistive part of the input impedance. As a consequence, both the real and imaginary parts of the impedance vary widely with this geometrical parameter. Figure 2 shows the real and imaginary parts of such an impedance as a function of frequency, with a parametric variation with respect to $\delta_d$. When the gaps are small and the stored capacitive energy is high, the curves associated with the real part of the impedance define a relatively narrow bell. However, when the dimensions of the gaps are non negligible with respect to the wavelength, and accordingly the gaps store less capacitive energy, the overall impedance bell appears lower, much wider, and shifted toward higher frequencies. This clearly indicates that the gaps capacitance is a key design parameter that can be tuned in order to obtain a wider matching bandwidth of the connected dipole array.

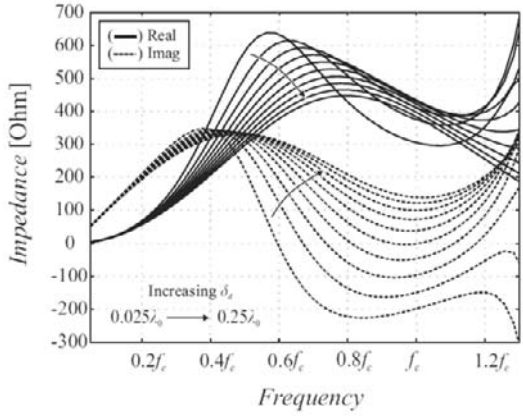


Figure 2: Active impedance of a connected dipole array as a function of frequency for different gap widths, given $h_d = 0.3\lambda_c$, $w_d = 0.05\lambda_c$, $d_x = d_y = 0.5\lambda_c$.

It was shown in [9] that an optimized value of the gap width allows designing a connected dipole array with 40% relative bandwidth, capable to scanning up to 45° in all azimuthal planes. This performance is achieved considering an ideal feeding of each dipole element: a uniformly distributed electric field impressed over the dipole gap region. Based on this theoretical design, a more complex design, including realistic feeding lines, has been performed and it is described in next section.

## 3 Prototype array

The first prototype array developed at TNO is shown in Fig. 3. The dipoles are printed on one side of a low permittivity ($\varepsilon_r = 2.2$) thin Duroid substrate, and electrically connected to form a unique long dipole periodically fed. The element spacing is 15.52 mm, which is about half wavelength at 9 GHz. The impedance transformation from the wave impedance of the free space, 377 Ω, at the aperture level, to 50 Ω at the connector, is performed with two wavelengths long transmission lines, printed on the same printed circuit boards in a egg-crate configuration (Fig. 3).

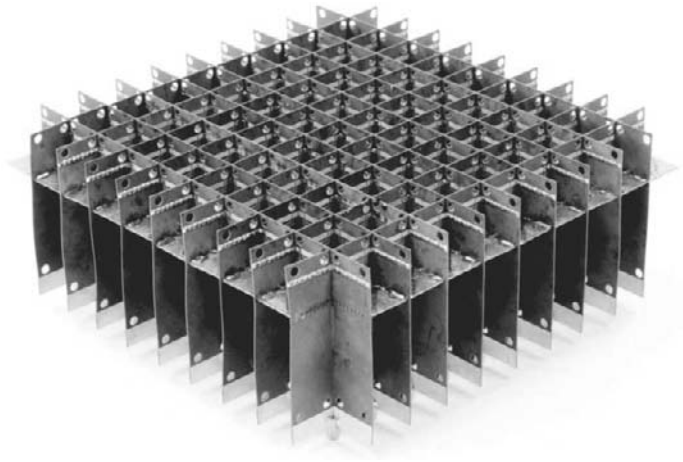

Figure 3: Prototype array.

The transition from coplanar strip-lines (CPS) to coplanar waveguide (CPW) and then to microstrip (MS) performs the balanced to unbalanced conversion, together with a wideband impedance transformation. As already highlighted in the previous section, the feeding gap of each dipole is an important design parameter and from the curves in Fig. 2, it appears that the best matching would be achieved for $\delta_d = 0.15\lambda_0$. However, such large gaps would require feeding lines (for instance coplanar strip lines) with interconductor distances so large that they would start radiating strongly cross-polarized fields. Actually, this radiation mechanism is very similar to the one of tapered slot antennas and it is in fact the main cause of their high cross-polarization characteristics (see Fig. 4).

The solution of this problem is the use of a double feed for each periodic cell, as shown in Fig. 5. In this case, the effective capacitance required in each gap is essentially the half of the required value, since the two feeds are connected in series. In this case, much narrower gaps can be used to obtain

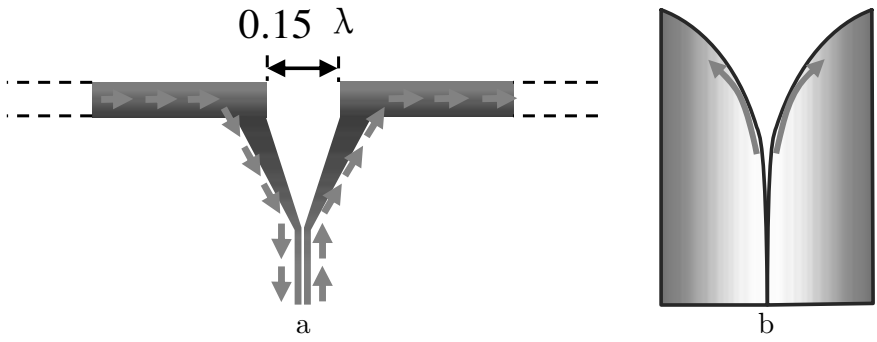


Figure 4: (a) Large gaps require feeding lines with large inter-conductor distances. (b) These give rise to strongly cross-polarized fields as in tapered slot antennas.

similar impedance curves, with respect to the single feed configuration. With such small gaps, the dipoles can be fed by transmission lines with negligible cross-polar radiation. This arrangement of the feeding lines, implemented with a CPS power divider (Fig. 5), was shown to improve the bandwidth of the array, [9]. A ground plane is included at a height of approximately $0.3\,\lambda_0$ (with $\lambda_0$ being the wavelength at 9 GHz) from the centre of the dipole, acting as a backing reflector.

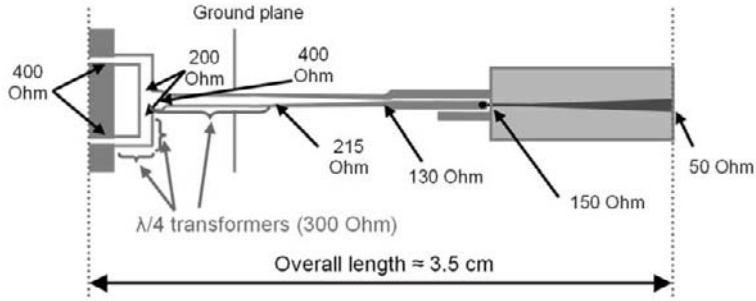


Figure 5: Double feed of the array element, with impedance transformation from 400 to 50 Ohms.

Figure 6 shows the active reflection coefficient of a central port of the finite array prototype when scanning toward broadside. From the measured curves, two unexpected resonance were observed at about 7 GHz and 8.5 GHz. Triggered by such observation, full-wave simulations of the entire structure, including the complete feeding network, were performed. The comparison between simulations and measurements is relatively good, indicating that the numerical tools are able to efficiently describe the wave phenomena in place. Note that the measurements include the summation of

all significant co-polarized S parameters for the investigated port, while the equivalent simulations are performed using the full wave simulator tool CST Microwave Studio and account for the entire finite array ($8 \times 8$ elements).

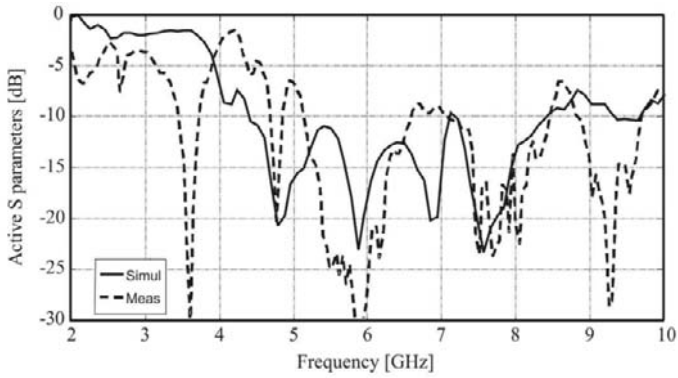


Figure 6: Active reflection coefficient of a central element of the finite array.

In order to analyse the nature of such resonances, further simulations were carried out assuming an infinite periodic array analysis. The reflection coefficient in the presence of the feeding lines was significantly different from those that were simulated in the design phase without the inclusion of the long matching network. In Fig. 7, the simulated active reflection coefficient when the array is radiating toward $\theta = 0°$ and $\varphi = 0°$ is reported. It is apparent that the array is completely mismatched at 5.25 and 7 GHz. At those frequencies, the simulations explicitly show the coexistence of common and differential modes in the long transmission lines. In Fig. 8, a schematic view of the electric current distribution along the feeding lines shows common mode propagation at 7 GHz, in correspondence of the resonance, while at 8 GHz the designed differential mode is dominant. It should be noted that these resonances are sharp and the radiation patterns, not reported here for brevity, do not indicate polarization degradation. However, the same simulations realized for the array radiating toward $\theta = 45°$ and $\varphi = 45°$ also show significant increases of the cross-polarized field levels. In practice, the scanning performance of the prototype array is limited by common modes excited in the vertical feeding lines. Needless to say that the infinite array configurations, while of great help in understanding the physics, overestimate the coherence of these standing waves, which are much less strong in a finite array (Fig. 6).

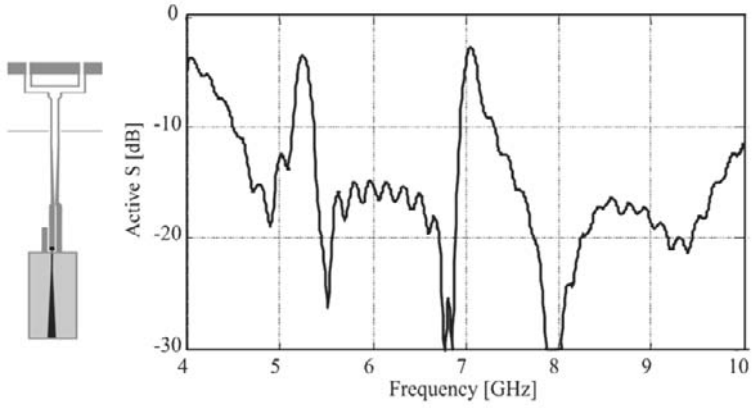


Figure 7: Active reflection coefficient for an infinite array when radiating towards $\theta = 0°$ and $\varphi = 0°$.

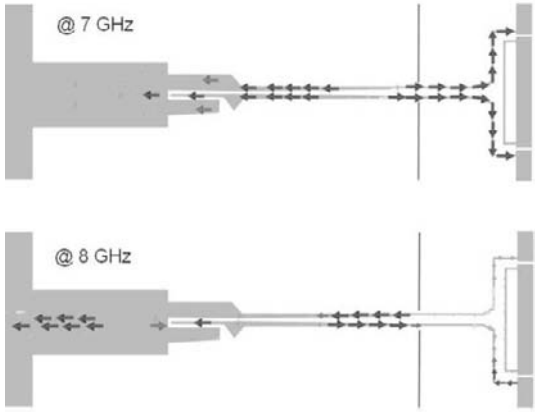


Figure 8: Surface current distribution at 7 and 8 GHz.

## 4 Common mode analysis

In order to analyse the common-mode resonance, we considered the simplified case of an infinite two-dimensional array of dipoles with periodicity $d_x$ and $d_y$, as shown in Fig. 9. The array elements are fed by CPS lines, whose length is equal to $l$. For sake of generality, no backing reflector is introduced. However, typically connected arrays involve the presence of a backing reflector. Accordingly, the transmission line lengths are in the order of a quarter of the free space wavelength. This is the length necessary to reach the ground-plane level, where the electronic circuits are located.

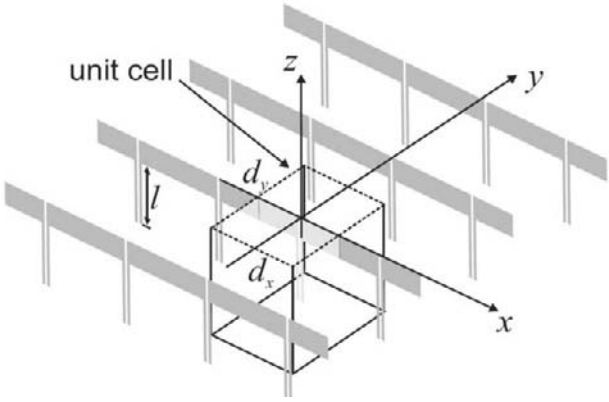


Figure 9: Geometry of a two dimensional array of dipoles fed by CPS lines.

As an example, in the most standard design situation in which the periodicity of the array is about half wavelength, and the vertical lines are a quarter wavelength, two neighboring feeding lines and the electrical connection via the dipole constitute a one wavelength continuous electric path ($d_x + 2l = \lambda$) and create a strong cross-polarizing standing wave. The active input impedance for $d_x = d_y = 15$mm, $l = 7.5$mm, is shown in Fig. 10. In addition to the expected grating lobe and the guided pole resonances, a peak of the impedance appears at 10 GHz. By observing the vector current distribution, the resonance can be recognized as associated with common-mode distribution in the CPS lines (Fig. 11). According to the third definition of cross-pol by Ludwig, [11], common-mode currents along z radiate strong

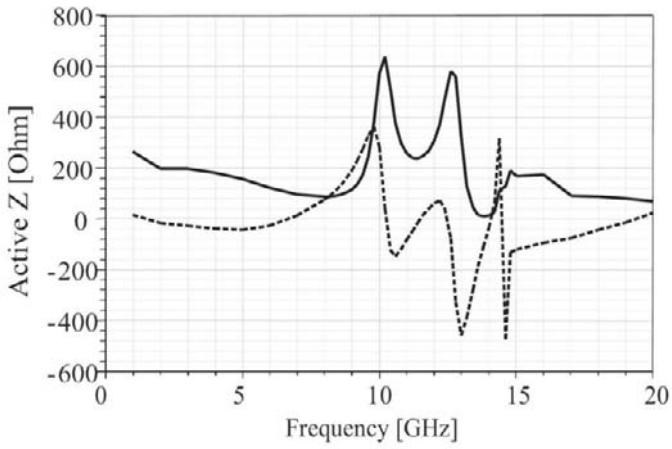


Figure 10: Real (–) and imaginary (- -) part of the active input impedance, for $\theta = 45°$ and $\varphi = 45°$.

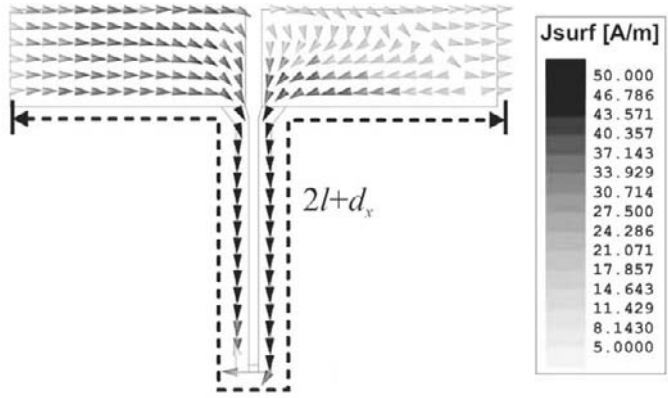


Figure 11: Surface current distribution at 10 GHz.

cross-polarized fields when scanning on the diagonal plane. In Fig. 12, the ratio between co-pol and cross-pol fields rapidly increases in proximity of the resonance at 10 GHz. Therefore, to ensure low cross-pol level, the length of the path $2l + d_x$ should be significantly shorter than a wavelength in order to shift the common-mode resonances at higher frequencies, outside the operational bandwidth of the array.

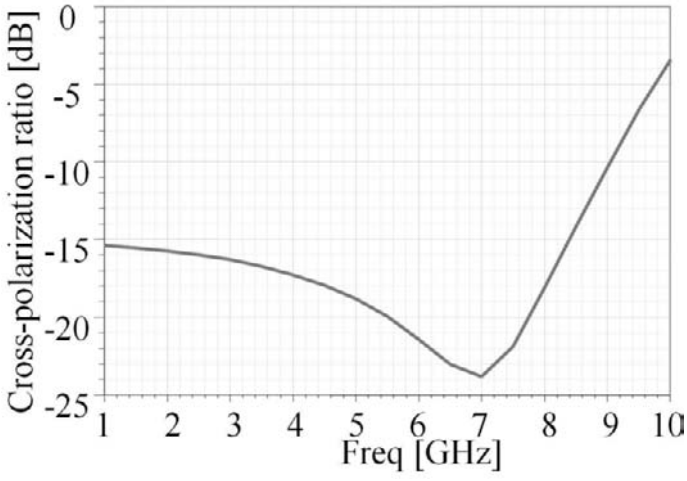


Figure 12: Cross-pol level when pointing at $\theta = 45°$ and $\varphi = 45°$.

## 5 Resonance-free array design

A CPS-to-CPS transformer, based on aperture coupling, has been designed to shorten the length of continuous current paths and to reject common-mode propagation. A schematic view of the component is shown in Fig. 13, where the ground plane on which the slot is etched is assumed to be infinite along $x$. The component is divided in two parts separated by the ground plane. The part at $z = h$, hereinafter the primary circuit, comprises a transition from CPS lines to Grounded CPS (GCPS) lines, then a power divider that splits the circuit in two equal halves, which are eventually re-connected in correspondence of a coupling slot. The secondary circuit at $z = -h$ is the same as the primary, but mirrored with respect to the slot. The initial input from the CPS lines can be associated with a differential-mode or a common-mode type of current. The common mode in input corresponds to a zero of electric current in correspondence of the slot. In turn, this translates in no electric current being excited in the secondary circuit of the transformer.

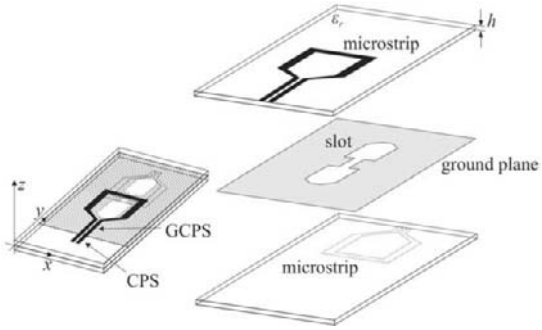


Figure 13: Geometry of the transformer.

The condition for high transmission levels of the differential mode is $Z_{\text{cell}} \ll Z_{\text{slot}}$, where $Z_{\text{slot}}$ is the impedance of the slot and $Z_{\text{cell}}$ is the connected array element loading. Therefore, the bandwidth of the transformer is wider for low values of $Z_{\text{cell}}$. Normally, the input impedance of an evenly sampled array ($d_x = d_y$) in the presence of a backing reflector is about $\zeta_0 \approx 400\,\Omega$. However, since $Z_{\text{cell}}$ is proportional to $d_x/d_y$, lower impedances can be obtained by considering a denser sampling of the array in the longitudinal direction. For example, with 4 feeds per cell ($dx = \lambda_0/8$), the input impedance at each feed point becomes $Z_{\text{cell}} = \zeta_0/4 \approx 100\,\Omega$. The CPS-to-CPS or CPS-to-MS (balun) transitions can be made compact on high permittivity dielectric ($\varepsilon_r = 10$), and the same number on T/R modules can be kept by means of power dividers (Fig. 13).

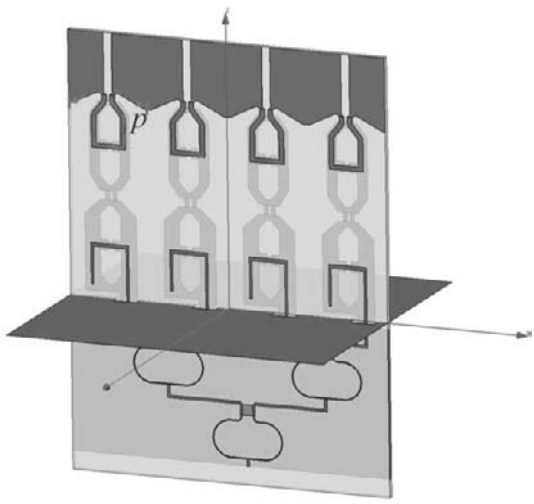


Figure 14: Geometry of a unit cell of a connected array with periods $d_x = d_y = \lambda_0/2$.

Figure 15 shows the cross-pol ratio as a function of the frequency for the geometry depicted in Fig. 14. For an array designed to work until 10 GHz, the cross-pol level remains lower than -14 dBs within the band of the array, while the common-mode resonance appears at a higher frequency (11 GHz). This is because the path $p$, shown in Fig. 14, has an electric length shorter than one wavelength at the frequencies within the operational band of the array, avoiding the occurrence of resonances.

An alternative design, which avoids a dense array sampling and the use of several power dividers in the feeding network, has also been developed. This common mode rejection structure, which is based on the combination

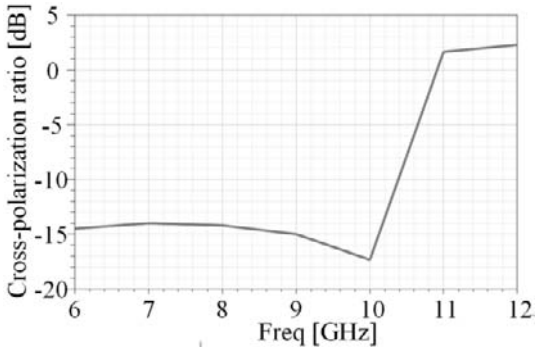


Figure 15: Cross-pol level when pointing at $\theta = 45°$, $\varphi = 45°$, for the geometry in Fig. 14.

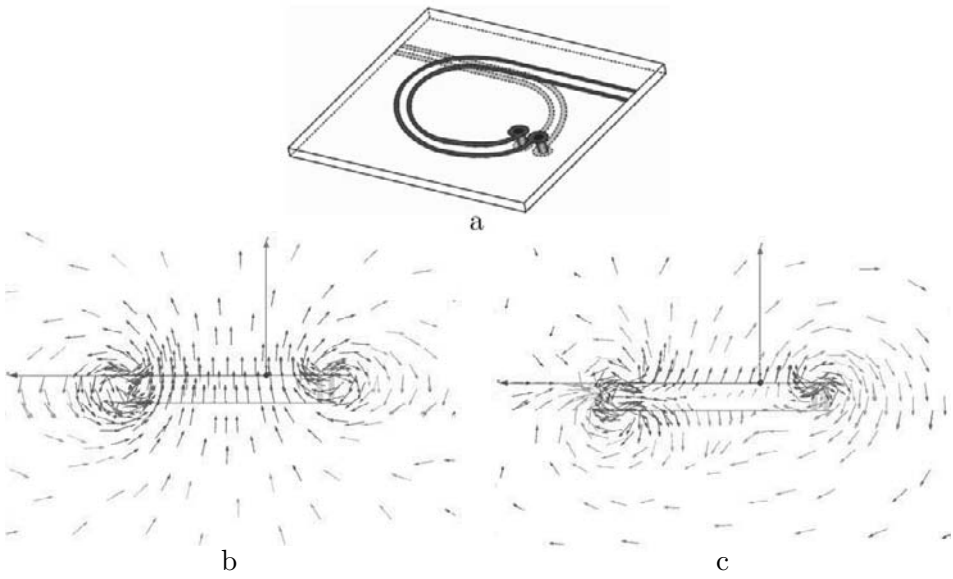


Figure 16: Loop geometry (a) and the associated magnetic field in a cross section at 7 GHz (b) and 15 GHz (c).

of a loop and a sleeve balun, has been optimized for a higher frequency band. In order to clarify the working principle of such a structure, it is important to focus the attention first on a single loop, as for example the one in Fig. 16(a). If the loop is fed with a common mode distribution, we can observe the following behavior of the currents in the two lines: in the lower frequency range, the currents flowing in the loop have equal phase, while at higher frequencies different portions of the loops are flown by currents with different phases. This is confirmed by the magnetic filed distributions shown in Fig. 16(b) and 16(c). These pictures show the magnetic field in a cross section of the loop structure, calculated via Ansoft HFSS, at 7 and 15 GHz, respectively. When most electric currents in the loop are in phase (Fig. 16(b)), there is a coherent adding of the magnetic fields. This produces a magnetic field circuitation with high contributions in the center of the selected cross section. The second configuration, at 15 GHz, corresponds to the case in which the electric currents in the loop are essentially divided in two parts with opposite phases, generating cancelling magnetic fields, which in turn produce a magnetic field circuitation with close to zero contributions in the center of the selected cross section (Fig. 16(c)).

As a consequence, at frequencies higher than a certain threshold, the average distributed inductance of the loop becomes lower and lower, creating a strong impedance discontinuity. The mismatch is such that almost

no common-mode propagation is allowed through the component. This effect is quantified in Fig. 17, by the S-parameters pertinent to differential (Fig. 17(a)) and common mode (Fig. 17(b)). A 10 dBs common-mode rejection is observed from about 9 to 22 GHz, while no blockage is observed by the differential mode up to 16 GHz. At this point, it is clear that although the single loop is sufficient to achieve the wanted suppression of the common mode, nevertheless the conversion from a balanced (CPS) to an unbalanced (micro-strip) line has not yet been performed. As shown in Fig. 18(d), if a CPS to micro-strip transformation is added below the ground plane level (Fig. 18(a)), cross-pol deteriorates (continuous curve). A single sleeve balun would also fail, due to electrical connection between adjacent elements (Fig. 18(b) and dotted curve). In a connected structure, in fact, the continuity of the current at the dipole edges prevents the resonance condition present in the case of a single resonant antenna which is at the base of the sleeve balun working principle. The joint use of loop and sleeve balun (Fig. 18(c) and dashed curve) recreates these conditions and allows the cross-pol field to be at least 14 dBs lower than the co-pol field, within the operational band (10.5–14.5 GHz; Fig. 18(e)), in all the scanning planes.

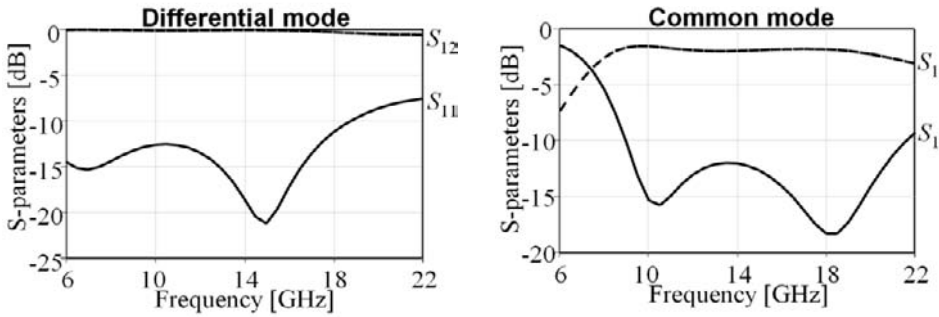


Figure 17: S-parameters of the loop for the differential mode (a) and the common mode (b).

## 6 Conclusions

In the last decades, the number of antennas on board of modern radar and communication platforms has shown a tremendous increase. An interesting and significant example is given by typical RF functions on board of multifunction frigates. These range from 200 MHz up to 18 GHz. The complete band in between these two frequencies is allocated to several functions, including: UHF communication, Electronic warfare Support Measure (ESM),

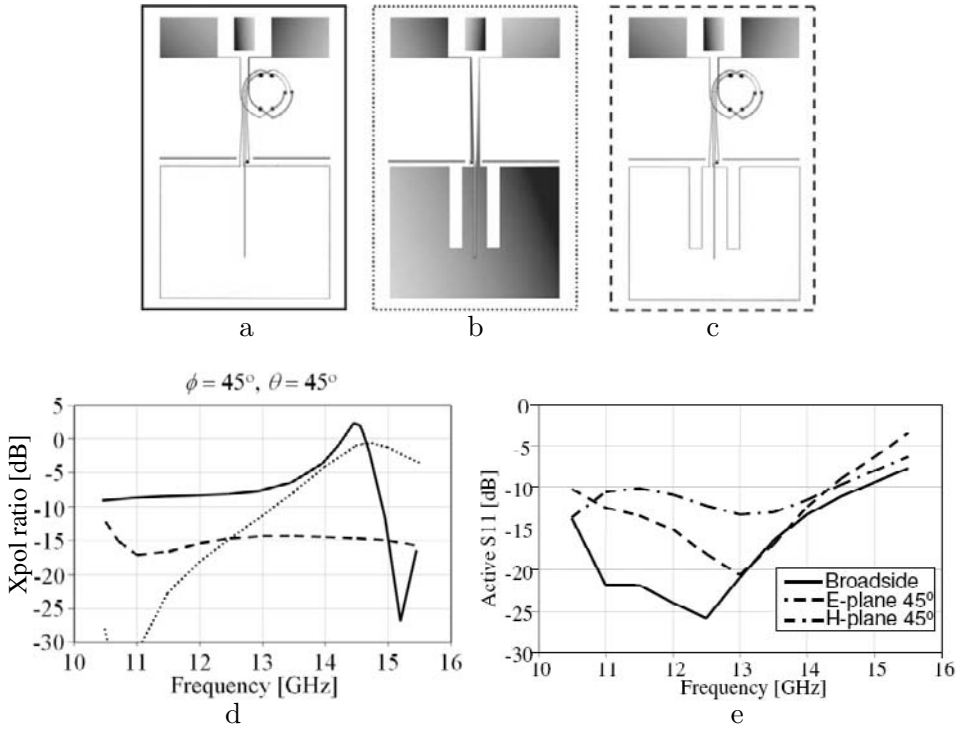


Figure 18: (d) Cross-pol levels at $\theta = 45°$, $\varphi = 45°$ for three configurations: loop (a), sleeve balun only (b) and loop + sleeve balun (c). (e) Active reflection coefficient for configuration (c).

Electronic Counter Measure (ECM), radar, navigation, Identification Friend or Foe (IFF), Joint Tactical Information Distribution System (JTIDS), SHF Satcom etc. Often these antennas use different polarizations and frequencies. Furthermore, demands on antenna size reduction and higher levels of integration have become more and more stringent, in order to reduce costs, increase efficiency and satisfy structural integration requirements. These trends and needs push for the development of flexible antenna solutions that can cover wide bandwidths or multiple frequency bands, in order to serve different functionalities. In this contribution, the development of a novel connected phased array concept, started at TNO, has been presented. An important issue related to the excitation of spurious common mode resonances in the feeding lines of the array has been highlighted and discussed in detail. The solution to this problem, consisting in a common mode rejection structure integrated in the antenna, has also been presented. The final innovative wide-band phased array concept presented in this contribution is characterized by excellent performances, in terms of bandwidth and polarization purity, over large scanning ranges.

# Bibliography

[1] Y. S. Kim and K. S. Yngvesson, "Characterization of tapered slot antennas feeds and feed array," *IEEE Trans. Antennas Propag.*, vol. 38, pp. 1559–1564, Oct. 1990.

[2] M. C. van Beurden, A. B. Smolders, M. E. J. Jeuken, G. H.Ċ. van Werkhoven, and E. W. Kolk, "Analysis of wide-band infinite phased arrays of printed folded dipoles embedded in metallic boxes," *IEEE Trans. Antennas Propag.*, vol. 50, no. 9, pp. 1266–1273, Sept. 2002.

[3] M. A. Gonzalez de Aza, J. Zapata, and J. A. Encinar, "Broad-band cavity-backed and capacitively probe-fed microstrip patch arrays," *IEEE Trans. Antennas Propag.*, vol. 48, no. 5, pp. 784–789, May 2000.

[4] W. S. T. Rowe, R. B. Waterhouse, and C. T. Huat, "Performance of a scannable linear array of Hi-Lo stacked patches," *IEE Proc. Microw., Antennas and Propag.*, vol. 150, no. 1, pp. 1–4, Feb. 2003.

[5] H. Wheeler, "Simple relations derived from a phased array antenna made of an infinite current sheet," *IEEE Trans. Antennas Propag.*, vol. 13, pp. 506–514, 1965.

[6] R. C. Hansen, "Linear connected arrays," *IEEE Antennas Wireless Propag. Lett.*, vol. 3, pp. 154-156, 2004.

[7] A. Neto and J. J. Lee, "Ultrawide-band properties of long slot arrays," *IEEE Trans. Antennas Propag.*, vol. 54, no. 2, pp. 534–543, Feb. 2006.

[8] J. J. Lee, S. Livingston, R. Koenig, D. Nagata, and L. L. Lai, "Compact light weight UHF arrays using long slot apertures," *IEEE Trans. Antennas Propag.*, vol. 54, no. 7, pp. 2009–2015, July 2006.

[9] A. Neto, D. Cavallo, G. Gerini, and G. Toso, "Scanning performances of wide band connected arrays in the presence of a backing reflector," *IEEE Trans. Antennas Propag.*, vol. 57, no. 10, pp. 3092–3102, Oct. 2009.

[10] A. Neto *et al.*, "Common mode, differential mode and baluns: the secrets," 31st *ESA Antenna Workshop Proc.*, Noordwijk, the Netherlands, 18–20 May 2009.

[11] A. C. Ludwig, "The definition of cross polarization," *IEEE Trans. Antennas Propag.*, vol. AP-21, pp. 116–119, Jan. 1973.

# Sunflower antenna: synthesis of sparse planar arrays for satellite applications

**Maria C. Viganò**[†], **Cyril Mangenot**[*], **Giovanni Toso**[*], **Gerard Caille**[‡], **Antoine G. Roederer**[†], **Ioan E. Lager**[†] and **Leo P. Ligthart**[†]

[†] *Delft University of Technology, IRCTR, Mekelweg 4, 2628 GA, Delft, the Netherlands. (m.c.vigano@tudelft.nl)*

[‡] *Thales Alenia Space Toulouse, 26 Avenue J.F. Champollion, 31037 Toulouse Cedex 1, France.*

[*] *European Space Agency, ESTEC Keplerlaan 1, 2200 AG, Noordwijk, the Netherlands.*

**Abstract**

This paper gives an overview of recent advancements on the design of an innovative sparse array for multibeam satellite applications. Just using a non-uniform placement of the radiators, without resorting to any excitation taper, an array antenna able to satisfy stringent requirements in terms of sidelobe level and beamwidth has been designed. In order to reduced the number of active controls, differently sized sub-arrays, composed of 1, 2 or 3 elementary square array tiles, are used in the design.

## 1 Satellite communication: an overview

Nowadays satellite communication is able to connect the complete Earth, providing, through multiple beam antennas, down-link and up-link coverage over a field of view for personal communication, and direct broadcast over linguistic areas. This coverage is guaranteed by several overlapping spots, generated by large antenna apertures, adopting both frequency and polarization reuse. An example of Europe coverage by means of different overlapping spots is given in Fig. 1.

In the past, these apertures have been usually generated using reflector based architectures [1]. The disadvantage of this configuration is mainly due to the lack of space on board of the satellite: if, for example, a 1:4 frequency reuse scheme is adopted with a one feed per beam architecture, 3–4 reflectors are needed. Another possibility is to use a Focal Array Fed Reflector (FAFR) [2], able to generate the different beams with a single aperture. Unfortunately this option is quite difficult to implement.

Antennas for Ubiquitous Radio Services in a Wireless Information Society
I.E. Lager and M. Simeoni (Eds.). 
doi:10.3233/978-1-60750-487-0-43

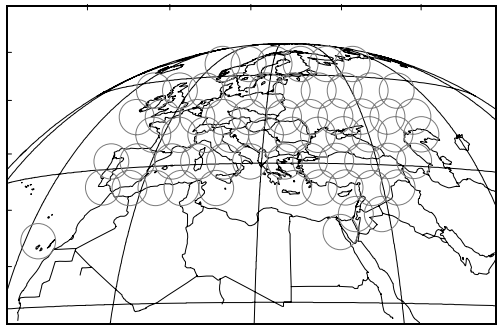

Figure 1: Example for a European multibeam coverage.

An alternative solution to the available ones, more appealing in terms of mass and spacecraft accommodation, consists of employing phased array antennas. Based on a single planar aperture, phased arrays would be a natural choice to generate multiple beams but they have been often discarded essentially because of their complexity and cost [3]. One way to make the phased array solution more competitive consists in reducing as much as possible the number of active elements and using all High Power Amplifiers (HPA) at the same working point while maintaining under control the main radiative characteristics [4].

Uniformly spaced array antennas have been studied in depth and several methods, requiring an amplitude taper to be applied to the radiators, have already been formulated in order to obtain a required radiation pattern. All these methods result in the need for a phase shifter and an amplifier for each array element. In order to reduce the number of controls and to shape the beam without resorting to an amplitude taper, uniformly fed sparse arrays can be used.

The synthesis of aperiodic arrays has been addressed several times in the past [5]–[16]. While in the 60s and 70s the solutions proposed were essentially deterministic [5]–[10], in the last years procedures based on statistic global optimization techniques have been mainly presented [11]–[14]. Recently, this interesting problem has been addressed again in [15]–[17], improving the solutions proposed by Willey [7] and Doyle [9].

Deterministic solutions are to be preferred to statistical algorithms for two main reasons: firstly, they allow obtaining real time results and, secondly, these synthesis techniques offer a solution with a controllable accuracy. Moreover, the results obtained applying deterministic methods may be directly used or adopted as the starting point for a global optimization approach.

The synthesis of aperiodic arrays has recently gained a renewed interest especially for the design of multibeam satellite antennas [17, 18]. Most of the techniques presented for the design of aperiodic arrays deal with the case of linear arrays. In the case of a planar array design, the easiest approach is to synthesize two linear arrays and, then, project them on two (orthogonal) axes via pattern multiplication [19]. If this simplification is not done, the designer has a higher number of degrees of freedom but the problem increases also in complexity.

In this paper the equi-power sub-arrays constituting the aperiodic array antenna are placed on a lattice reproducing the positions of the sunflower seeds, opportunely adjusted according to a desired tapering law. This particular non-uniform lattice is selected, as explained in the following sections, essentially because it guarantees a favorable radial and azimuthal spreading of the element positions. In this way, the pattern in the sidelobes and grating lobes regions tends towards a plateau-like shape [6], avoiding the presence of high narrow peaks and completely overruling onset of grating lobes (GL's). Moreover, by manipulating the element positions with the presented technique, the beamwidth can be adjusted and the sidelobe level (SLL) kept under an assigned value without using any amplitude taper. This planar array can be considered in the design of a transmit direct radiating array for a communication antenna deployed on a geostationary satellite.

## 2 Sparse array antenna synthesis

Starting from a regular spiral placement of the elements, able to guarantee a good spreading of the energy associated to SLL and GL's in a planar array and to obtain a quite uniform filling of the given aperture, the position of the radiators are then modified according to a proper density taper.

The chosen reference spiral is the Fermat spiral (Fig. 2) which has the property of enclosing equal areas within every turn. This spiral is quite often found in nature. In particular, there are leafs and seeds whose positions can be obtained by sampling a Fermat spiral equation. When it is important to have a uniform subdivision of the space, the parameters ruling the angular and radial placement along the spiral are related to the Golden Ratio [20]. More in details: if the angular distance between successive elements is chosen to equal the Golden angle (approximately 2.399963 radians – an irrational value), it is impossible to have two or more elements in the spiral array characterized by the same $\phi$ angle. Thanks to this interesting property, the element packing result to be efficient, as it will be clearly shown in Figs. 3 (a) and 4 (a).

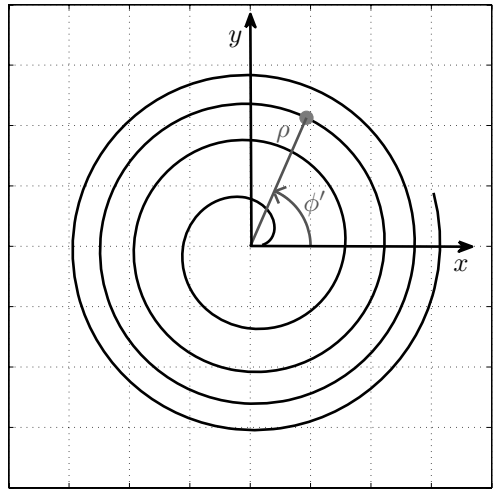


Figure 2: The Fermat spiral and its associated coordinate system.

## 2.1 Uniform spiral array

Let us consider elements placed along a spiral like the one depicted in Fig. 2, according to the following equations [21]

$$\rho_n = s\sqrt{\frac{n}{\pi}}, \quad \text{for } n = 1, \ldots, N \tag{1}$$

$$\phi'_n = 2\pi n\beta_1, \quad \text{for } n = 1, \ldots, N \tag{2}$$

where $\rho_n$ is the distance from the spiral center to the $n^{\text{th}}$ element, $n = 1, \ldots, N$, with $N$ denoting the total number of elements, the parameter $\beta_1$ controls the angular displacement $\phi'$ between two consecutive elements, and the parameter $s$ denotes the distance between the elements in the $xOy$ plane. Assume a sparse array deployed on a circular aperture of radius $R_{ap}$ along the Fermat spiral, with element locations given by the expression (1) and (2). In this manner, the positions of the elements in the sunflower array depend only on $n$ via a trivial equation. This placement strategy is illustrated in Fig. 3 (a), that presents such an array consisting of 250 elements.

It can be demonstrated [17, 21] that this kind of array element placement leads to an almost uniform distance $s$ between the radiators. This property is attractive when the interest focuses on avoiding GL, only, without a control of the SLL. As for the SLL, it remains around 17 dB, irrespective of the number of elements in the array and the spacing factor $s$ (see Fig. 3 (b)). This is consistent with the element distribution replicating a uniform current distribution on a circular aperture.

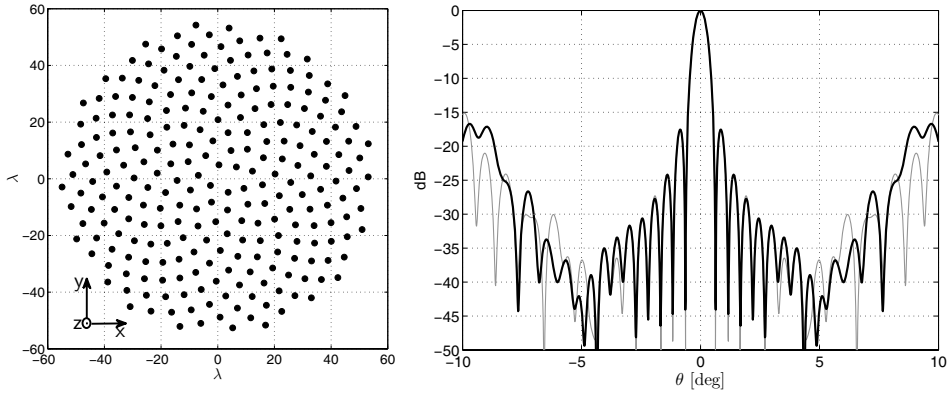


a b

Figure 3: Uniform sunflower array antenna consisting of 250 elements, assembled according to the algorithm described in [21]. (a) Distribution of the 250 elements; (b) pertaining array factor in the $\{x = 0\}$–plane (thick, black line) and $\{y = 0\}$–plane (thin, gray line); the angle $\theta$ measures the tilting with respect to the $Oz$ axis.

It is now clear that the only possibility to control the SLL, as well, is by introducing a density taper. In the next section it will be demonstrated how, by translating a Taylor amplitude tapering law [22] into a corresponding spatial density law, the SLL can be drastically reduced.

## 2.2 Non-uniform element placing

The spiral aperiodic lattice with a uniform element density introduced in the previous paragraph is an excellent starting point to apply a space tapering process. The spreading of the elements in the spiral arms guarantees an optimal behavior in terms of GL even when the inter-element spacing is larger than $\lambda$. In order to be able to control the SLL it is possible to vary the elements positions with respect to the array center, thus obtaining an effect similar to an amplitude taper.

The space taper technique presented here consists of choosing a reference amplitude distribution whose pattern satisfies the assigned requirements and emulates it by varying the radiator distance from the center. Specifically, a Taylor amplitude taper law with a certain SLL and $\bar{n}$ [22] has been selected as a reference and the locations of the elements in the sparse array are determined by means of a simple, 2 steps algorithm.

Let $A(r)$ denote the Taylor amplitude taper and $R_{\mathrm{ap}}$ the radius of the envisaged circular aperture. Firstly, $N$ positions $\rho_n$, $n = 1, \ldots, N$ are selected

by sequentially applying the relations

$$2\pi \int_{R_{n-1}}^{\rho_n} A(r) r \mathrm{d}r = \frac{2\pi}{2N} \int_0^{R_{ap}} A(r) r \mathrm{d}r, \quad n = 1, \ldots, N \tag{3}$$

$$2\pi \int_{R_{n-1}}^{R_n} A(r) r \mathrm{d}r = \frac{2\pi}{N} \int_0^{R_{ap}} A(r) r \mathrm{d}r, \quad n = 1, \ldots, N \tag{4}$$

with $R_0 = 0$ and $R_N = R_{\mathrm{ap}}$. Note that Eq. (3) emulates the desired taper by equating the surface integral over the annular ring delimited by the interval between $R_{n-1}$ and $\rho_n$ to half of the $n^{\mathrm{th}}$ part of the total aperture excitation. Subsequently, the element positions are determined by choosing their pertaining azimuth angle $\phi_n$ according to

$$\phi_n' = 2\pi n \frac{\sqrt{5}+1}{2}, \quad \text{for } n = 1, \ldots, N. \tag{5}$$

It should be noted that the effectively obtained aperture radius will be lower than the initially targeted $R_{\mathrm{ap}}$. Nevertheless, in the case when a large number of elements is used, this deviation will have a negligible impact on the obtained beamwidth.

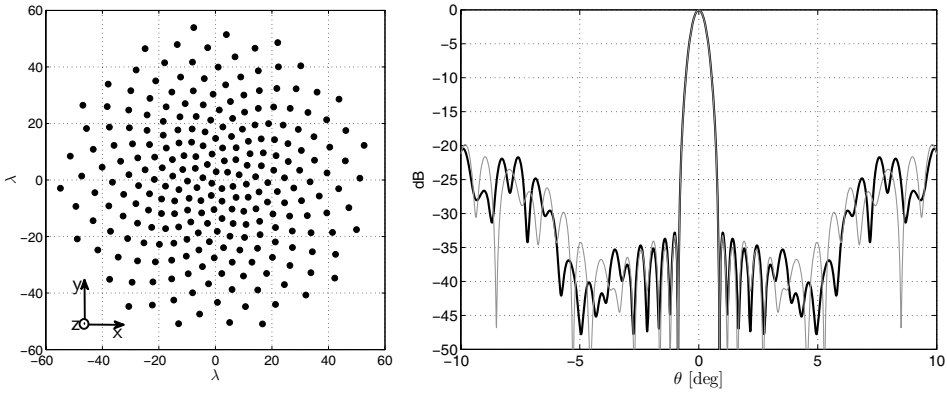


a b

Figure 4: Tapered sunflower array antenna consisting of 250 elements. (a) Distribution of the 250 elements; (b) pertaining array factor in the $\{x = 0\}$–plane (thick, black line) and $\{y = 0\}$–plane (thin, gray line); the angle $\theta$ measures the tilting with respect to the $Oz$ axis.

The result of this placement strategy is illustrated in Fig. 4 (a) where a $56\,\lambda$ radius aperture is filled with 250 elements distributed in a manner such that obtains a pattern similar to the one achievable with a Taylor amplitude law characterized by an SLL = 32 dB and $\bar{\mathrm{n}} = 4$. A total number $N = 250$ is

selected as an example. The array factor shown in Fig. 4 (b) clearly evidences the effect of the density taper on the reduction of the SLL, especially the ones close to the main-beam.

## 3 Application to a GEO satellite communication problem

The transmitting antenna considered in this study is operating in the Ka-band (19.7–20.2 GHz) and may have a maximum diameter of 1.5 m. The starting point considers a quasi-circular, direct radiating array with dimensions deemed to be sufficient for providing the required maximum gain and beam-width (see Table 1). The array must generate 64 spot beams. The total frequency band is divided into 4 sub-bands, and each of them is assigned to a set of beams so that there are no adjacent pencil beams using the same frequency resource. Figure 1 shows the footprint on the Earth of these 64 pencil beams.

The procedure described in the previous section has been extended and generalized also for the case in which the radiators are not all identical. In view of all elements being fed with the same power while, in turn, consisting (per type) of different numbers of equally fed individual radiators, it is obvious that the amplitude of the signal fed to the elements will differ, per type. Let

$$B_{\mathrm{E}}(m) = N_{\mathrm{r}}(m)\sqrt{\frac{P_{\mathrm{E}}(m)}{N_{\mathrm{r}}(m)}}, \quad \text{for } m = 1, \ldots, M \tag{6}$$

be the relevant amplitude, where $P_{\mathrm{E}}(m)$ is the (identical) power quotient delivered to the relevant element. Assume now that the total number of elements per type is fixed beforehand. With these prerequisites, each element is placed inside concentric rings of radii $R_{n-1} < R_n$, $n = 1, \ldots, N$, with

Table 1: Mission Requirements

| | |
|---|---|
| Number of spots | 64 |
| Spot diameter | 0.65° |
| Inter-spot distance | 0.56° |
| Rx band | 29.5 – 30.0GHz |
| Tx band | 19.7 – 20.2GHz |
| Frequency reuse | 1:4 |
| EOC gain | 43.8dBi |
| SLL1 over the interfering areas | 20dBi |
| SLL2 over the Earth | 25dBi |
| SLL3 over the whole visible space | 30dBi |

$R_0 = 0$ and $R_N = R_{ap}$ (the radius of the complete aperture). The remaining radii $R_n$ are calculated iteratively, by solving the integral equation

$$2\pi \int_{R_{n-1}}^{R_n} A(r) r \mathrm{d}r = B_{\mathrm{E}}(m)\big|_n, \quad \text{for } n = 1, \ldots, N \tag{7}$$

with $B_{\mathrm{E}}(m)\big|_n$ denoting the element amplitude associated with the type $m$ to which the element $n$ belongs.

This extension of the previously discussed formulation allows a further reduction of the number of elements, by using small sub-arrays in the array center and larger ones at the periphery. Different configurations are possible depending on how the sub-arrays are formed. Note that, from a technological point of view, it is really convenient to have sub-arrays composed of a different number of identical basic 'bricks'.

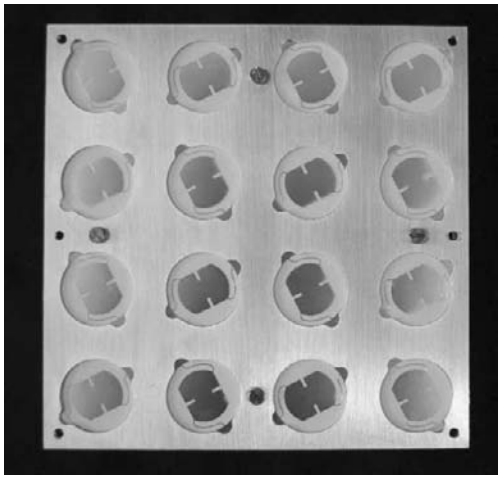

Figure 5: Square tile consisting of 16 patches.

In order to prove the concept here presented, a demonstrator, working at 7.5 GHz, has been realized. As elementary tile, a square sub-array consisting of 16 cavity backed patches, whose design was provided by Thales Alenia Space France, has been used (see Fig. 5). Thanks to the particular elements orientation and to the proper design of the feeding line embedded in the tile, this sub-array guarantees a perfect circular polarization over the $\theta$-range of interest. These basic elements have been grouped in larger sub-arrays consisting of 1, 2 or 3 square tiles (see Fig. 6) and used as radiators in the array environment. In this way it has been possible to better exploit the available antenna aperture with a reduced number of active chains, and at the same time, keep the complexity of the configuration low by using the same basic tile for assembling the three types of sub-arrays.

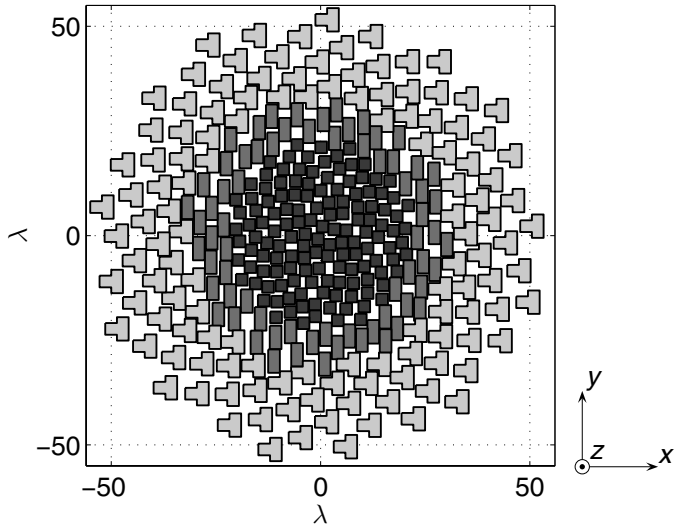


Figure 6: Position of the sub-arrays in the sun-flower configuration. All sub-arrays receive the same power.

The results achieved with the presented configuration are shown in Figs. 7 and 8. In the first one it is possible to appreciate how the taper applied to the sub-array positions can shape the pattern, reducing in a significant way the SLL in the desired field of view.

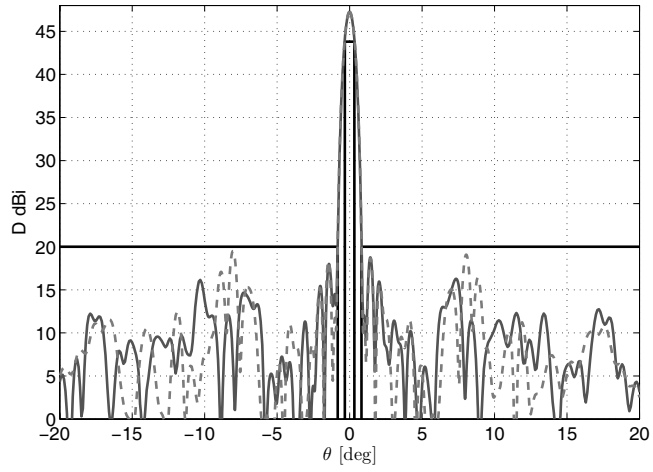


Figure 7: Radiation pattern at boresight for the configuration in Fig. 6 in the $\{x = 0\}$–plane (continuous, dark gray line) and $\{y = 0\}$–plane (dashed, gray line); the angle $\theta$ measures the tilting with respect to the $Oz$ axis. The design mask is indicated by continuous, black lines.

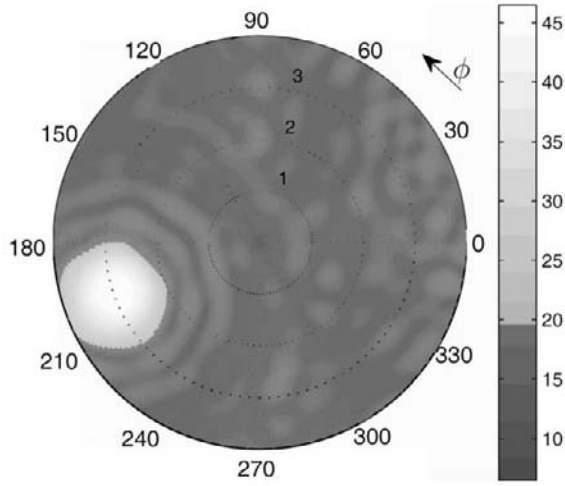


Figure 8: Pattern for the discussed array configuration with the beam pointing at Europe's edge.

The array factors in the $\{x = 0\}$ and $\{y = 0\}$ planes have been plotted in Fig. 7 for the beam pointing at boresight. The radiation pattern resulting from the sunflower configuration can be considered almost rotationally symmetric over Europe ($\theta \in [-4°, 4°]$).

Figure 8 represents the array radiation pattern when the beam is pointing at Europe's edge. Thanks to the color choice, with a threshold at the 20 dBi level, it is possible to notice that the SLL is not exceeding the requested level but remains under 19 dBi. In both cases, the achieved results comply with the demanding requirements given in Table 1 both when the beam points at boresight and when it points at the edges of Europe.

## 4 Conclusions

An analytic synthesis procedure to design aperiodic planar arrays which guarantees the control of SLL, GL and beamwidth without introducing any amplitude tapering has been presented. Starting from an array deployed on a non-regular lattice and characterized by a uniform spatial density of the elements, the density function has been modified in order to fit a reference amplitude tapering. The design technique has been applied for the design of a transmit Direct Radiating Array for a multibeam satellite communication mission. Three different kinds of sub-arrays have been used in the array synthesis in order to reduce the number of controls while maintaining good performances satisfying the mission requirements.

## 5 Acknowledgement

This work has been realized in the framework of a PhD activity supported by ESA-ESTEC and Thales Alenia Space France.

## Bibliography

[1] Y. Cailloce, G. Caille, I. Albert, and J. M. Lopez, "A Ka-band direct radiating array providing multiple beams for a satellite multimedia mission," in *Proc. IEEE 2000, Int. Conf. Phased Array Systems and Technology*, pp. 403–406, May 2000.

[2] C. Mangenot, P. Lepeltier, J. L. Cazaux, and J. Maurel, "Ka-band fed array focal reflector receive antenna design and developments using MEMS switches," in *Proc. JINA conf., 2002*, vol. 2, pp. 337–345, November 2002.

[3] R. J. Mailloux, *Phased Array Antenna Handbook*, Artech House, Boston, 2005.

[4] G. Caille, Y. Cailloce, C. Guiraud, D. Auroux, T. Touya, and M. Masmousdi, "Large multibeam array antennas with reduced number of active chains," in *Proc. Second European Conference on Antennas and Propagation – EuCAP*, Edinburgh, UK, November 2007

[5] H. Unz, "Linear arrays with arbitrarily distributed elements," *IEEE Trans. Antennas Propag.*, vol. 8, no. 2, pp. 222–223, March 1960.

[6] A. Ishimaru, "Theory of unequally-spaced arrays," *IEEE Trans. Antennas Propag.*, vol. 10, no. 6, pp. 691–702, November 1962.

[7] R. E. Willey "Space tapering of linear and planar arrays," *IEEE Trans. Antennas Propag.* vol. 10, no. 4, pp. 369–377, July, 1962.

[8] R. Harrington, "Sidelobe reduction by nonuniform element spacing," *IEEE Trans. Antennas Propag.*, vol. 9, pp. 187–192, March 1961.

[9] W. Doyle, "On approximating linear array factors," *RAND Corp Mem RM-3530-PR*, February 1963.

[10] M. I. Skolnik, "Chapter 6. Nonuniform Arrays," in *Antenna Theory, Part I*, R. E. Collin and F. Zucker (eds), New York, McGraw-Hill, 1969.

[11] R. L. Haupt, "Optimized element spacing for low sidelobe concentric ring arrays," *IEEE Trans. Antennas Propag.*, vol. 56, no. 1, pp. 266–268, January 2008.

[12] R. L. Haupt, "Thinned arrays using genetic algorithms," *IEEE Trans. Antennas Propag.*, Vol. 42, pp. 993–999, July 1994.

[13] A. Trucco, "Synthesis of aperiodic planar arrays by a stochastic approach," in *Proc. MTS/IEEE Oceans'97 Conf.*, pp. 820–825, Halifax, Nova Scotia, Canada 1997.

[14] M. C. Viganò, G. Toso, S. Selleri, C. Mangenot, P. Angeletti and G. Pelosi, "GA optimized thinned hexagonal arrays for satellite applications," in *IEEE Antennas Propagat. Symp. Dig.*, pp. 3165–3168, Honolulu, USA, June 2007.

[15] O. M. Bucci, M. D'Urso, T. Isernia, P. Angeletti and G. Toso, "A new deterministic technique for the design of uniform amplitude sparse arrays", in *30$^{th}$ ESA Antenna Workshop*, Noordwijk, the Netherlands, May 2008.

[16] O. M. Bucci, M. D'Urso, T. Isernia, P. Angeletti and G. Toso, "Deterministic synthesis of uniform amplitude sparse arrays via new density taper techniques", accepted for publication in *IEEE Trans. Antennas Propag.*

[17] M. C. Viganò, G. Toso, G. Caille, C. Mangenot and I. E. Lager, "Sunflower array antenna with adjustable density taper," *Int. Journal of Antennas and Propagation, Hindawi Publ. Corp.*, vol. 2009, Article ID 624035.

[18] G. Toso, C. Mangenot and A. G. Roederer, "Sparse and thinned arrays for multiple beam satellite applications," in *29$^{th}$ ESA Antenna Workshop on Multiple Beams and Reconfig. Antennas*, Noordwijk, the Netherlands, April 2007.

[19] M. C. Viganò, I. E. Lager, G. Toso, C. Mangenot, G. Caille, "Projection based methodology for designing non-periodic, planar arrays," in *Proc. 38$^{th}$ European Microwave Conference – EuMC*, pp. 1624–1627, Amsterdam, the Netherlands, October 2008.

[20] P. Atela, C. Gole and S. Hotton, "A dynamical system for plant pattern formation: rigorous analysis," *Journal of Nonlinear Science*, vol. 12, Is. 6, pp. 641–676, Oct. 2002.

[21] D. W. Boeringer, "Phased array including a logarithmic spiral lattice of uniformly spaced radiating and receiving elements," *U.S. Patent No. 6433745 B1*, Silver Spring, MD, US, April 2002.

[22] T. Taylor, "Design of circular apertures for narrow beamwidth and low sidelobes," *IEEE Trans. Antennas Propag.*, vol. 8, no. 1, pp. 17–22, January 1960.

# The relativity of bandwidth – the pursuit of truly ultra wideband radiators

**Dani P. Tran**[†], **Cristian Coman**[‡], **Fatma M. Tanyer-Tigrek**[†], **Andrei Szilagyi**[*], **Massimiliano Simeoni**[†], **Ioan E. Lager**[†], **Leo P. Ligthart**[†] and **Piet van Genderen**[†]

[†]*International Research Centre for Telecommunications and Radar (IRCTR), Faculty of Electrical Engineering, Mathematics and Computer Science, Delft University of Technology, 2628 CD, Delft, the Netherlands (f.m.tanyer-tigrek@tudelft.nl),*

[‡]*NATO Consultation, Command and Control Agency (NC3A), Surveillance & Reconnaissance Resource Centre, 2597 AK The Hague, the Netherlands,*

[*]*Military Equipment & Technologies Research Agency, Aeroportului Street, No. 16, Bragadiru, 077025, Jud. Ilfov, Romania.*

**Abstract**

An overview on the design of increasingly wider bandwidth radiators that are amenable to being integrated in array configurations is presented. The initial step is represented by moderate bandwidth radiator of the cavity backed patch antennas. The bandwidth characteristics are then substantially increased by combining coplanar waveguide (CPW) feedings and profiled dipoles, the result being radiators with unprecedented performances. This type of radiators are further refined for improving their time-domain adequacy or for ensuring intrinsic filtering properties.

## 1 Introduction

Larger bandwidth is one of the most frequently invoked requirements in present day radio applications: it is indispensable for ensuring the needed resolution in radar applications and it is, together with increasingly sophisticated protocols, the driving force behind enhancing the data rate in the communication channels. With reference to the latter, it is worth noting that the adoption of the First Report and Order by the Federal Communication Commission (FCC) [1] that permitted the commercial operation of Ultra Wide Band (UWB) technology unleashed a research activity of considerable proportions for developing the appropriate means for transforming the UWB technology from a high-end utility into a quotidian commodity.

Literally, the FCC defines an antenna as being UWB when it has a

Antennas for Ubiquitous Radio Services in a Wireless Information Society
I.E. Lager and M. Simeoni (Eds.). 
doi:10.3233/978-1-60750-487-0-55

fractional (relative) bandwidth of 20%, this value being 25% in the case of the radar domain [2]. Nevertheless, this (apparently) simple estimator leaves room for several side notes. Firstly, one must observe that, as resolution and data rate are *systems* related features, so should bandwidth be thought of in relation to the *supported system*. It then follows that, especially in the case of array antennas, an ingenious system design may supplement for limitations of the elements constituting it, thus inducing some relativity in the interpretation of the bandwidth. For example, by assembling on the same aperture several moderate bandwidth radiators having different, but contiguous, operational bandwidths, the collective performance of the array will be (ultra) wide band. Furthermore, by restricting the assessment of the radiator capabilities to their *impedance matching bandwidth* (the one that is accounted for in [2]), the UWB qualifier may turn out to be insufficiently substantiated. The impedance matching over a certain bandwidth should be complemented *over the same bandwidth* by a series of additional features, such as stable radiation characteristics, extremely low group delay, etc. Moreover, when the radiators are to be integrated in array environments, avoiding the onset of grating lobes makes miniaturization an imperative factor when the arrays are to be operated over an (ultra) wide bandwidth.

Addressing in a systematic and innovative manner this type of aspects provided the grounds for the International Research Centre for Telecommunications and Radar (IRCTR) to initiate in 2004 the Wide Band Sparse Element Array Antennas (**WiSE**) project. One of its two directions of activity was represented by compiling a catalogue of moderate to (ultra) wide band radiators amenable to being included in (planar) array antennas. This contribution summarizes some of the most notable achievements of this line of research. To benign with, Section 2 discusses a number of cavity backed patch type radiators. Although they are characterized by a moderate bandwidth (in the range of 10%) these antennas are excellently adapted for being employed in planar arrays. The next step is represented by the presentation in Section 3 of a class of CPW-fed radiators having an omnidirectional radiation followed, in Section 4, by the introduction of some extremely valuable variants that offer unidirectional radiation. The catalogue is completed in Section 5 by the discussion of some multi-frequency radiators. The account will be finalized by drawing some conclusions.

## 2 Cavity backed patch radiators

The possibilities offered by the cavity backed patch topology were recognized already in the early stages of the **WiSE** project. It should be observed

that, although examples of remarkably wide band radiators of this type are available in the literature [3, 4], this configuration yields, in general, a moderate bandwidth. This is the more so the case when, in view of ensuring technological reproducibility and compactness, a stratified, microwave laminate technology is used. Nevertheless, these radiators are extremely well suited to array environments and posses some interesting features, such as a potentially high polarization purity. Moreover, the topology lends itself to an accurate numerical modeling using, for example, the boundary-integral, resonant modes expansion (BI-RME) method [5], the application of which to the cavity backed patch architectures being elaborately discussed in [6]. This numerical tool can constitute the computational engine in complex and effective optimization schemes, as discussed in [6], as well.

These favorable properties provided the grounds for a number of radiators of this type to be designed, manufactured and physically validated within the **WiSE** project, both as individual antennas and integrated in arrays. In the following, a selection of the most representative outcomes of this research line will be discussed.

## 2.1 Cavity backed (stacked) patch antennas – initial experiments

The first type of antennas in this class that were developed within the **WiSE** project concerned probe-fed, circular patches, possibly with an additional parasitic patch, the generic configuration for the latter, more complex, variant being shown in Fig. 1. The geometrical parameters of the radiator were subject to grid-search optimization strategies for enhancing the operational bandwidth in the targeted X frequency band. This notoriously computation time consuming operation was greatly reduced by resorting to an accurate, semi-analytic approach combining the BI-RME and mode-matching methods with a Generalized Admittance description of the complete chain consisting from the succession of the various waveguide sections that can be recognized in Fig. 1 (a) (see [6, 7] for a detailed description of this formalism). This procedure allowed designing a number of moderate band elementary antennas. A particularly relevant design referred to a pair of antennas having the operational bandwidths[1] $7.9 \div 8.4\,\mathrm{GHz}$ and $8.6 \div 9.3\,\mathrm{GHz}$, respectively. These antennas were initially, tested as individual radiators and, subsequently, integrated in a non-periodic, shared aperture, planar array containing 31 and 32 elements of the two kinds, respectively [7].

The array antenna experiments provided a clear evidence of the high

[1] All operational bandwidths quoted in this work are defined with respect to a VSWR $\leqslant$ 2 condition, with VSWR denoting the Voltage Standing Wave Ratio.

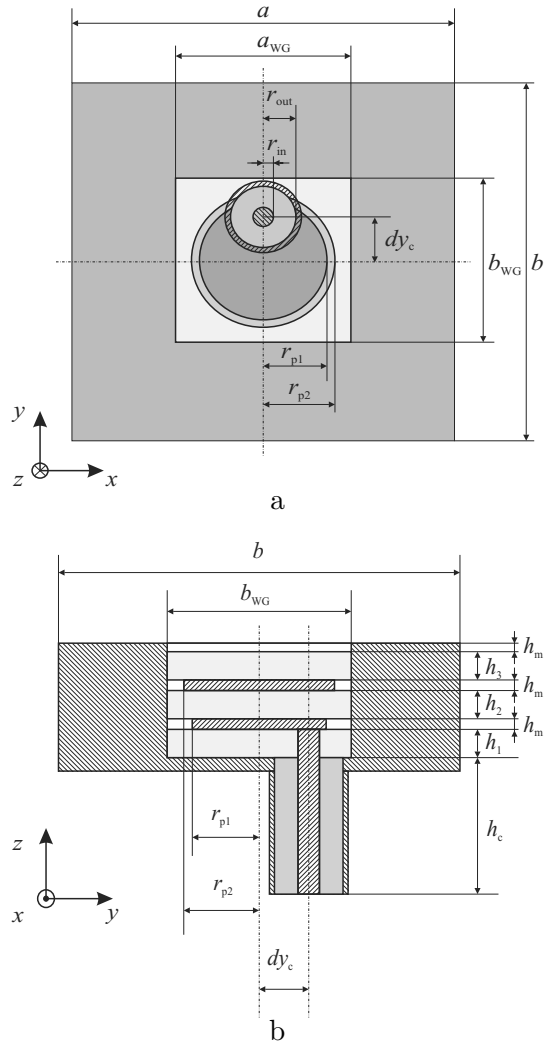


Figure 1: The configuration concerning the double patch antenna. (a) Top view; (b) axial cross-section.

level of isolation between the elements ensured by the cavity enclosure. In this sense, the measured reflection coefficient plots in Fig. 2 is characterized by a high degree of uniformity of this parameter for elements embedded in a highly non-uniform array environment. This behavior could only be obtained when the individual radiators were well isolated from each other, an effect that can only be attributed to the employed cavities.

The experience gained in this phase of the project laid the basis for developing a coplete family of such radiators, as will be shown below. All

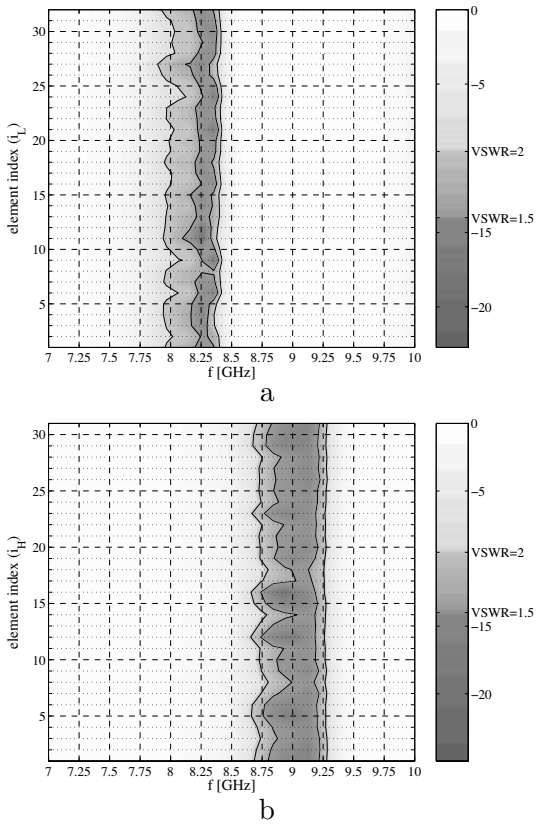


Figure 2: The frequency dependence of the active reflection coefficient for each elementary radiator in the two sub-arrays; the solid contours indicate the levels corresponding to VSWR=2 and VSWR=1.5, respectively. (a) Performance of the sub-array $SA_L$ operating in the $7.9 \div 8.4$ GHz bandwidth; (b) performance of the sub-array $SA_H$ operating in the $8.6 \div 9.3$ GHz bandwidth.

hereafter discussed radiators share the two main benefits already attested by the configuration shown in Fig. 1: a superior inter-element separation and a remarkable ease of manufacturing due to the use of vias for emulating the cavity enclosure. Additionally, some of the radiators will also benefit from another advantage of the embedded patch configuration, namely from the fact that the aperture radiation ensures a higher polarization purity.

## 2.2 High polarization purity cavity backed patch antennas

For assembling an array antenna consisting of radiating elements having high polarization purity, a special design has been implemented. The resulting antenna, shown in Fig. 3, consists of a cavity embedded microstrip

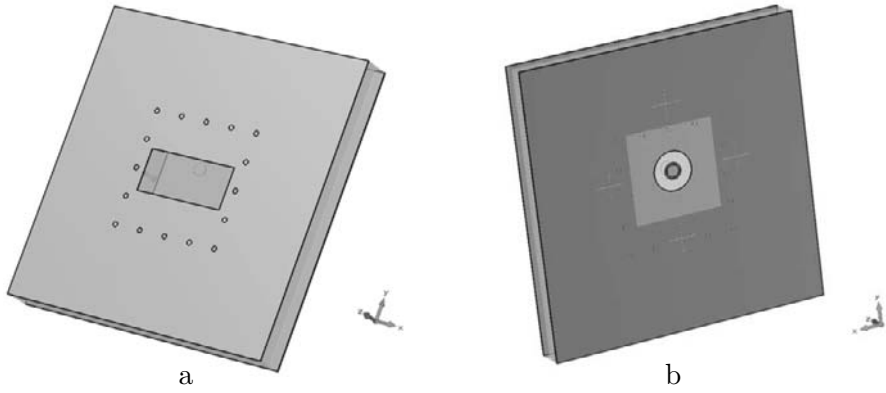

a b

Figure 3: The elementary radiator designed for the polarization agile array (a) Front view; (b) back view.

patch which is radiating through a rectangular slot. This particular geometry was selected in order to provide a good inter-element isolation between neighboring elements in the array environment, this feature being provided, as already indicated, by the cavity enclosure of the antenna. As before, the metallic walls are emulated by rows of equally-spaced metal plated through holes. The antenna is fed from the rear so to enable compact array arrangements. The elongated shape of the radiating slot provides high polarization purity to the radiated field. The antenna is manufactured with standard multilayer printed circuit board technology.

## 2.3 The cavity-backed slotted-patch antenna

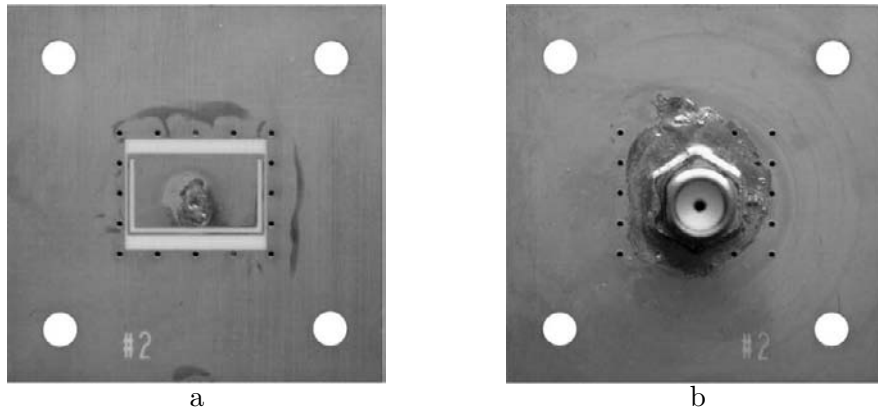


a b

Figure 4: The cavity-backed U-slot patch antenna. (a) Top view; (b) Bottom view.

With the goal of designing an antenna that would be amenable to be integrated in planar arrays, operate over reasonably wide frequency bands and be produced in an inexpensive and reliable manner, the cavity-backed U-slot patch (CUP) antenna [9] has been introduced. The idea behind the CUP antenna relies on the fact that the only method for inhibiting the surface waves propagation that allows for using compact elementary antennas is the cavity enclosure of the radiators themselves (see the overview in [10] and the references therein). This procedure results in the so-called cavity-backed patch antennas (CBPAs). The main features of the CBPAs are: miniaturization, suppression of surface waves, electromagnetic shielding from the neighboring circuitry and reduced backward radiation. The miniaturization can be achieved by filling the cavity hosting the antenna with higher permittivity dielectric materials, while all other aforementioned features derive directly form the use of the cavity enclosure. In view of ensuring an increased impedance bandwidth, the radiator to be enclosed in the metallic cavity is chosen as a U-slot patch antenna. The resulting ensemble, the *CUP antenna*, was described for the first time in [11], where its potential for phased array applications was demonstrated. It is very compact, allowing for closely packed array arrangements that yield wide grating lobes-free scanning. The radiator can be manufactured in standard printed circuit board (PCB) technology from a single microwave laminate, this ensuring its economical and accurate production [12]. The experimental prototype designed at IRCTR, displayed in Fig. 4, has bulk dimensions of about half a wavelength at the operational frequency of 10 GHz and exhibits a matching bandwidth of about 10% at the expense of a poor cross-polarization level (about -10 dB below the co-polar component) for observation angles away from the boresight direction (see Fig. 5).

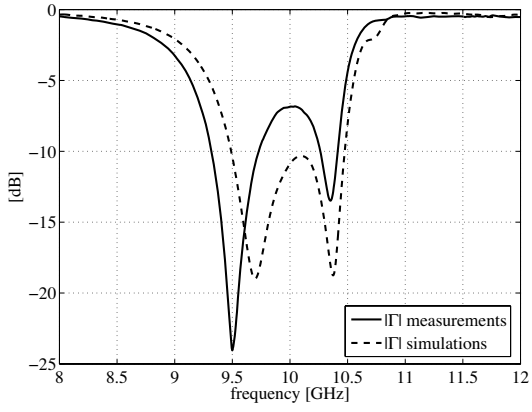


Figure 5: Simulated and measured return loss concerning the cavity-backed slotted-patch antenna.

# 3 CPW fed omnidirectional UWB radiators

The **WiSE** project set itself the task of developing antennas ensuring a 50% *system* operational bandwidth. In this respect, the radiators described in Section 2 offer a bandwidth of only around 10%. While preliminary studies demonstrated that such radiators may be assembled in arrays that meet the 50% bandwidth requirement, the resulting architecture turned out to be very complex and to have a relatively low gain and insufficient aperture efficiency. Consequently, the explorations turned towards developing truly UWB elements that could directly yield the aimed at operational bandwidth.

A strategic choice for achieving this goal was opting for a Coplanar Waveguide (CPW) feeding. A first type of antennas in this category is characterized by an omnidirectional radiation pattern. In the following, this type will be exemplified by means of two representative radiators referred to as the 'Eared' and the 'Tulip' loop antennas.

## 3.1 The 'Eared' antenna

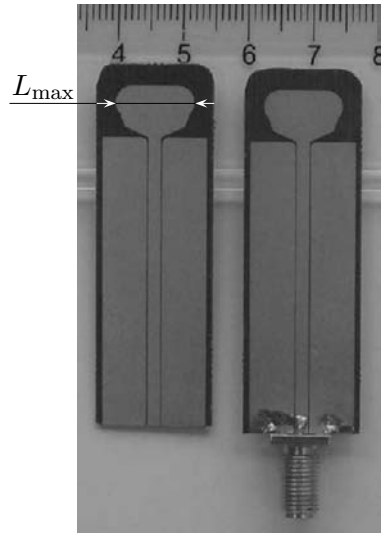


Figure 6: The 'Eared' antenna.

A physical implementation of the 'Eared' antenna is shown in Fig. 6. The device is etched on a commercially available Rogers Rogers RT/duroid® 5870 [13] high frequency laminate with a relative permittivity $\epsilon_r = 2.33$ at an operating frequency of $f_0 = 9\,\text{GHz}$. The maximum linear dimension of this device, denoted as $L_{\max}$ in Fig. 6, amounts to 12 mm. The radiator consists

of several sections the effects of which on the antenna performance being investigated in detail in [14, 15]. The feeding sections were extended in order to facilitate the measurement of the device's matching and radiation characteristics. The simulated and measured return loss frequency dependencies are presented in Fig. 7, with the simulated results predicting an operational bandwidth of 150% stretching between 6.5 GHz and 45 GHz. Note that the measurements were limited by the operational bandwidth of the employed connector. The antenna has omnidirectional radiation patterns with low cross-polar components (i.e. −25 dB at the desing frequency) [14, 15].

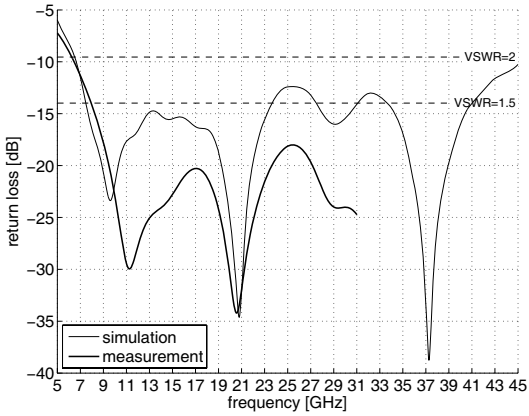


Figure 7: Simulated and measured return loss frequency dependencies concerning 'Eared' antenna.

The initial 'Eared' antenna was re-engineered for making it suitable to Impulse Radio applications, the targetted frequency range stretching, in that case, between 3.1 and 10.6 GHz. That variant was shown to have an impedance bandwidth of 169%, between 2.7 and 33 GHz. The Impulse Radio variant was also subject to a time domain performance assessment, the measured results evidencing remarkably low group delay variations that were below 4 ns up to 10 GHz [16].

Since, as mentioned in Section 1, the aim of the **WiSE** project was to assess the performance of the designed radiators in array environments, two *linear* arrays composed of 7 and 15 'Eared' antenna were manufactured, the latter device being presented in Fig. 8. The frequency and scanning angle dependences of the (combined) array reflection coefficient magnitude which are presented in Fig. 9 attest that the linear array has an operational bandwidth of 61%, between 8 GHz and 15 GHz. Furthermore, an excellent impedance matching was obtained for scanning angles between $\vartheta_0 = 0^\circ$ and $\vartheta_0 = 60^\circ$ over the whole frequency band, with $\vartheta_0$ measuring the tilting from the $Oz$ axis in the $\{y = 0\} -$ plane.

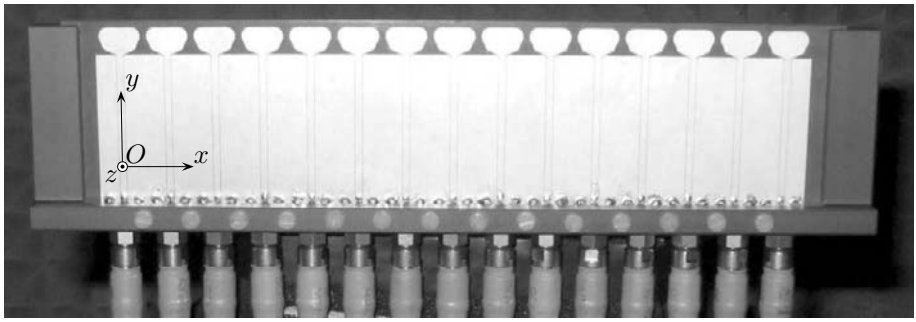


Figure 8: Linear array of 15 'Eared' antennas.

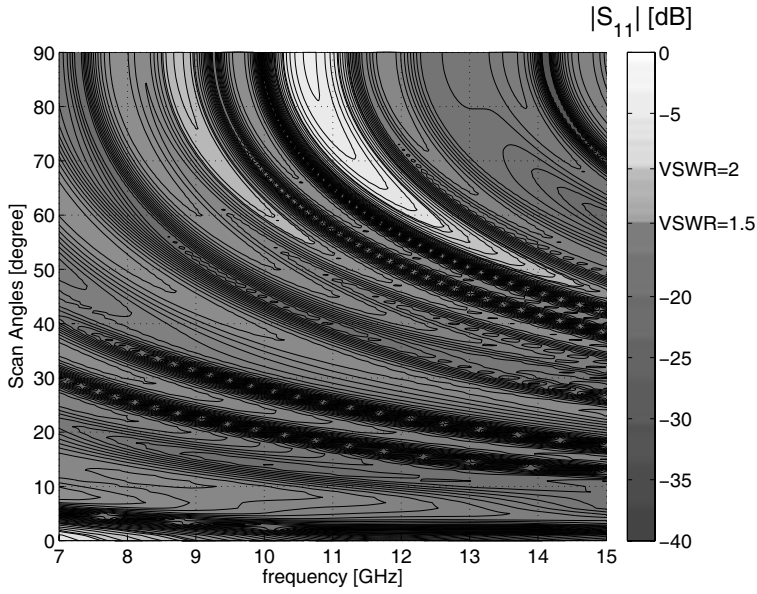


Figure 9: Frequency and scanning angle dependencies of the (combined) array reflection coefficient magnitude.

## 3.2 The 'Tulip' loop antenna

The second CPW fed antenna developed within **WiSE** was the so-called 'Tulip' loop antenna, a sample of which being shown in Fig. 10. The device is manufactured from the commercially available Rogers Rogers RO/duroid® 4003 high frequency laminate [17], with a relative permittivity $\epsilon_r = 3.55$ at an operating frequency of $f_0 = 10\,\mathrm{GHz}$. The radiation is ensured by the loop and the tuning stub inside it controls the impedance matching of the antenna. The maximum dimension of the antenna, denoted by $L_{\max}$ in Fig. 10, is 11 mm. The feed sections were again extended due to the

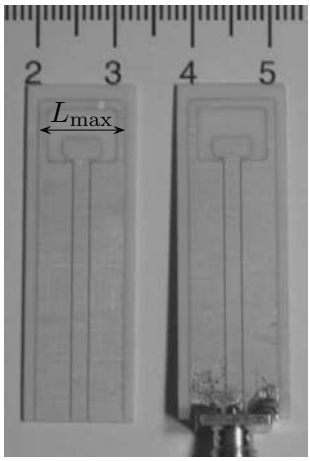


Figure 10: The 'Tulip' loop antenna.

reasons already discussed in Section 3.1. The frequency characteristic of the magnitude of the reflection coefficient of the antenna is presented in Fig. 11, the measured result indicating an operational bandwidth of 70%, stretching between 7.2 GHz and 15 GHz. Similarly to the case of the 'Eared' antenna, the 'Tulip' loop antenna has an omnidirectional radiation pattern (see [18]).

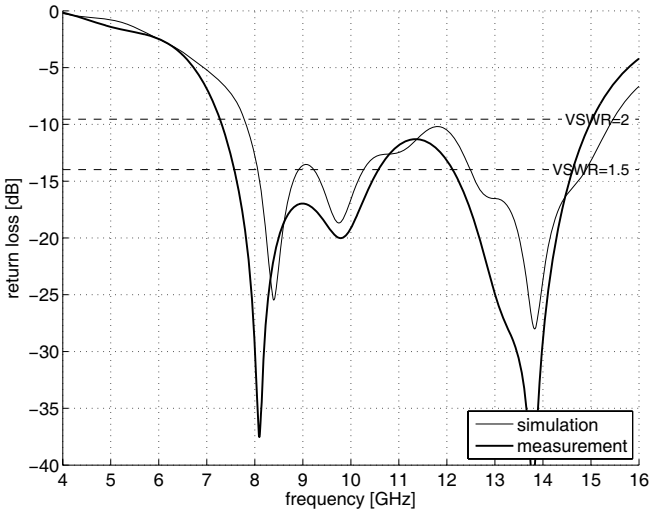


Figure 11: Simulated and measured return loss frequency dependencies concerning the 'Tulip' loop antenna.

For investigating the array performance of the 'Tulip' loop antenna, a *linear* array consisting of 4 such elements was manufactured, the device

being illustrated in Fig. 12. The feeding sections of the individual radiators were separated by rows of equi-spaced slots in order to mitigate the strong coupling that was evidenced by the initial numerical experiments effectuated on this type of arrays [19]. The frequency and scanning angle dependencies of the (combined) array reflection coefficient magnitude are presented in Fig. 13. Except for a small region corresponding to scanning angles $\vartheta_0 \geqslant 60^\circ$ ($\vartheta_0$ measuring the tilting from the $Oz$ axis in the $\{y = 0\} -$ plane) and frequencies $f \geqslant 13.6\,\mathrm{GHz}$, the array performance satisfies the VSWR $\leqslant$ 2 condition by a large margin. An elaborate discussion on the measured performance of this array antenna is given in [20].

## 4 CPW-fed unidirectional antennas

The CPW-fed antennas presented in Section 3 have clearly demonstrated UWB capabilities. Nevertheless, these devices are all characterized by omni-directional radiation patterns, a feature that induces certain limitations for both incorporating them in (planar) arrays and for using them in hand-held communication devices. An intense effort was then invested in obtaining CPW-fed radiators that maintain their UWB properties even when a backing ground plane is added. The results of this research activity is illustrated by two remarkable devices, the so-called 'diapason' and 'dispersion-free' antennas that are hereafter analyzed.

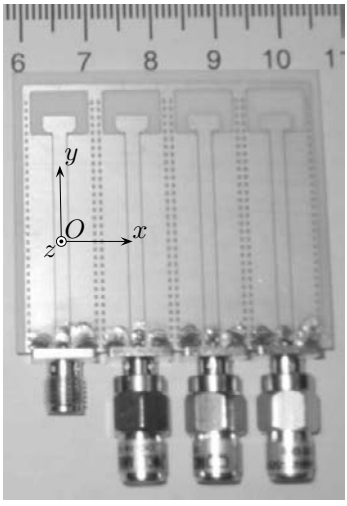


Figure 12: Linear array of CPW fed, printed, loop antennas.

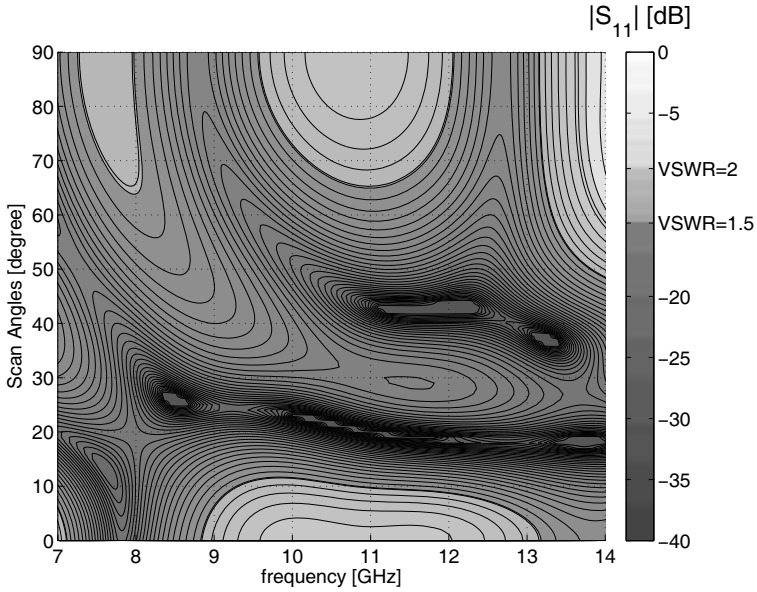


Figure 13: Frequency and scanning angle dependencies of the (combined) array reflection coefficient magnitude for the array shown in Fig. 12.

### 4.1 The 'diapason' antenna

Over the past 60 years, microstrip and UWB antennas have been constantly a topic of intense investigation and they seemingly reached their maturity. However, it is generally recognized that the former suffer from a reduced operational bandwidth while the latter are non-directive. The radiator displayed in Fig. 14, referred to as the 'diapason' antenna, demonstrates how the ease of fabrication and directivity of the microstrip antennas can be reconciled with UWB performance.

The antenna is fed by an off-axis grounded coplanar waveguide (CPWG), with the two ground plates that are visible in Fig. 14 being electrically connected to the waveguide's ground. The employed asymmetric diapason stub counter-balances the reactance and the susceptance of the ring-loop slot antenna. The device is supposed to be etched on a Rogers Rogers RT/duroid ® 5880 microwave laminate [13], with 1/2 oz copper-cladding and a 5.5 mm substrate thickness. The overall dimensions are $12.5 \times 12.5 \times 5.5$ mm, this representing a 1 to 3 reduction with respect to the antenna presented in [21].

With these choices, the radiator displays unprecedented and unparalleled, multiple-octave impedance bandwidth performance, as shown in Fig. 15. The obtained operational bandwidth is approximately 100 times larger than the one reported in [21]. The key to obtaining this feature was provided by

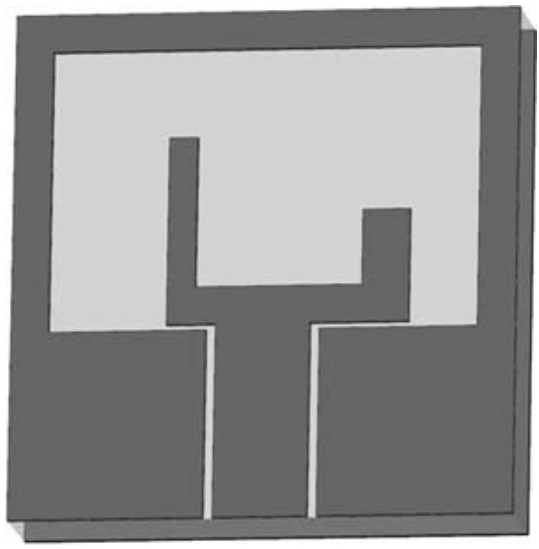

Figure 14: The 'diapason' antenna.

the innovative combination between an off-axis feeding and the unique unbalance matching method. The result is the simplest and smallest, broadside, unidirectional, super wide-band antenna ever recorded.

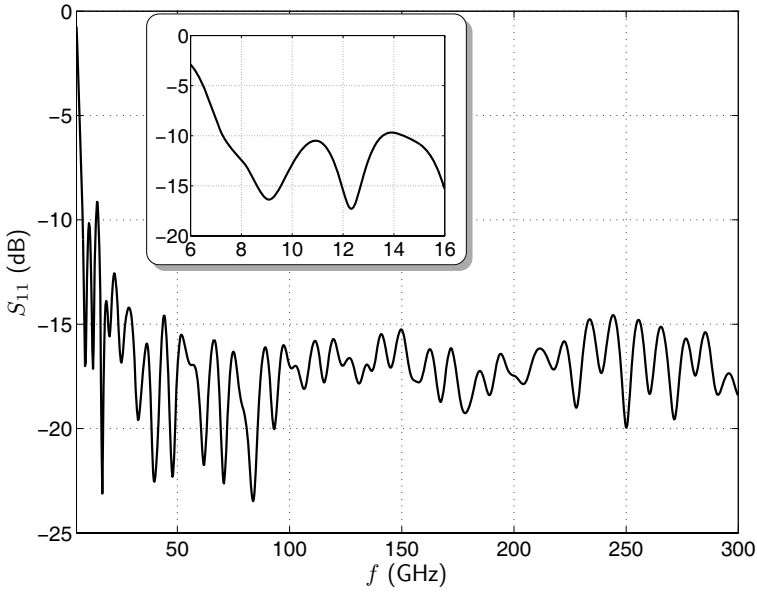


Figure 15: Simulated input reflection coefficient for the 'diapason' antenna. The inset shows a zoom-in on the X-band behavior of the antenna.

### 4.2 The 'dispersion-free' antenna

The ability of radiators to transmit undistorted pulses, as required, for example, by Impulse Radio applications, is decisively influenced by a dispersion free operation. In this respect, it has been observed that dispersion is associated with structures that have multiple inflection points in their frequency characteristics. By succeeding to circumvent this shortcoming, IRCTR managed to devise a radiator that is characterized by both extremely low dispersion and UWB impedance matching characteristics. This device, termed as the 'dispersion-free' antenna, is depicted in Fig. 16.

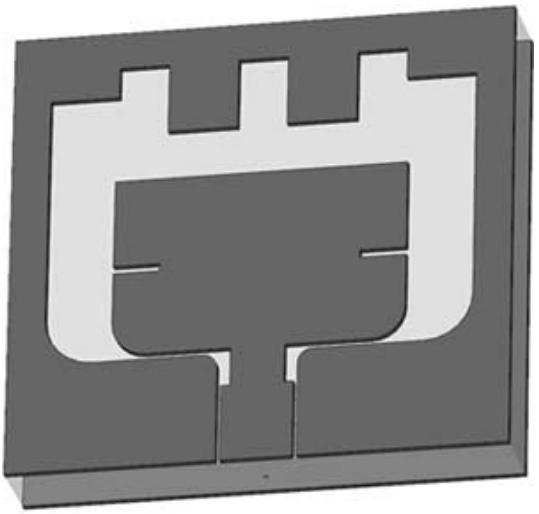

Figure 16: The 'dispersion-free' antenna.

The radiator consists of a grounded substrate having a patch and a ring etched on its top side. As was the case with the 'diapason' antenna, the patch is fed by a CPWG, with the ring being grounded. The structure is kept small for allowing for susceptance matching in the higher segment of the operational frequency band. The *notches* in the patch physically force the currents to flow along longer paths, making the patch (virtually) longer; this makes it possible to neutralize the reactance in the lower end of the frequency bandwidth. The *stubs* at the upper-side of the grounded ring are extruded down to form capacitive gaps that provide paths for the flow of the displacement currents. In this manner, more degrees of freedom are created for tuning the antenna at lower frequencies. To conclude with, the carves at the feeding point (the 'neck') of the patch allow a smooth CPWG to patch transition. More details on the design and working principles of this radiator can be found in [22], that article discussing a first previous version of the 'dispersion-free' antenna.

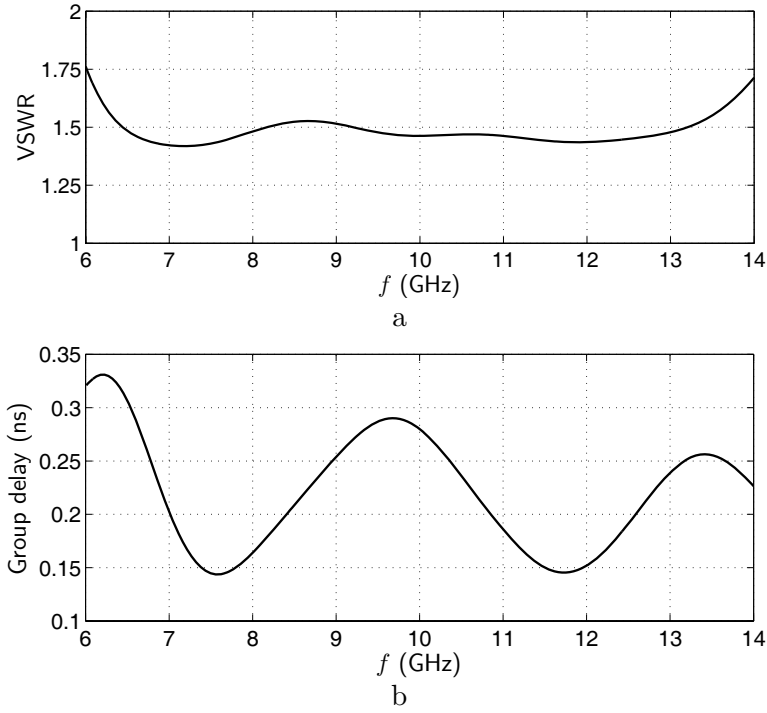


Figure 17: Frequency characteristics of the 'dispersion-free' antenna. (a) VSWR analysis; (b) group delay analysis.

The frequency characteristics of the 'dispersion-free' antenna are presented in Fig. 17. The plots demonstrate a remarkably wide and flat impedance bandwidth and, at the same time, an extremely low group delay behavior. In both respects, the presently discussed device evidences clearly superior performances to those of the radiator reported in [22].

## 5 Multi-frequency antennas

A particularly interesting feature to be implemented in a radiator is ensuring *controllable* filtering properties, the result being sometimes referred to as a 'filt-antenna'. This type of devices turned out to be extremely adequate for the **WiSE** $\mathsf{DEMO}_4$[2] demonstrator, a concrete instantiation of the concept being represented by the UWB antenna for tactical radio-location and navigation (RAD-NAV) shown in Fig. 18. Through its embedded filtering capabilities, this device safeguards the following frequency bands:

[2] $\mathsf{DEMO}_4$ demonstrator: a complex, wearable receive antenna system for a METRA defined application.

- the fixed and mobile satellite RAD-NAV bands $L_1$ through $L_5$;
- the industrial, scientific and medical (ISM) ISM2.5G and ISM5.8G radio bands as defined by the Radio communication sector of the International Telecommunication Union (ITU-R);
- the complete FCC unlicensed UWB band (3.1 up to 10.6 GHz).

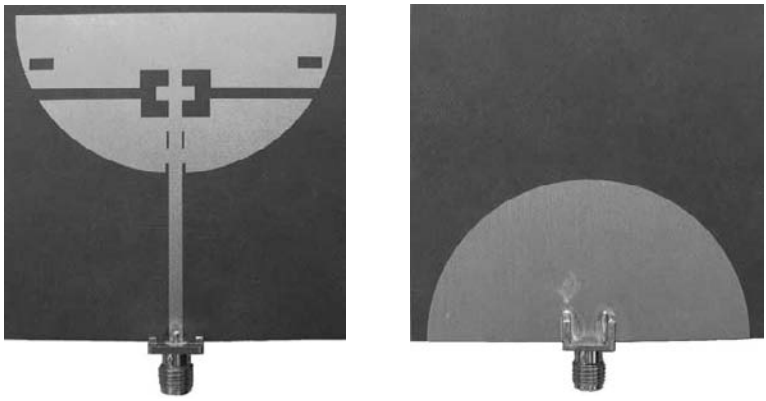

a b

Figure 18: The 'RAD-NAV' antenna. (a) Front side; (b) back side.

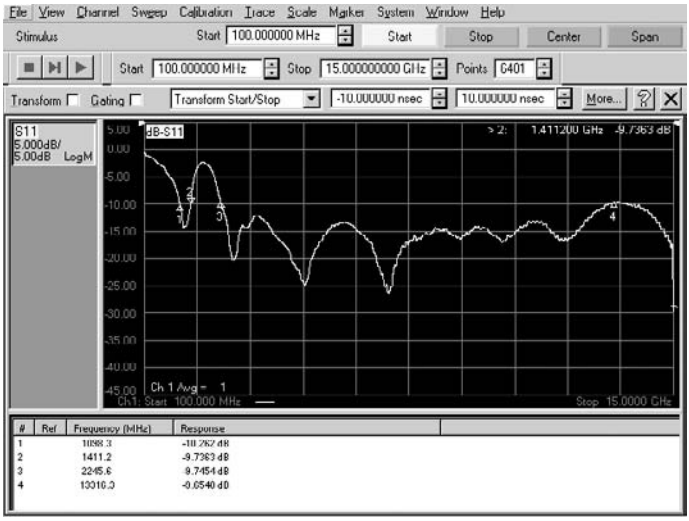


Figure 19: Vector network analyzer snapshot certifying the frequency selective properties of the 'RAD-NAV' antenna.

The antenna architecture consists of two identical, semi-elliptic patches that are anti-simetrically placed on the two sides of a dielectric slab. The

lower patch acts as a ground plane while the upper one, fed by means of a microstrip line, represents the radiating element. Several notched shapes are etched away from the radiator for matching and/or filtering purposes. The antenna is manufactured from a Rogers Rogers RT/duroid® 5880 microwave laminate [13], with 1/2 oz copper-cladding and a 0.787 mm substrate thickness, the overall dimensions being $60 \times 60 \times 0.787$ mm. Note that the design can be easily scaled up and down for accommodating the stringent requirements pertaining to the **DEMO**$_4$ demonstrator.

The measurement results in Fig. 19 are suggestive for the excellent radiation properties of the manufactured device. Note that these results were obtained in an electromagnetically extremely polluted environment, with simultaneous effects of connections, ends, edges, transitions, direct, multiple and multipath reflections, and disturbances caused by adjacent equipment. The fact that the measured were in very good agreement with the simulated predictions is manifest for the robustness of the employed design (a truly 'plug-and-play' design).

## 6 Conclusions

The elementary antenna research and development activities within the **WiSE** project were summarized. some high performance, easily manufacturable variants of cavity backed, patch antennas were presented, insisting on their suitability to being embedded in planar arrays. Several CPW fed, UWB radiators, having both omnidirectional and unidirectional radiation patterns were then discussed. The elements of the former variety were shown to operate adequately in linear arrays. As for the latter group, they set new standards in the printed array area, with record breaking impedance bandwidths and extremely low group delays. The manners to implement filtering properties in UWB antennas were also demonstrated.

## 7 Acknowledgement

The research reported in this work was effectuated within the frame of the "Wide Band Sparse Element Array Antennas" (WiSE) project, a scientific undertaking financed by the Dutch Technology Foundation (Stichting Technische Wetenschappen – STW). This support is hereby gratefully acknowledged.

## Bibliography

[1] Federal Communication Commission, "FCC 02-48 – First report and order: Revision of Part 15 of the commission's rules regarding ultra-wideband transmission systems," Washington, DC, released April 22, 2002.

[2] IEEE Std 1672-2006, "IEEE standard for ultrawideband radar definitions," IEEE-SA Standards Board, November 10, 2008.

[3] S. D. Targonski, R. B. Waterhouse, D. M. Pozar, "Design of wide-band aperture-stacked patch microstrip antennas," *IEEE Trans. Antennas Propag.*, vol. 46, no. 9, pp. 1245–1251, Sept. 1998.

[4] R. B. Waterhouse, "Design and scan performance of large, probe-fed stacked microstrip patch arrays," *IEEE Trans. Antennas Propag.*, vol. 50, no. 6, pp. 893–895, June 2002.

[5] G. Conciauro, M. Gugliemi, R. Sorrentino, *Advanced Modal Analysis. CAD Techniques for Waveguide Components and Techniques*, John Wiley & Sons, Ltd., Chichester, 1999.

[6] C. I. Coman, *Shared Aperture Array Antennas Composed of Differently Sized Elements Arranged in Sparse Sub-arrays*, dissertation, Delft University of Technology, January, 2006.

[7] C. I. Coman, I. E. Lager, and L. P. Ligthart, "The design of shared aperture antennas consisting of differently sized elements," *IEEE Trans. Antennas Propag.*, vol. 54, no. 2, pp. 376–383, Feb. 2006.

[8] M. Simeoni, I. E. Lager, "The cavity-backed slotted-patch antenna," Scientific report IRCTR-S-05-06, May, 2006.

[9] I. E. Lager, M. Simeoni, "Experimental investigation of the mutual coupling reduction by means of cavity enclosure of patch antennas," in *Proc. 1$^{st}$ European Conference on Antennas and Propagation – EuCAP*, Nice, France, November 2005.

[10] N. C. Karmakar, "Investigations into a cavity-backed circular-patch antenna," *IEEE Trans. Antennas Propag.*, vol. 50, no. 12, pp. 1706–1715, Dec. 2002.

[11] M. Simeoni, C. I. Coman, and I. E. Lager, "Cost-effective array antennas for narrow-beam, wide-angle scanning applications," in *Proc. 36$^{th}$ European Microwave Conference – EuMC*, pp. 1790–1793, Manchester, UK, Sept. 2006.

[12] I. E. Lager, M. Simeoni, and L. P. Ligthart, "Technological antenna design – An instrument for the mass-production of antenna systems," in *Proc.* 11$^{th}$ *Int. Symp. on Antenna Technology and Applied Electromagnetics*, pp. 44–45, Saint-Malo, France, June 2005.

[13] Rogers Corporation, "Rogers RT/duroid® 5870/5880 high frequency laminates," [Online]. Available: www.rogerscorp.com.

[14] F. M. Tanyer-Tigrek, D. P. Tran, I. E. Lager, L. P. Ligthart, "CPW-fed, quasi-magnetic, printed antenna for ultra wide-band applications," *IEEE Antennas Propag. Mag.*, vol. 2, pp 61–70, 2009.

[15] F. M. Tanyer-Tigrek, D. P. Tran, I. E. Lager, L. P. Ligthart, "Over 150% bandwidth, quasi-magnetic, printed antenna," in *IEEE Antennas Propagat. Symp. Dig.*, San Diego, CA, July 2008.

[16] F. M. Tanyer-Tigrek, I. E. Lager, L. P. Ligthart, "Experimental validation of the time-domain behavior of the UWB, 'Eared' Antenna for Impulse Radio Applications," accepted for presentation at the $4^{th}$ *European Conference on Antennas and Propagation – EuCAP*, Barcelona, Spain, april 2010; also issued as Scientific Report IRCTR-S-018-09.

[17] Rogers Corporation, "Rogers RO4000® series high frequency circuit materials," [Online]. Available: www.rogerscorp.com.

[18] F. M. Tanyer-Tigrek, D. P. Tran, I. E. Lager, L. P. Ligthart, "Wide-band Tulip-Loop Antenna," *Proc.* $3^{rd}$ *European Conference on Antennas and Propagation – EuCAP*, pp. 1446–1449, Berlin, Germany, March 2009.

[19] F. M. Tanyer-Tigrek, I. E. Lager, L. P. Ligthart, "CPW-fed printed loop antenna for ultra wide-band applications and its linear array performance," submitted to *IEEE Antennas Propag. Mag.*; also issued as Scientific Report IRCTR-S-004-09.

[20] F. M. Tanyer-Tigrek, I. E. Lager, L. P. Ligthart, "Experimental validation of a linear array consisting of CPW fed, UWB, printed, loop antennas," *IEEE Trans. Antennas Propag.*, (in press); also issued as Scientific Report IRCTR-S-001-09.

[21] D. P. Tran, "A novel uni-directional, off-axis CPW-fed, matched by unbalanced fork-stub, UWB ring slot antenna printed on single layer PCB with back plane," in *IEEE Antennas Propagat. Symp. Dig.*, San Diego, CA, July 2008.

[22] D. P. Tran, F. M. Tanyer-Tigrek, I. E. Lager, and L. P. Ligthart, "A novel unidirectional radiator with superb UWB characteristics for X-band phased array applications," in *Proc.* $3^{rd}$ *European Conference on Antennas and Propagation – EuCAP*, pp. 1617–1621, Berlin, Germany, March 2009.

# Reconfigurability, new materials: future challenges for antenna design and simulation

**Anja K. Skrivervik**[†], **Julien Perruisseau-Carrier**[‡], **Frédéric Bongard**[*] and **Juan R. Mosig**[†]
[†]*Laboratoire d'Electromagnétisme et d'Acoustique, Ecole Polytechnique Fédérale de Lausanne, CH-1015 Lausanne, Switzerland (anja.skrivervik@epfl.ch),*
[‡]*Centre Tecnòlogic de Telecomunicacions de Catalunya (CTTC), Barcelona, Spain,*
[*]*JAST Innovation in Antennas, PSE-C, CH-1015 Lausanne, Switzerland.*

**Abstract**

Re-configurability is one of the key features in modern wireless communications. Indeed, the increase of services provided imply an optimized management of the electromagnetic spectrum, along with strong miniaturization in order to allow for the cohabitation of all these services on small handheld devices. Reconfigurable antennas are one possible answer to these challenges. In this paper, we will present designs of reconfigurable antennas and feeding networks using recent technologies, namely MEMS (Micro Electro Mechanical Systems) and Metamaterials.

## 1 Introduction

The electromagnetic spectrum available for wireless communication is becoming more and more saturated, as new services in the field of wireless communications [1], military communication systems [2], space communication platforms, collision avoidance systems [3, 4] and others emerge. This trend sets an increasing challenge on antenna engineers: on one hand, the number of services having to cohabite in a small volume increases rapidly, while the spectrum is not unlimited. A possible solution to the challenges due to this increase of demands is reconfigurability: only one antenna will be used for all the applications, its characteristics being modified according to the situation. Although multiband antennas can also be used to transmit several standard with a single antenna, advantages of reconfiguration are, among others, useful out-of-band rejection at the reconfigurable antenna level, and reconfigurable antennas can potentially be tuned to an indefinite number of operation frequencies (cognitive radio).

Antennas for Ubiquitous Radio Services in a Wireless Information Society
I.E. Lager and M. Simeoni (Eds.). 
doi:10.3233/978-1-60750-487-0-75

A consequence of this is that the gained space can be used either to optimize the antenna characteristics, or for other system elements. Another important advantage is that antenna future requirements can be taken into account during its design, allowing thus for a new life after the end of one service. This latter point is especially appealing in the field of satellite antennas. MEMS are useful and versatile devices to achieve antenna reconfigurability: they can be embedded directly into the radiating element itself, in order to activate different parts of it, or to change its resonance frequency, polarization and radiation patterns. But they can also be in the antenna matching network as switches or tunable capacitors and in the antenna feeding network of array antennas as tunable phase shifters or delay lines. This usefulness of MEMS has been demonstrated through the boom of publications on MEMS tunable antennas over the last years : we find frequency reconfigurable antennas [5–21], antennas with tunable radiation pattern [22–33], polarization reconfiguration [34–36] or combinations of all this. MEMS tunable elements are also good candidates for reconfigurable reflectarrays [37–42, 46] or for MIMO antennas [43–45].

In recent years, there has been a rapidly growing interest in engineered materials commonly called 'metamaterials'. Metamaterials (MTMs) are broadly defined as artificial composite materials specifically engineered to produce desired unusual electromagnetic properties not readily available in nature. Among the unusual properties MTMs can exhibit, the one that has retained most of the attention is negative refraction, which is achieved when both the permittivity and the permeability of a medium are negative. Such MTMs are referred to usually in the literature as left-handed media (LHM).

Most of the well demonstrated microwave applications of MTMs rely on the transmission line (TL) approach, which mostly results in 1D or 2D planar structures which can be conveniently analyzed, realized and measured [46, 47]. In principle, bulky 3D MTMs could be obtained by geometrical aggregation of 2D structures. In all cases, TL-based MTMs are ideally suited for integration and combination with MEMS, electronic chips and miniaturized devices (see for instance [46, 47]).

MTMs have produced very interesting concepts in the antenna field. The richness of their dispersion has been exploited for leaky-wave antennas with forward/backward scanning capabilities, miniaturization of resonant antennas, directivity and gain enhancement and multi-band behavior. Again, most of these concepts have been demonstrated with TL-based MTMs and in particular with the so-called balanced composite right/left-handed transmission line (CRLH TL) [46,47], for which a typical dispersion diagram is shown in Fig. 1.

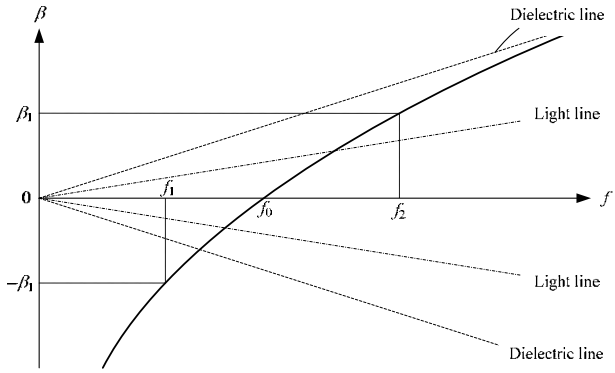


Figure 1: Typical dispersion diagram for a balanced CRLH TL.

Avoiding technicalities, it can be just said that the CRLH TL usually shows a large negative phase constant at low frequency. This leads to a small guided wavelength $\lambda_g = 2\pi/|\beta|$ which allows to obtain a given phase-shift with a smaller physical length and also to obtain a $\lambda_g/2$ field distribution over a physically small distance [50]. In both cases the antenna and its eventual beamforming network can be miniaturized.

In general, it can be said that the MTMs achieved improvements over conventional antennas are size reduction, dual/multi-band behavior, enhanced directivity and novel functionalities. Most of the well demonstrated antenna applications can be found in two distinct classes: leaky-wave antennas and resonant antennas.

*a. Leaky-wave antennas*

It is known that leaky-wave (LW) radiation occurs when the phase velocity of a wave propagating along an open structure exceeds the velocity of light (fast-wave propagation). As can be seen on the dispersion diagram of Fig. 1, the CRLH TL exhibits a fast-wave region around the transition frequency $f_0$, where $\beta$ remains between the two light lines. As a result, a simple open CRLH TL can be used as a leaky-wave antenna (LWA) in this frequency range [46, 47].

The most interesting particularity of these antennas is that they can radiate in the forward ($f > f_0$) and backward ($f < f_0$) directions with continuous scanning through broadside (at $f_0$). In contrast, conventional LWAs can radiate forward or backward, depending on the mode used, but they do not allow broadside radiation. Moreover, it is noticeable that CRLH TL LWAs radiate in their dominant mode, thereby not requiring any special feeding system as is the case for conventional LWAs using higher order radiating modes.

Improved versions of these antennas have been subsequently proposed. For instance, varactors have been included in each cell of the CRLH TL to achieve beam-scanning and tunable beamwidth at a fixed frequency [51, 52]. Obviously, MEMS could be used in similar applications.

*b. Resonant antennas*

As mentioned, miniaturized resonant antennas can be obtained by making use of the large negative phase constant $\beta$ that can be achieved at low frequency [53]. This principle has also been applied to dipole antennas [54].

The CRLH TL also allows obtaining low values of $|\beta|$ (positive or negative), hence large values of $\lambda_g$, which can be used for the design of enlarged half-wavelength resonant antennas with enhanced gain due to larger radiation aperture. A CRLH TL at the transition frequency $f_0$ (infinite wavelength) acts a zero order resonator, whose resonant frequency does not depend on its total size. Using this principle, zero order resonant antennas have been proposed [50]. These structures can be made much smaller than conventional $\lambda/2$ patch antennas. Ring antennas obtained by wrapping around the two ends of a CRLH TL have been proposed. The miniaturized square ring antenna of [56] uses the $\beta = 0$ point, whereas the circular ring antenna of [57] is operated in the two first right-handed/left-handed resonant modes (perimeter $= \lambda$). This antenna can be fed at different points to achieve circular polarization.

CRLH phase shifting lines can also be advantageously used in series-fed antenna arrays. They allow for size reduction of the feed network and reduction of the beam squinting with frequency, as explained in [58]. A recent review on leaky-wave and resonant antennas based on the CRLH TL can be found in [59].

This paper presents recent advances in our laboratory in the fields of reconfigurable antennas and antennas using MTMs. Section 2 is devoted to the presentation of MEMS based reconfigurable antennas, while Section 3 presents results on MTMs and MTM based antennas. Some final conclusions are raised in Section 4.

## 2 MEMS based reconfigurability

Reconfigurability in an antenna can be provided by two different strategies [60]: The device providing reconfigurability can be placed either in the

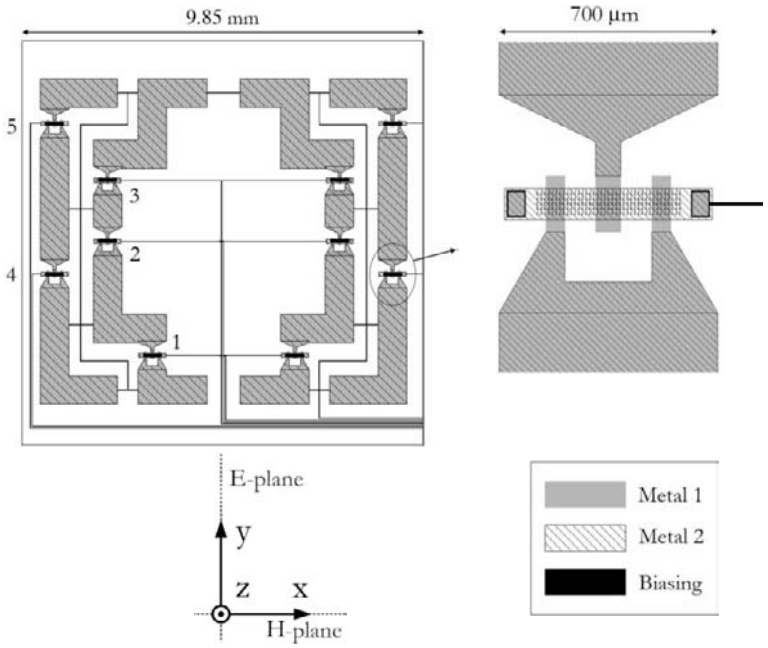


Figure 2: Illustrative for the principle of a MEMS tunable reflectarray cell, with a zoom in on the MEMS bridge.

antenna feeding circuit or in the radiating aperture itself. Obvious antenna application are steerable phased arrays and multiband antennas, while polarization, and frequency reconfigurability can be achieved working in the radiation aperture or on the feeding network. In this section we will first present an example of MEMS reconfigurable reflectarray elements, where the tunable MEMS element are located on the element itself [63–65]. We will then show an example on a MEMS controlled true time delay line (TTDL), as it could be used, for instance, in steerable phased arrays.

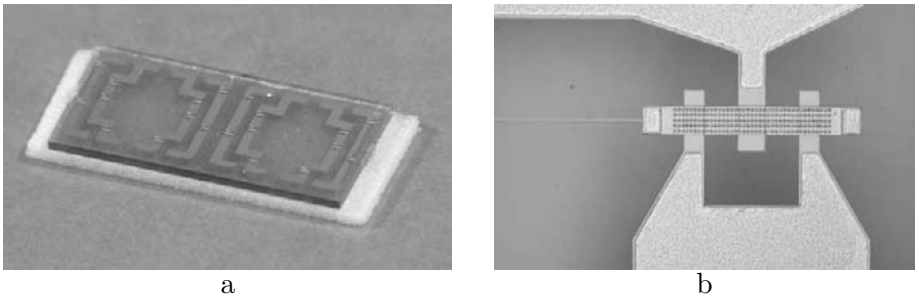

a b

Figure 3: Photograph of the reflectarray cells fabricated by VTT-Finland. (a) A reflectarray cell; (b) zoom in on the MEMS bridge.

An example of a MEMS tunable reflectarray element is depicted in Fig. 2. It represents the layout of a reflectarray cell, consisting of two concentric printed loop antennas, interrupted by MEMS switches acting as series capacitors. The phase of the cell's reflection coefficient is varied by actuating the proper MEMS. A photograph of the physical device is shown in Fig. 3, and the resulting reflection coefficient phase versus MEMS state is depicted in Fig. 4. The cells were fabricated by VTT-Finland.

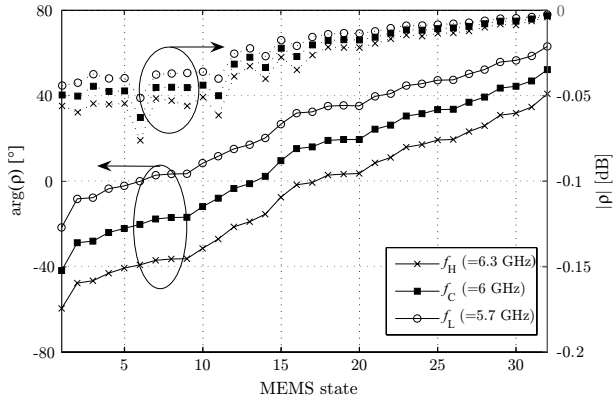


Figure 4: Phase of the cell's reflection coefficient versus the MEMS' states.

Beside the design of MEMS reconfigurable antennas, EPFL-LEMA has been active in the design of tunable microwave and millimeter wave circuits using distributed MEMS. Typical designs are tunable TTDLs [68] and artificial TLs [67]. A large emphasis has also been put on the theoretical background and the efficient design of such periodically loaded structures [68, 69]. The principle of a MEMS tunable TTDLs is shown in Fig. 5: it

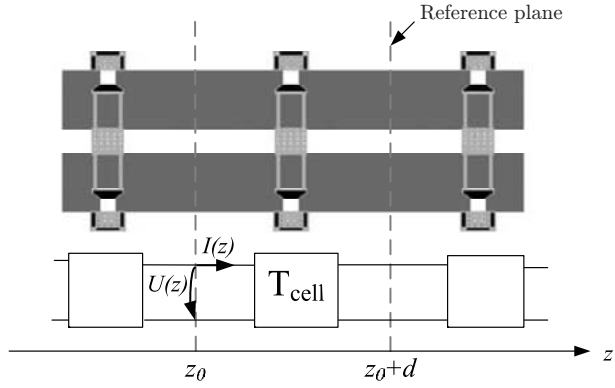


Figure 5: Illustrative for the principle of a distributed TTDL.

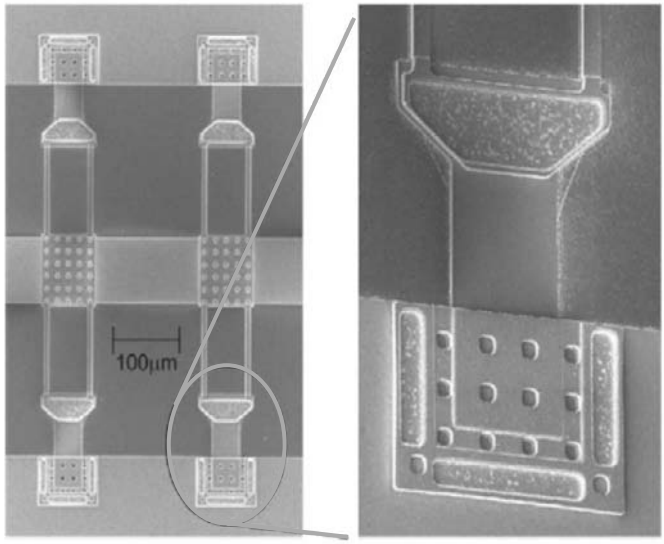


Figure 6: Detail of the realized TTDL. (a) General view; (b) zoom in on a MEMS capacitor.

consists of a TL (in this case a coplanar waveguide) which is periodically loaded with MEMS capacitors.

A SEM image of a part of the realized line is shown in Fig. 6, and the measured differential delay between the up and down states in Fig. 7.

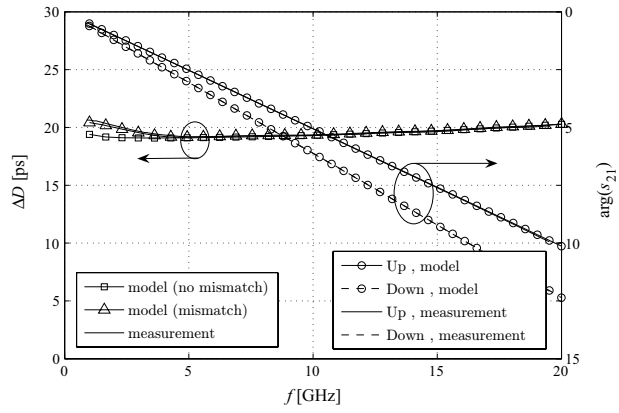


Figure 7: Predicted and measured differential delay.

# 3 MTMs and MTM based antennas

## 3.1 One dimensional MTMs

As mentioned in the introduction, one interesting family of one dimensional MTM is made of the so called CRLH TL. These lines consist of ordinary TLs (usually printed circuits) which are periodically loaded by series capacitors and parallel inductors. EPFL-LEMA has extensively studied these structures [67-75]. The equivalent circuit of a unit cell of such a line is depicted in Fig. 8.

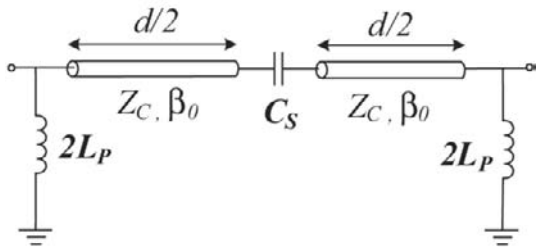


Figure 8: The equivalent circuit for the unit cell of a CRLH TL.

A straightforward calculation of the Bloch (omega-beta) diagram of this type of structure shows usable lower and upper frequency bands, where the circuits exhibits, respectively, left-handed and right-handed behavior, separated by a transition band,as depicted in Fig. 9.

A typical realization of such a structure in a CPW host TL is shown in Fig. 10. Such devices allow the realization of very compact phase shifters.

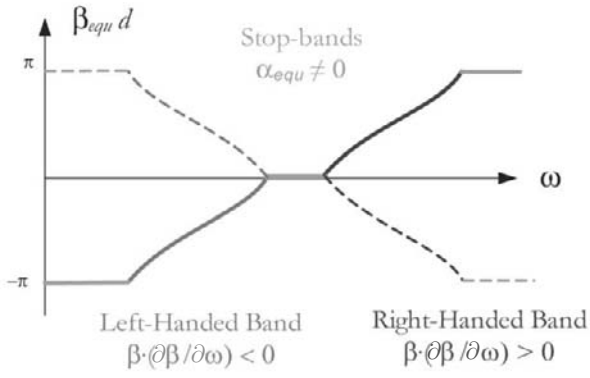


Figure 9: The Bloch diagram of a CRLH TL.

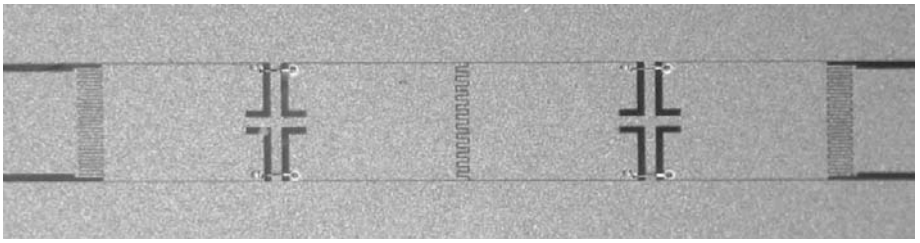

Figure 10: Example of a fabricated CRLH TL.

The next logical step is a combination of MEMS and metamaterial concepts to design and realize a MEMS tunable CRLH TLs. The final device and its equivalent circuit are shown in Fig. 11 [61,62].

It consists of a coplanar waveguide (CPW) TL (which is of course right-handed) periodically loaded with series capacitors and parallel inductors. This periodical loading will artificially induce a left-handed behavior. The frequency band of this left-handed behavior is tuned by changing the value of the series capacitors, made of MEMS bridges.

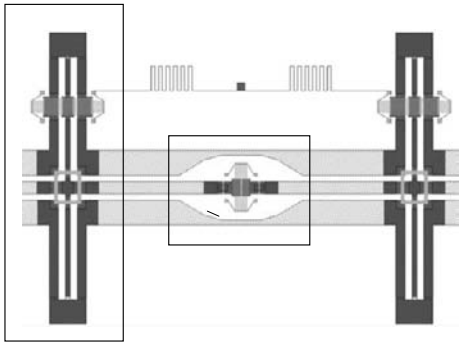

a

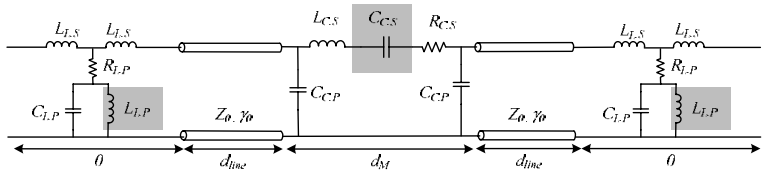


b

Figure 11: Illustrative for a MEMS tunable CRLH TL elementary cell. (a) General view; (b) equivalent circuit.

### 3.2 CRLH TL based on a lattice network unit cell

A brand-new promising idea in the area of 1D-MTMs, recently developed by EPFL-LEMA, is to use a unit cell under the form of a lattice network, i.e. a circuit with crossed diagonal arms [72–74]. This novel CRLH TL, referred to as 'type X', exhibits the following advantages over its conventional counterpart:

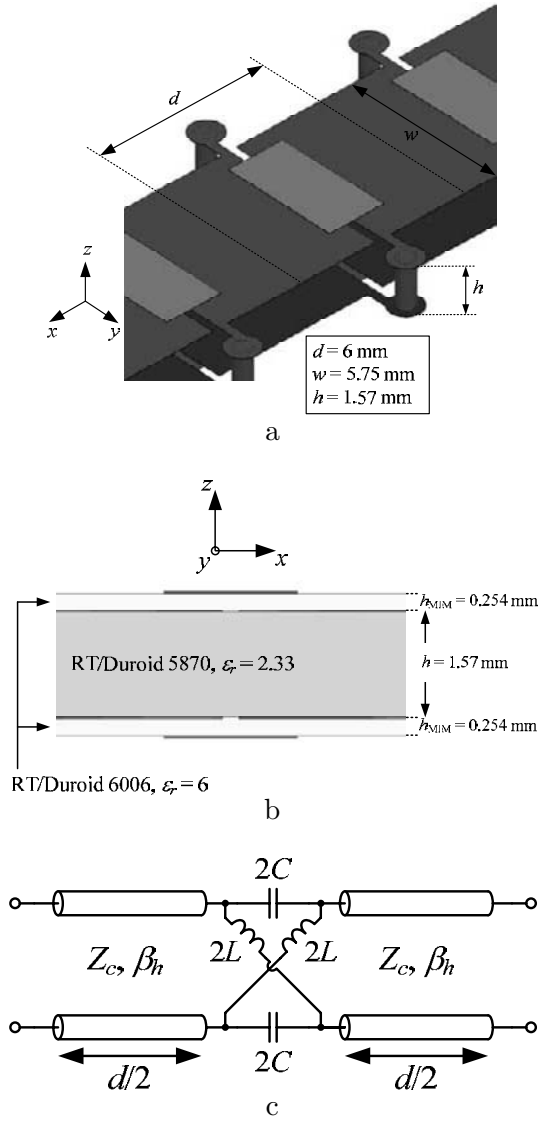


Figure 12: Example of CRLH TL implementation in parallel stripline technology [73]. (a) General view; (b) transverse cross-section; (c) equivalent circuit.

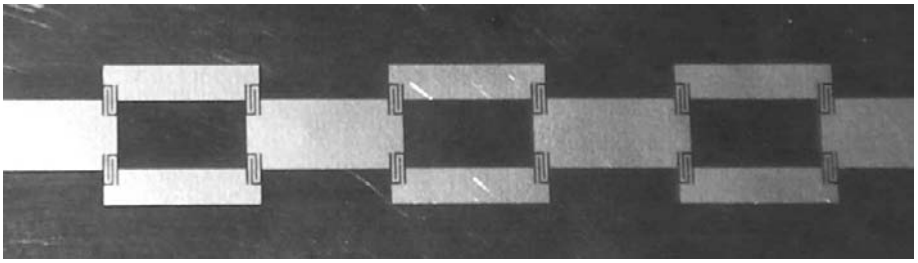

Figure 13: Picture of the type X CRLH TL realized in CPW-like technology.

- All-pass behavior (no stop-bands below the LH band and above the RH band). As a result, the LH band extends down to DC;
- Frequency-independent Bloch impedance;
- Larger group velocity, hence a reduced frequency variation of the phase response.

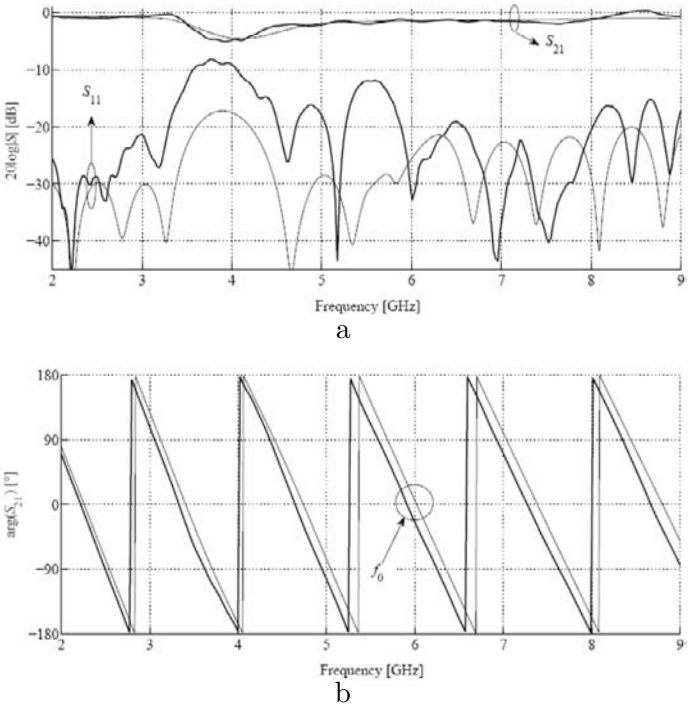


Figure 14: Measured (thick line) and simulated (thin line) frequency dependence of the S parameters of the 10-cell type X CRLH TL shown in Fig. 13. (a) Magnitude plot of the $S_{11}$ and $S_{21}$ parameters; (b) phase plot of the $S_{21}$ parameter (the phase of $S_{11}$ is skipped for clarity).

The concept has been successfully implemented in both parallel stripline and CPW-like technologies (Figs. 12 and 13). As shown in Fig. 14, prototypes following these preliminary concepts show a reasonable agreement between theoretical predictions and measurements in a large frequency band (2–9 GHz). Further improvements both at the technological and at modeling levels are under way.

An alternate implementation of this X CRLH TL design in a silicon based micromachined CPW with finite width ground planes is shown in Fig. 15 [74].

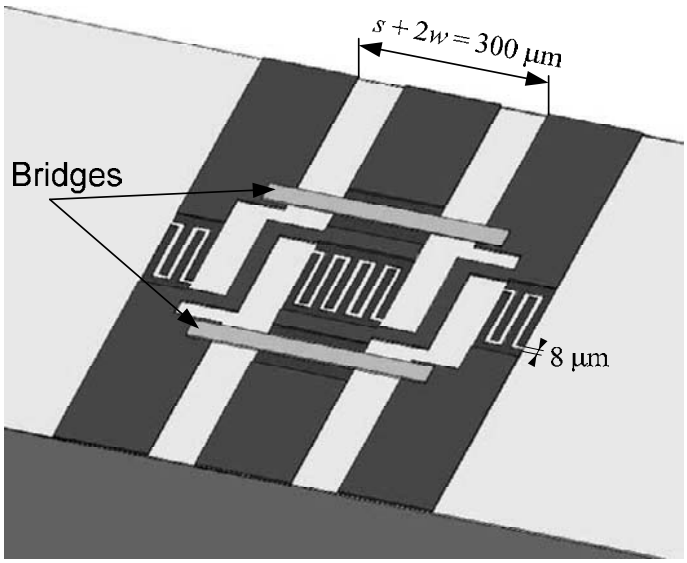


Figure 15: Unit cell of the proposed type X CRLH TL in micromachined CPW with finite width ground planes. The substrate is Silicon, $h = 525\,\mu$m, $\varepsilon_r = 11.9$, covered by a thinn layer of $SiO_2, h = 0.5\,\mu$m, $\varepsilon_r = 3.9$. There are three metallization layers: Metal 1 (Pt), $h = 0.4\,\mu$m, Metal 2 (Al), $h = 3\,\mu$m, and Metal 3 (Al), $h = 3\,\mu$m.

As we use a single shunt inductance in each slot of the CPW, bridges are needed to connect the two ground planes in order to minimize the excitation of the parasitic odd CPW mode. The structure has been designed to be balanced with a transition frequency $f_0 = 17.5$ GHz. The possible reconfiguration of this structure using MicroElectroMechanical Systems (MEMS) technology is a very interesting prospect.

Figure 16 shows a possible implementation of a X- CRLH-TL reconfigurable by means of MicroElectroMechanical system (MEMS). The system should provide 2-bit digital control with minimum loss at high frequencies while taking advantage of the all-pass X cell behaviour [75].

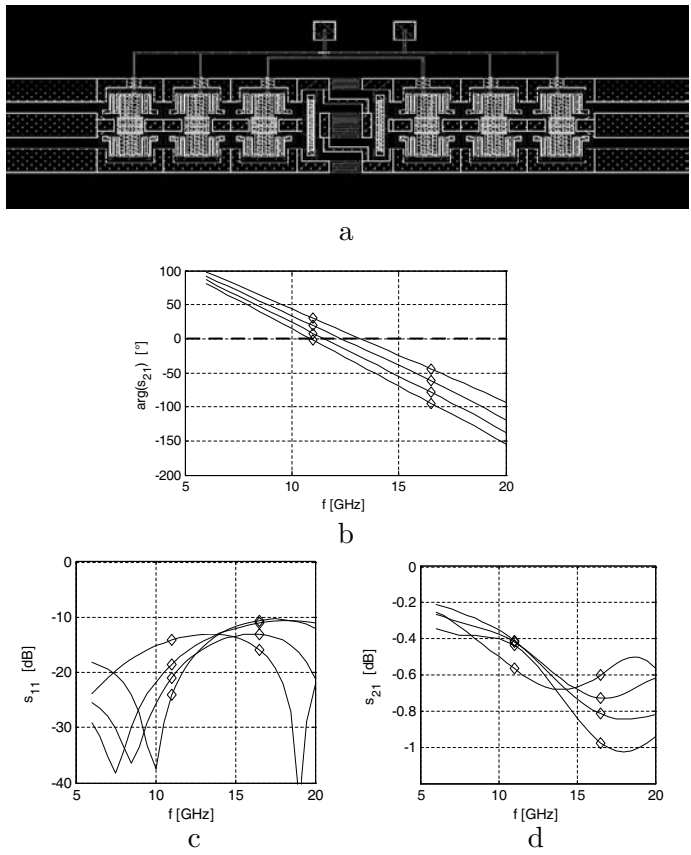


Figure 16: Explicative for the two-bits MTM/MEMS reconfigurable phase-shifter. (a) General view; (b) frequency dependence of the phase for the 4 states; (c) matching dependence of the phase for the 4 states; (d) insertion loss dependence of the phase for the 4 states.

The novel type X unit cell can be potentially used to improve the performances of most of the reported CRLH TL applications, provided that it is possible to implement the required series capacitances in both conductors of the host TL used. If these capacitances can be MEMS-controlled the promise of reconfigurable antennas is very appealing. Two well-demonstrated CRLH TL antenna systems – the leaky-wave antenna [46, 47] and the series-fed array [76] – could benefit from this device.

### 3.3 Three-D MTMs for planar antennas

In addition to the planar MTMs previously discussed, we have assessed the ability of certain types of 3D (or bulky) MTMs to behave as a material

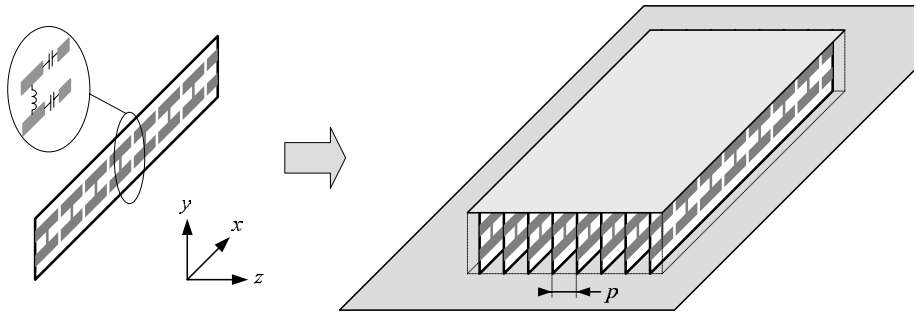


Figure 17: Volumetric layered TL-based MTM obtained by stacking 1D planar CRLH TLs implemented in CPS technology. The structure can be used as a substrate for microstrip patch antennas.

filling with exotic properties when used as a substrate for microstrip patch antennas. The richness of the dispersion curve of such MTM can lead to miniaturization or multi-frequency capabilities.

The retained solution is based on a recently proposed topology of volumetric MTMs based on the TL approach [77]. These structures are obtained by layering several planar TL-based MTMs on top of each other. The idea is to take benefit of the non-resonant nature of planar TL-based MTMs to realize volumetric structures (meta-slabs). A possible implementation of such a structure is shown in Fig. 17. It consists of a stacking of 1D CRLH TLs implemented in a coplanar stripline (CPS) host TL [78].

Figures 18 and 19 show two practical realisations of microstrip antennas involving such a meta-substrate [78]. In them, a conventional slot-fed patch

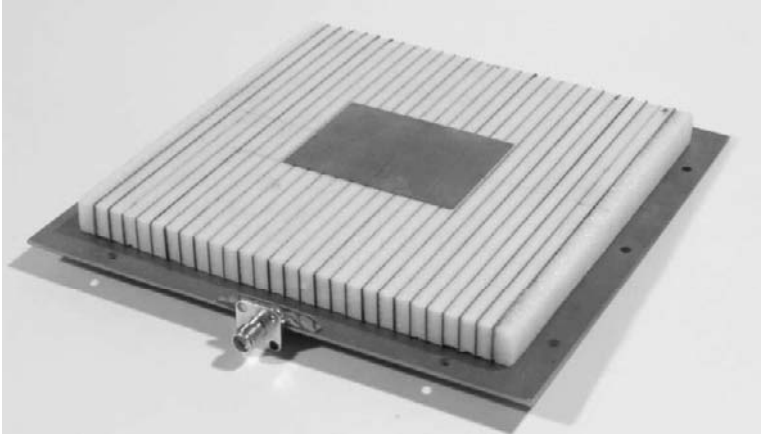

Figure 18: Aperture coupled meta-patch antenna using a full-size meta-slab.

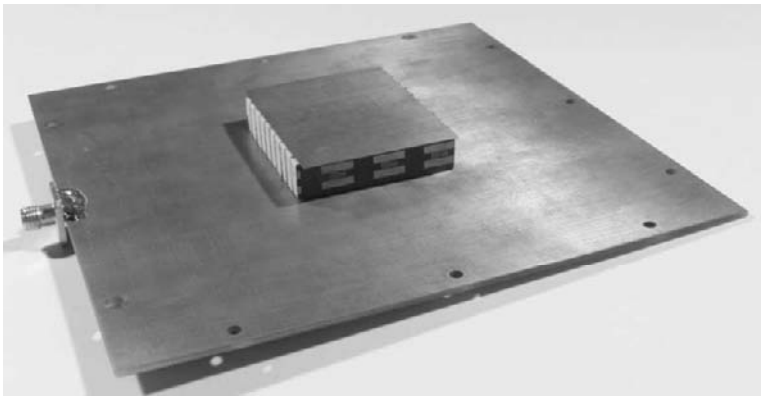

Figure 19: Aperture coupled meta-patch antenna using a reduced meta-slab.

resides of a meta-slab whose transverse dimensions are larger or identical to the patch dimensions.

The initial research consists in matching the dispersion diagram of the 3D MTM with the antenna observed resonances. This is not an easy task as witnessed by the complex behavior of the input impedance (Fig. 20). However it is clear that, when compared with the result for a patch on a traditional substrate, the lower resonant mode is reduced (potential miniaturization) and many new resonances appear. The problem is that the intrinsic modes of the MTM slab are modified by the patch itself and can couple strongly to

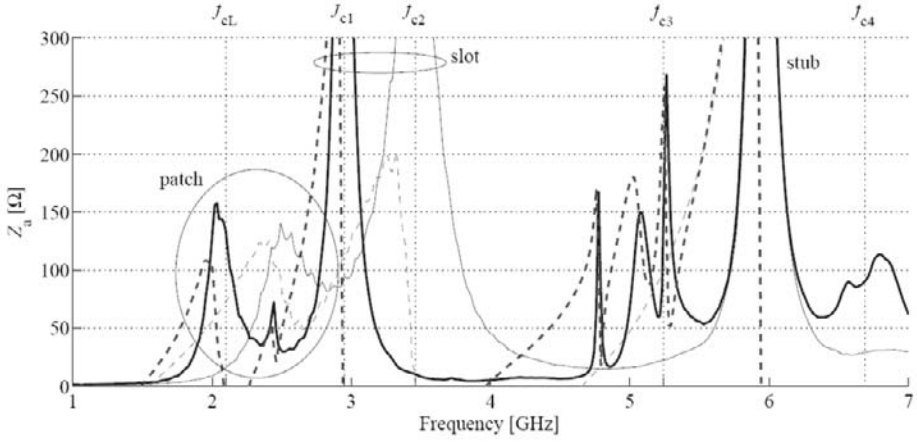


Figure 20: Measured input impedance of the antenna shown in Fig. 19. Thin line: same antenna with a foam substrate in place of the meta-slab. Continuous line: real part; dashed line: imaginary part.

patch resonances. This coupling must be further understood and controlled before resulting in practical applications.

## 4 Conclusions

This paper has surveyed two recent technologies, MEMS and electromagnetic metamaterials, aimed at facilitating one of the most sought-after functionalities in the antenna domain: reconfigurability. The paper concentrates in the most outstanding developments in our laboratory, EPFL-LEMA. These are far from being unique, as most research groups in the world exhibit nowadays some activities in these areas. They are intended to be considered just as representative examples, witnessing the potential power of these new technologies. The domain of applications is particularly enhanced and enlarged when a combination of both technologies is considered. Indeed, some type of metamaterials, like the one-dimensional composite right-left handed transmission lines, are particularly well suited for integration with MEMS and exciting applications are currently blossoming [79]. Despite these successes, these new areas are far from being mature. Additional theoretical research is still needed to understand and fully harness some encountered complex phenomena, like the modal coupling in three-dimensional metamaterial-based antennas, as evidenced in the previous section of this paper.

## Bibliography

[1] J. T. Aberle, F. Zavosha, and D. T. Auckland, *E-tenna Corp.*, Del Mar, Calif., EE Times Dec 5, 2001 (9:03 AM) URL: http://www.commsdesign.com/story/OEG20011205S0052

[2] L. Corey, "Phased Array Development at DARPA", *IEEE Int. Symp. On Phased Array Systems and Technology*, Boston, 2003.

[3] J. Schobel, T. Buck, M. Reimann, M. Ulm, M. Schneider, "W-band RF-MEMS subsystems for smart antennas in automotive radar sensors," in *Proc.* 34$^{\text{th}}$ *Eur. Microwave Conf.*, Amsterdam, The Netherlands, Oct. 12–14, 2004, pp. 1305–1308.

[4] D. Sievenpiper, H. J. Song, H. P. Hsu, G. Tangonan, R. Y. Loo, J. Schaffner, "MEMS-based switched diversity antenna at 2.3 GHz for automotive applications", 5$^{\text{th}}$ *Int. Symp. Wireless Personal Multimedia Communications*, Vol. 2, pp. 762–765, October 2002.

[5] D. E. Anagnostou, G. Zheng, M. T. Chryssomallis, J. C. Lyke, G. E. Ponchak, J. Papapolymerou, and C. G. Christodoulou, "Design, fabrication, and mea-

surements of an RF-MEMS-based self-similar reconfigurable antenna," *IEEE Trans. Antennas Propag.*, Vol. 54, pp. 422–432, Feb. 2006.

[6] P. Panaïa, C. Luxey, G. Jacquemod, R. Staraj, G. Kossiavas, L. Dussopt, F. Vacherand, and C. Billard, "MEMS-based reconfigurable antennas," in *IEEE Int. Symp. on Industrial Electronics*, 2004, Vol. 1, pp. 175–179.

[7] L. M. Feldner , C. D. Nordquist and C. G. Christodoulou, "RF MEMS reconfigurable patch antenna", in *Proc. of Antennas and Propagat. Soc. Int. Symp.*, 2005, Vol. 2A, 3–8 July 2005, pp. 338–391.

[8] C. Zhang, S. Yang, H. K. Pan, A. E. Fathy, S. El-Ghazaly, and V. K. Nair, "Development of reconfigurable mini-nested patches antennas for universal wireless receivers using MEMS," in *Proc. of IEEE AP-S Int. Symp. USNC/URSI*, Albuquerque, NM 2006.

[9] E. Erdil, K. Topalli, M. Unlu, O. A. Civi, and T. Akin, "Frequency tunable microstrip patch antenna using RF MEMS technology," *IEEE Trans. Antennas Propag.*, Vol. 55, no. 4, pp. 1193–1196, Apr. 2007.

[10] S. Onat, L. Alatan, S. Demir, "Design and Implementation of a Triple-Band Re-Configurable Microstrip Antenna," in *Proc. of the* $9^{\text{th}}$ *European Conference on Wireless Technology*, pp. 326–329, Sept. 2006.

[11] Z. Yijun; Z. Shouzheng, "Slot antenna with MEMS switches and fractals," *Microwave Conference Proceedings, 2005. APMC 2005. Asia-Pacific Conference Proceedings*, Vol. 1, Dec. 2005.

[12] B. Manimegalai, V. Periyasamy, L. Vishwanathan, S. Raju, V. Abhaikumar, "A novel MEMS based fractal antenna for multiband wireless applications," *Microwave Conference Proceedings, 2005. APMC 2005. Asia-Pacific Conference Proceedings*, Vol. 2, Dec. 2005.

[13] C. Shafai, L. Shafai, R. Al-Dahleh, D. D. Chrusch , S. K. Sharma, "Reconfigurable Ground Plane Membranes for Analog/Digital Microstrip Phase Shifters and Frequency Agile Antenna," *2005 International Conference on MEMS,NANO and Smart Systems, ICMENS*, pp. 287–290, 2005.

[14] S. Liu, M.-J. Lee, C. Jung, G.-P. Li, F. De Flaviis, "A frequency reconfigurable circularly polarized patch antenna by integrating MEMS switches," in *Proc. AP-S Int. Symposium 2005*, Washington, DC, 3–8 July 2005, Vol. 2A, pp. 413–416.

[15] M. Mowler, B. Lindmark, J. Oberhammer, G. Stemme, "A 2-bit reconfigurable meander slot antenna with RF-MEMS switches," *Antennas and Propagation Society International Symposium, 2005 IEEE*, Vol. 2A, pp. 396–399, 3–8 July 2005.

[16] O. Kivekäs, J. Ollikainen, and P. Vainikainen, "Frequency-tunable internal antenna for mobile phones," in *Proc. 12th Int. Symp. on Antennas (JINA)*, Nov. 2002, Vol. 2, pp. 53–56.

[17] J-M. Laheurte, "A switchable CPW-fed slot antenna for multifrequency operation," *Electronics letters*, 2001, Vol. 37, pp. 1498–1500.

[18] C. Luxey , D. Dussopt, J. Le Sonn, J. Laheurte, "Dual frequency operation of a CPWfed antenna controlled by PIN diodes," *Electronics letters*, 2000, Vol. 36, pp. 2–3.

[19] S. Pioch, N. Adellan, J. M. Laheurte, P. Blondy, A. Pothier, "Integration of MEMS in Frequency-Tuneable Cavity-Backed Slot Antennas," in *Proc. 12th Int. Symp. on Antennas (JINA)*, Nice, Nov. 2002.

[20] W. H. Weedon, W. J. Payne, G. M. Rebeiz, J. S. Herd and M. Champion, "MEMS-switched reconfigurable multi-band antenna: design and modeling," in *Proc. of the 1999 Antenna Applications Symposium*, Monticello, IL, Sept. 15–17, 1999.

[21] D. Anagnostou, M. T. Chryssomallis, J. C. Lyke, C. G. Christodoulou, "Reconfigurable Sierpinski gasket antenna using RF-MEMS switches", in *Proc. Antennas and Propagation Society International Symposium, 2003*, Vol. 1, 22–27 June 2003.

[22] A. Hajimiri, A. Komijani, A. Natarajan, R. Chunara, X. Guan, and H. Hashemi, "Phased Array Systems in Silicon," *IEEE Communications Magazine*, Vol. 42, pp. 122–130, August 2004.

[23] H. Sagkol, K. Topalli, M. Unlu, O. A. Civi, S. Koc, S. Demir, T. Akin, "A monolithic phased array with RF MEMS technology," in *Proc. Antennas and Propagation Society International Symposium, 2002*, Vol. 4, 16–21 June 2002.

[24] K. F. Sabet, L. P. B. Katehi, K. Sarabandi, "Modeling and design of mems-based reconfligurable antenna arrays," in *Proc. Aerospace Conference, 2003*, Vol. 2, March 8–15, 2003.

[25] J. H. Schaffner, D. F. Sievenpiper, R. Y. Loo, J. J. Lee, S. W. Livingston, "A wideband beam switching antenna using RF MEMS switches," in *Proc. Antennas and Propagation Society International Symposium, 2001*, Vol. 3, 8–13 July 2001.

[26] J.-C. Chiao, Y. Fu, I. M. Chio, M. DeLisio, L.-Y. Lin, "MEMS reconfigurable Vee antenna," in *Proc. Int. Microwave Symp., 1999 IEEE MTT-S*, Vol. 4, 13–19 June 1999, pp. 1515–1518.

[27] G. H. Huff, J. T. Bernhard, "Integration of packaged RF MEMS switches with radiation pattern reconfigurable square spiral microstrip antenna," *IEEE Trans. on Antennas and Propagat.*, Vol. 54, No. 2, Feb. 2006, pp. 464–469.

[28] C. W. Jung, F. De Flaviis, "RF-MEMS capacitive series switches of CPW and MSL configurations for reconfigurable antenna application," in *Proc. IEEE Antennas and Propagat. Soc. Int. Sym. 2005*, Vol. 2A, 3–8 July 2005.

[29] C. W. Jung, M.-J. Lee, G. P. Li, F. De Flaviis, "Reconfigurable scan-beam single-arm spiral antenna integrated with RF-MEMS switches," *IEEE Trans. on Antennas and Propagat.*, Vol. 54, No. 2, Feb. 2006, pp. 455–463.

[30] W. Guoan, T. Polley, A. Hunt, J. Papapolymerou, "A high performance tuneable RF MEMS switch using barium strontium titanate (BST) dielectrics for reconfigurable antennas and phased arrays," *IEEE Antennas and Wireless Propagation Letters*, Vol. 4, 2005.

[31] L. Petit, L. Dussopt, J.-M. Laheurte, "MEMS-Switched Parasitic-Antenna Array for Radiation Pattern Diversity," *IEEE Trans. on Antennas and Propagat.*, Vol. 54, No. 9, Sept. 2006, pp. 2624–2631.

[32] X. Guo, Z. Lai, M. Cai, J. Chen, "Fitting SOC miniature MEMS reconfigurable antenna," 6th *International Conference on ASIC, ASICON 2005*, Vol. 2, 24–27 Oct. 2005.

[33] X.-S. Yang, B.-Z. Wang, Y. Zhang, "A reconfigurable Hilbert curve patch antenna," in *Proc. IEEE Antennas and Propagat. Soc. Int. Symp. 2005*, Vol. 2B, 3–8 July 2005.

[34] L. Le Garrec, I. Roch-Jeune, M. Himdi, R. Sauleau, O. Millet, L. Buchaillot, "Microactuators and microstrip antenna for polarization diversity," in *Proc.* 5th *Workshop on MEMS for millimeterWAVE communications (MEMSWAVE)*, Uppsala (Sweden), 30 June–2 July 2004.

[35] R. N. Simons, C. Donghoon, L. P. B Katehi, "Polarization reconfigurable patch antenna using microelectromechanical systems (MEMS) actuators," in*Proc. IEEE Antennas and Propagat. Society Int. Symp., 2002*, Vol. 2, 16–21 June 2002.

[36] R. N. Simons, C. Donghoon, L. P. B Katehi, "Microelectromechanical systems (MEMS) actuators for antenna reconfigurability," in *Proc. IEEE International Microwave Symposium (MTT-S) Digest, 2001*, Vol. 1, 20–25 May 2001.

[37] H. Legay, B. Pinte, M. Charrier, A. Ziaei, E. Girard, R. Gillard, "A steerable reflectarray antenna with MEMS controls," in *Proc. IEEE Int. Symp. on Phased Array Systems and Technology, 2003*, 14–17 Oct. 2003.

[38] J. M. Zendejas, J. P. Gianvittorio, and Y. Rahmat-Samii, "Magnetic MEMS reconfigurable frequency-selective surfaces," *J. Microelectromech. Syst.*, Vol. 15, No. 3, pp. 613–623, Jun. 2006.

[39] J. P. Gianvittorio and Y. Rahmat-Samii, "Reconfigurable patch antennas for steerable reflectarray applications," *IEEE Trans. Antennas Propag.*, Vol. 54, pp. 1388–1392, May 2006.

[40] J. Perruisseau, H. Legay, J. Lenkkeri, J.-P. Polizzi, E. Jung, A. K. Skrivervik, "Design and realization of a MEMS Tuned Reflectarray," *MEMSWAVE 2007.*

[41] S. V. Hum, G. McFeetors, M. Okoniewski, "Integrated MEMS Reflectarray Elements," in *Proc. of The European Conference on Antennas and Propagation: EuCAP 2006*, 6–10 November 2006, Nice, France.

[42] O. Bayraktar, K. Topalli, M. Unlu, et al., "Reconfigurable Reflectarray Using RF MEMS Technology," in *Proc. of The European Conference on Antennas and Propagation: EuCAP 2006*, 6–10 November 2006, Nice, France.

[43] S. Avrillon, A. Pothier, L. Mercier and P. Blondy, "A Novel Reflectarray using Integrated Band Reject," in *Proc. of* 35th *European Microwave Week*, Paris, Oct 2005.

[44] B.A. Cetiner, H. Jafarkhani, Q. Jiang-Yuan, H. J. Yoo, A. Grau, F. De Flaviis, "Multifunctional reconfigurable MEMS integrated antennas for adaptive MIMO systems," *IEEE Communications Magazine*, Volu. 42, No. 12, Dec. 2004, pp. 62–70.

[45] B. A. Cetiner, E. Akay, E. Sengul, E. Ayanoglu, "A MIMO System with Multifunctional Reconfigurable Antennas," *IEEE Antennas and Wireless Propagation Letters*, Vol. 5, No. 1, Dec. 2006.

[46] C. Caloz and T. Itoh, *Electromagnetic Metamaterials: Transmission Line Theory and Microwave Applications*: Wiley-Interscience and IEEE press, 2006.

[47] G. V. Eleftheriades and K. G. Balmain, *Negative-Refraction Metamaterials: Fundamental Principles and Applications*: Wiley-Interscience and IEEE press, 2005.

[48] C. Caloz and T. Itoh, "Transmission Line Approach of Left-Handed (LH) Materials and Microstrip Implementation of an Artificial LH Transmission Line," *IEEE Transactions on Antennas and Propagation*, Vol. 52, pp. 1159–1166, May 2004.

[49] A. Sanada, C. Caloz, and T. Itoh, "Planar Distributed Structures With Negative Refractive Index," *IEEE Transactions on Microwave Theory and Techniques*, Vol. 52, pp. 1252–1263, April 2004.

[50] A. Lai, C. Caloz, and T. Itoh, "Composite Right/Left-Handed Transmission Line Metamaterials," *IEEE Microwave Magazine*, 2004, pp. 34–50.

[51] S. Lim, C. Caloz, and T. Itoh, "Electronically Scanned Composite Right/Left Handed Microstrip Leaky-Wave Antenna," *IEEE Microwave and Wireless Components Letters*, Vol. 14, pp. 277–279, June 2004.

[52] S. Lim, C. Caloz, and T. Itoh, "Metamaterials-Based Electronically Controlled Transmission-Line Structure as a Novel Leaky-Wave Antenna With Tunable Radiation Angle and Beamwidth," IEEE Transactions on Microwave Theory and Techniques, vol. 52, pp. 2678-2690, December 2004.

[53] C. J. Lee, K. M. K. H. Leong, and T. Itoh, "Design of Resonant Small Antenna Using Composite Right/Left-Handed Transmission Line," in *Proc. IEEE Antennas and Propagation Int. Symp. (AP-S) and USNC/URSI Meeting*, Washington, DC, 2005.

[54] H. Iizuka and P. S. Hall, "Left-Handed Dipole Antennas and Their Implementations," *IEEE Transactions on Antennas and Propagation*, Vol. 55, pp. 1246–1253, May 2007.

[55] A. Rennings, S. Otto, C. Caloz, and P. Waldow, "Enlarged Half-Wavelength Resonator Antenna With Enhanced Gain," in *Proc. IEEE Antennas and Propagation Int. Symp. (AP-S) and USNC/URSI Meeting*, Washington, DC, 2005, pp. 683–686.

[56] F. Qureshi, M. A. Antoniades, and G. V. Eleftheriades, "A Compact and Low-Profile Metamaterial Ring Antenna With Vertical Polarization," *IEEE Antennas and Wireless Propagation Letters*, Vol. 4, pp. 333–336, 2005.

[57] S. Otto, A. Rennings, C. Caloz, P. Waldow, and T. Itoh, "Composite Right/Left-Handed Lamda-Resonator Ring Antenna for Dual-Frequency Operation," in *Proc. IEEE Antennas and Propagation Int. Symp. (AP-S) and USNC/URSI Meeting*, Washington, DC, 2005, pp. 684–687.

[58] G. V. Eleftheriades, M. A. Antoniades, and F. Qureshi, "Antenna applications of negative-refractive-index transmission-line structures," *IET Microw. Antennas Propag.*, Vol. 1, pp. 12–22, February 2007.

[59] C. Caloz, T. Itoh, and A. Rennings, "CRLH Metamaterial Leaky-Wave and Resonant Antennas," *IEEE Antennas and Propagation Magazine*, Vol. 50, pp. 25–39, October 2008.

[60] A. K. Skrivervik, P. Crespo-Valero, "MEMS in antennas," *MEMSWAVE 2005 Conference*, Lausanne, June 23–24, 2005, pp. 25–30.

[61] J. Perruisseau-Carrier, T. Lisec, and A. K. Skrivervik, "Circuit Model and Design of Silicon-Integrated CRLH-TLs Analogically Controlled by MEMS," *Microw. and Optical Tech. Lett.*, Vol. 48, pp. 2496–2499, Dec 2006.

[62] J. Perruisseau-Carrier, T. Lisec, and A. K. Skrivervik, "Analog and Digital MEMS-Variable Composite Right/Left Handed Transmission Lines," in *Proc. 2006 ANTEM, International Symposium on Antenna Technology and Applied Electromagnetics and URSI/CNC Canadian Radio Sciences Conference*, Montréal, Canada, 2006.

[63] J. Perruisseau-Carrier, F. Bongard and A. K. Skrivervik, "Efficient Modeling and Design of Reconfigurable Reflecting Cells and Application to a MEMS-based Digital Implementation," *IEEE Trans. on Microwave Theory and Thechniques*, Dec 2008.

[64] J. Perruisseau-Carrier and A. K. Skrivervik, "Monolithic MEMS-Based Reflectarray Cell Digitally Reconfigurable Over a 360° Phase Range," *IEEE Antennas and Wireless Propagation Letters*, Vol. 7, pp. 138–141, 2008.

[65] J. Perruisseau-Carrier and A. K. Skrivervik, "A dynamically-controlled reflectarray element using embedded packaged MEMs switches," in *Proc. Antennas and Propagation Society International Symposium 2008*, 2008.

[66] J. Perruisseau-Carrier and A. K. Skrivervik, "Requirements and challenges in the design of high performance MEMS reconfigurable reflectarray cells," in *Proc.* 2nd *European Conference on Antennas and Propagation, EuCAP 2007*, Nov. 11–16 2007, Edinburg, UK.

[67] J. Perruisseau-Carrier, R. Fritschi, A. Skrivervik, "Controllable true-time delay line and left-handed transmission lines in MMIC technology," *Latsis Symposium 2005*, Lausanne, Switzerland, February 28–March 2 2005, p. 120.

[68] J. Perruisseau-Carrier, A. K. Skrivervik, "Tunable differential phase shifters using MEMS positive/negative phase velocity transmission lines," in *Proc. of URSI 2007, North American Radio Science Meeting URSI - CNC/USNC*, Ottawa, Canada, 2007.

[69] J. Perruisseau-Carrier, R. Fritschi, P. Crespo-Valero, A. K. Skrivervik, "Modeling of periodic distributed MEMS, application to the design of variable true-time delay lines," *IEEE Transactions on Microwave Theory and Techniques*, Vol. 54, No. 1, January 2006, pp. 383–392.

[70] J. Perruisseau-Carrier, A. K. Skrivervik, "A Bloch wave approach to the design of optimally matched non-effective medium composite right/left handed transmission lines," in *Proc. IET Microw., Antennas Propag.*, Vol. 1, No. 1, February 2007, pp. 50–55.

[71] J. Perruisseau-Carrier, A. K. Skrivervik, "Design of wideband high and low impedance meta-transmission lines," *Microwave and Optical Technology Letters*, Vol. 49, No. 8, August 2007, pp. 1926–1929.

[72] F. Bongard and J. R. Mosig, "A novel composite right/left-handed unit cell and potential antenna applications," in *Proc. IEEE Antennas and Propagation Int. Symp. (AP-S) and USNC/URSI Meeting*, San-Diego, CA, 2008, pp. 1–4.

[73] F. Bongard, J. Perruisseau-Carrier, and J. R. Mosig, "Enhanced CRLH Transmission Line Performances Using a Lattice Network Unit Cell," *IEEE Microwave and Wireless Components Letters*, Vol. 19, pp. 431–433, July 2009.

[74] F. Bongard, J. Perruisseau-Carrier and J. R. Mosig, "Enhanced periodic structure analysis based on a multiconductor transmission line model and application to metamaterials," *IEEE Transactions on Microwave Theory and Techniques*, Vol. 57, No. 11, pp. 2715–2726, 2009.

[75] J. Perruisseau-Carrier, F. Bongard, M. Fernndez-Bolaos, and J. R. Mosig, "Silicon-Integrated Fixed and Reconfigurable CRLH Unit Cells Based on the Lattice Topology," in *Proc. IEEE Antennas and Propagation Int. Symp. (AP-S) and USNC/URSI Meeting*, Charleston, SC, 2009.

[76] G. V. Eleftheriades, M. A. Antoniades, and F. Qureshi, "Antenna applications of negative-refractive-index transmission-line structures," *IET Microw. Antennas Propagat.*, Vol. 1, pp. 12–22, Feb. 2007.

[77] A. K. Iyer and G. V. Eleftheriades, "Volumetric layered transmission-line metamaterial exhibiting a negative refractive index," *Journal of the Optical Society of America B*, Vol. 23, pp. 553–570, March 2006.

[78] F. Bongard, J. R. Mosig, and M. Van der Vorst, "Investigations on volumetric layered transmission line metamaterials for antenna applications," in *Proc. European Conference on Antennas and Propagation (EuCAP)*, Edinburgh, UK, 2007.

[79] J. Perruisseau-Carrier, K. Topalli, and T. Akin, "Low-loss Ku-band Artificial Transmission Line with MEMS Tuning Capability," *IEEE Microw. Wireless Compon. Lett.*, Vol. 19, pp. 377–379, June 2009.

# Active arrays for satellite applications: the quest for increased power efficiency

**Cyril Mangenot**, **Giovanni Toso** and **Piero Angeletti**
*European Space Agency, Keplerlaan 1,*
*2200 AG, Noordwijk, the Netherlands (cyril.mangenot@esa.int)*

**Abstract**

Active array antennas have very attractive features but are quite complex and expensive. For this reason, they are today considered for space missions essentially when in flight beam reconfigurability or inertialess beam steering is required. However, array antennas may find wider applications in new potential LEO or MEO telecommunication constellations or as a way to generate very large space aperture thanks to digital processing. The paper presents an overview on the European ongoing activities on active phased arrays with a particular emphasis on the main limitations, challenges, possible improvements and opportunities.

## 1 Introduction

The topic of space antenna sub-systems is very wide due to the need to cover all types of applications including Earth Observation (EO), Telecommunications, Navigation, Science as well as Telecommand and Telemetry, manned spacecraft and user terminals. The optimization of performances such as end of coverage gain, polarization purity and beams isolation, mandatory for link budget and overall system capacity, strictly requires developing and maintaining in parallel several antenna technologies, concepts and architectures for the different operational frequencies, frequency bandwidths, radiating aperture diameters and scanning volume. This last parameter, which most often justifies the use of Active Arrays, widely changes with the applications and has a major impact on antenna concept selection. While for Synthetic Aperture Radar there is an agility need for $\pm 13$ degrees in elevation combined with no or limited scan in azimuth, for radiometry there is interest in $\pm 45$ to 60 degrees conical scan volume. Regarding Telecommunications, $\pm 9$ degrees is required from Geostationnary Orbit and $\pm 55$ degrees from Low Earth Orbit while user terminals request pointing toward the half hemisphere. Another domain such as Navigation asks for shaped isoflux beams over $\pm 13$ degrees from a Medium Earth Orbit. Such scan volumes

Antennas for Ubiquitous Radio Services in a Wireless Information Society
I.E. Lager and M. Simeoni (Eds.). 
doi:10.3233/978-1-60750-487-0-97

justify different array architectures and topologies optimization to minimize their complexity and cost.

This paper addresses the different array types that might be suitable to answer the very broad domain of application identified above and propose some way forward with high potential. The associated frequency domain extends from 400 MHz to 100 GHz.

## 2 Benefits/limitations of array antennas

Array antennas have intrinsic very attractive feature regarding beam flexibility but have not been extensively implemented until now for space applications. Array antennas benefit from space heritage mainly in the field of Synthetic Aperture Radar (SAR) such as ERS, Envisat, RADARSAT, for which one single beam with agility is required and where the pulsed mode reduces the constraints on power. It shall be noted that EO future instruments, such as the wide swath high-resolution radar, also require multiple beam capability, as this is the case for telecommunication applications. This implicitly paves a direction for digital beamforming and for more consideration to signal processing aspects. Beside EO applications, recent developments such as GLOBALSTAR and INMARSAT IV for mobile communication and SMOS for passive radiometer have demonstrated major interest and potential of array antennas. Outside Europe, major array antenna developments have been recently performed such as SPACEWAY and WGS (Wideband Gapfiller Satellite) in the United States and WINDS in Japan. From user terminal antenna, US is also very active as demonstrated with the first CONNEXION operational in flight aircraft entertainment system on some airline companies.

It should be mentioned that since the beginning of the eighties, although active arrays were very often originally considered for several programs, the detailed trade-off performed at the time of final mission implementation selected solutions based on reflector antennas. Preliminary selection was mainly justified by the large advantages of active arrays in terms of coverage flexibility, in flight reconfigurability, multiple beams generation by only one aperture and the avoidance of moving parts for beam steering. Solutions based on Active Antennas were nevertheless disregarded at that time due to their intrinsic drawbacks in terms of power consumption and dissipation, the limited radiated power capability for broadcasting and the overall achievable performance. Regarding complexity, maturity of technologies, mass budget when high gain is requested and overall cost, reflectors showed overall better characteristics. Arrays were selected only when no other alternatives with

the requested functionalities were available. Further to this, there have been specific applications, where the array antenna provided advanced capabilities and fixed beam or switched beam solutions resulted. Examples are the cylindrical arrays on Meteosat, permitting the images to be taken without disturbances by for instance mechanically scanning/switching antennas.

Accounting for the above, it is considered as strategic relevance for Europe to face in the most efficient way the very large number of constraints associated to array antenna subsystems and to concentrate all the efforts to further develop and improve this domain. It shall be noticed that US space industry benefits from large military investments in active antenna technology and in the future there is a risk that reconfigurable antennas could be relocated and reconfigured with minimal non-recurring costs to cover the needs of European operators.

This array optimization shall address all aspects (radio-frequency, mechanical and thermal) of space antennas as these arrays are characterized by a high integration level of all functions. An iterative process shall be implemented to ensure a competitive compromise between radio-electrical, mechanical and thermal performances, considering the platform interfaces. As demonstrated with ongoing developments, it shall be noted that the potential antenna architectures for array antenna systems are widely dependant on the available technologies and this requires a good knowledge of the state of the art.

As it is well known, a phased array antenna is a system obtained connecting a group of small radiators and organizing them in such that their received or transmitted signals are in the correct electrical relationship (phase and amplitude) with each other. While reflector antennas usually scan the beam by mechanically moving the reflector or the feed or both, a phased array can scan the beam electrically by changing the phasing of its elements. The primary reason for using arrays is to produce beams that can be modified (scanned or shaped) electronically. The circuitry, which controls the excitation of elements in an array, is called the Beam Forming Network (BFN).

Above description is in part already 'old fashioned' as with todays technologies available there are implementations possibilities such as digital beam forming in combination with signal processing which allow performing similar functions without RF BFN. In digital beamforming arrays, only the high power components, circuits and LNAs located near the antenna aperture are using analog circuits. All the amplitude and phase control functions, as well as the beamforming are performed digitally. With digital beam forming (DBF), very accurate beam control can be obtained and various array signal processing methods can be applied. This includes multiple beams with very

low side lobes, adaptive pattern control and direction of arrival (DOA) estimation. Digital signal processors can discriminate between incoming signals and interference allowing smaller user antennas. This type of arrays have been implemented in several defense program such as Skynet 5, Syracuse 3 or Spainsat and transposition to receive antenna for commercial application such as secured TTC links, telecom high gain antennas with a large number of beams, Earth Observation is to be promoted. The higher security level required even by commercial applications reinforces this demand. It is expected that digital beam forming network tiles for SAR application will allow implementing additional radar modes such as MTI, will make available true delay line for high resolution and make central electronics more generic. For telecommunication this type of beam-forming appears to be the only alternative for applications with a high number of beams and radiators (analog beam former becoming too complex).

Less complex arrays do not include scanning capability, such as the ERS antenna, or only phase-shifters to scan a beam, such as RADARSAT1 antenna or the reflectarray concept. To generate multiple scanned/shaped beams using the same antenna aperture, active phased arrays with amplification at each element have to be considered. Their capability to reconfigure the radiation pattern is particularly useful to cope with mission needs during the satellite lifetime.

Active phased arrays are also well known for being complex and expensive antennas and, as a consequence, only few space missions (around 10%) consider this type of antenna. This is not the case for ground and airborne radar where important funding mainly from the US defense programs have lead to large-scale production of T/R modules reaching a goal of 100 $ per module already in 1985. Unfortunately, this background is hardly reusable for space mission due to completely different requirements and operational constraints.

Another limiting factor to a wider application of antenna phased arrays in space mission is linked to the large mass and high power dissipation typically required, especially for the large active phased array configurations. This generates the need for new, ultra-light technologies and thermal hardware. With the progress in developments of more efficient T/R module, thermal aspects may be different, but the improvement on this parameter is not as quick as expected. Today (active) phased arrays for space missions are mostly considered when in flight beam reconfigurability or inertia-less beam steering is required. However, it is important to note that array antennas may find wider space applications in case LEO or MEO telecommunication constellations come again or as a way to generate very large space aperture thanks to digital processing associated to correlating arrays.

During the past 20 years, the basic elements and transmission lines present in phased array systems have evolved with a variety of microstrip, stripline and other printed radiators replacing the traditional dipoles, slots or horns, fed by coaxial lines or waveguides. The state of development in the two fields of devices and automation, has allowed one to produce phased arrays automatically at a larger integration level, and not by piecewise assembly, taking advantage of monolithic fabrication. Using digital processing or analog devices, the (active) phased arrays will have time-delay capability to make wideband performance possible. Other important features of array antennas are: the distribution of solid-state power amplification with graceful degradation and with the distributed lower power levels a lower risk of multipaction in the antenna. (Active) phased arrays can also be designed to conform to the surface of a spacecraft, vehicle or even human user (skin/clothes antennas).

Active phased array antennas enable to radiate or receive the signal directly are called 'Direct Radiating Arrays' (DRA). They can also be used to illuminate reflectors and, in this case, the antenna systems are called 'Array Fed Reflectors' (AFR). Feed arrays can compensate for the inherent distortions of large reflectors deployed in space, thanks to techniques monitoring the reflector surface or synthesize a desired radiation pattern by adjusting the feed coefficients and they can assist to move the complete multiple beam pattern over the coverage, therewith handling seasonal deviations in desired scanning/coverages, without moving the satellite too much (saving life time). Both types of arrays, Direct Radiating Arrays (DRA) and Array Fed Reflectors (AFR) will be addressed in this paper.

## 3 Space applications requesting array antennas

### 3.1 Earth observation

In the past SARs operating in C-band were mounted on board satellites which also hosted other types of instrument (e.g. ERS, ENVISAT). The tendency now is for dedicated satellites possibly used in constellation together with multiple beam instruments.

Next generation SAR asks for array antennas with cost efficient solutions and more flexibility (bi-static operation, receive only arrays; beamshaping, beam agility; polarization purity, interferometric capabilities). It is expected the need for wider bandwidth (reconnaissance), higher amplitude/phase stability, more sensitivity (science) and simultaneous multibeam reception possibly combined with large apertures in receive only.

There is also the need to reduce the cost of SAR instruments, active antennas being the main cost driver. With this objective, there will be an evolution towards a new generation of SAR active antennas with T/R modules using advanced technologies (GaN, SiGe, advanced packaging and interconnect concepts...) and possibly including frequency conversion or digitalization.

Special attention shall also be given to advanced calibration concepts to obtain significant reductions in cost and calibration time as compared with currently used techniques. Beside C and X-band instruments, side looking SAR and nadir looking ground penetrating radar operating in P-band (435 MHz) for Biomass and ice-sheet thickness measurement imposes severe constraints on antenna and very large aperture (typically 60 $m^2$) development is required.

Also in the area of passive reception of signals, e.g. GNSS signals, there is a requirement for antennas operating mainly at L-band capable of beam steering and tracking.

## 3.2 Mobile communications

Geo mobile mission needs are very demanding at antenna level regarding both reflectors (with diameter in the range from 9 to 12 meters) and focal array (made of more than 100 Tx/Rx feeds with shared aperture to generate overlapped beams). The large number of pencil beams together with the world coverage and the frequency reuse lead to reach today technology limit as illustrated by the very large complexity of Inmarsat IV feed array.

Beside the need for 25 meter reflector diameter and the move to S-Band frequency operation, major improvements on Digital components technology are required.

## 3.3 Mobile Digital Broadcasting Systems

Mobile Broadcasting missions require very large aperture (mass issue) and high EIRP (power consumption) which are today the two most difficult targets for arrays antenna. Considering also that only a reduce number of beams are required, it is not considered as appropriate to focus on array development for this type of mission. Nevertheless it shall be noticed that passive array fed reflector are sometime considered when multiple shaped beams are needed for the mission.

### 3.4 Conventional Fixed Telecommunications Service (mainly Ku-band)

Despite the continuous progress witnessed in terrestrial fixed communication networks capabilities, satellites are an attractive solution for broadcasting, multi-casting and point-to-point communications for their well-known coverage capability and limited ground infrastructure. The Fixed Telecommunications Service represents by far the largest Space market. Nevertheless, satellite networks are today often lagging behind terrestrial ones and they are not flexible enough to efficiently support the current trend toward bursty non-uniformly distributed traffic, both in space and time. However, this is not an intrinsic limitation and satellites, provided the necessary technology is developed with proper timing, can actually offer advantages in that respect in view of they inherently served large areas. To be successful, the next generation of telecommunication array antennas shall be able to:

- increase the EIRP and improve the power efficiency;
- provide in flight reconfigurability to comply with user needs and standard changes.

### 3.5 High Capacity Multi-Beam Systems (mainly Ka-band)

It is expected that the next generation of multi-media networks will see the satellite as an integral part of the global information infrastructure. In this framework, GEO satellites are expected to provide both trunking and access networks. The satellite component shall be able to cope in a flexible and yet efficient way with the evolution of terrestrial networks. The required antennas offering this flexibility are not today available and justify developments on arrays as this product has all the potentials to answer to the above demand.

To achieve these targets and respond to future communications requirements by means of space-based solutions, it is required to develop truly innovative systems keeping in mind current limited attitude to risk and the difficulty to anticipate market trends. At antenna level, this will require the development of a new generation of antenna sub-systems including tracking systems and techniques offering flexibility with cost effectiveness.

## 4 European space heritage on array antennas

Array antennas can be classified in several ways, for instance as:

- passive (phased) array antennas;

- semi-active array antennas;
- active (phased) array antennas.

*Passive (phased) arrays* deal with large aperture split in radiators with central amplification and, possibly, phase and amplitude control. In passive arrays, the BFN is an assembly of transmission lines, phase shifters and variable power dividers directly connected to the radiating elements. Passive arrays can be used to provide medium gain with either fixed or mechanically steered beams or with electronically steered ones. When gain requirements increase they are usually replaced by reflector antennas. Such a type of array may be adequate for communications and navigation satellites in a MEO/GEO orbit or for medium rate data transmission.

*Semi-Active arrays* consider custom designed hybrid circuits introduced between the elements and the power amplifiers. This allows them to operate all at their nominal level with optimum efficiency. Beam scanning or reconfiguration is achieved by phase-only signal control at the inputs of amplifiers. These arrays are often used to feed multibeam reflector antennas. Digital BFN on receive is a solution and way forward for the receive situation.

*Active (phased) arrays* use, at element level, distributed high-power generation for transmit and low-noise amplification for receive as well as phase and amplitude control (if required). Active arrays are well adapted for tracking low-Earth-orbiting satellites. The most common approach toward achieving fast-beam scanning is through the integration of monolithic microwave integrated circuit (MMIC) phase shifters with the antenna elements.

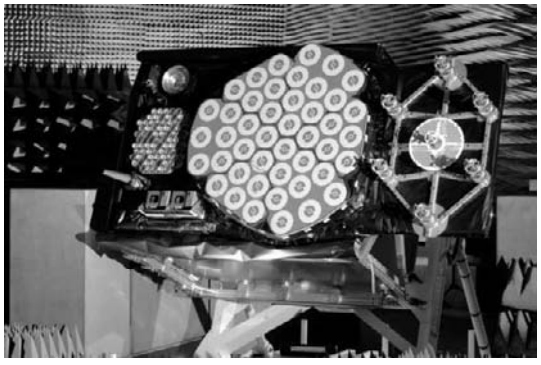

Figure 1: GALILEO IOV Payload Earth panel (Courtesy of Astrium-Uk, EADS-CASA Espacio and RYMSA).

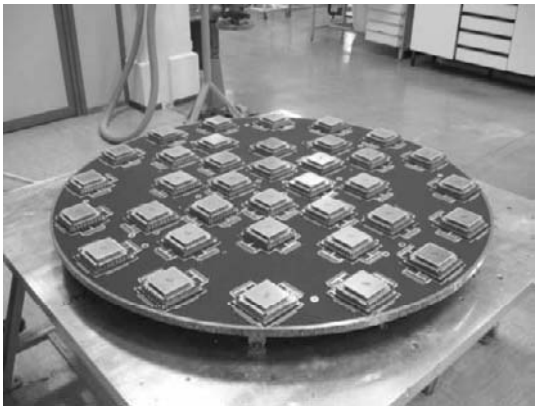

Figure 2: GSTBv2 Antenna Array (Courtesy of Thales Alenia Space Italy).

In some cases, *hybrid electro/mechanical arrays* combining mechanical steering with electrical steering/shaping are considered. This architecture is often used to reduce the number of active control thanks to electrical scanning in only one plane. This is often the case for mobile user terminals where azimuth scanning is performed by the antenna rotation and elevation agility is realized by a linear phased array.

*Passive (phased) arrays* are mainly implemented as:

- Direct Radiating Arrays in transmission or reception;
- reflectarray;
- lenses;
- hybrid electro/mechanical arrays;
- Array Fed Reflectors.

An example of Passive Array is given by the Navigation antenna for GALILEO. It shall provide an iso-flux fixed shaped beam in two sub-bands with the following requirements:

- gain: 15 dBi at $\pm 12^\circ$ Edge of coverage;
- circular polarization (RHCP); Axial Ratio: 0.8 dB;
- low band: 1164–1215 MHz, 1260–1300 MHz; high band: 1555–1595 MHz.

Two designs, developed under ESA contracts, are shown in Figs. 1 and 2.

*Semi-Active arrays* are mainly implemented as:

- Direct Radiating Arrays in transmission or reception;
- Array Fed Reflectors.

Figure 3: transmission antenna for a spun satellite at L2 Lagrange point (Courtesy of Thales Alenia Space France).

An example of semi-active array is given by the data transmission array as shown in Fig. 3.

This antenna is optimized to provide maximum gain for an angular coverage $\theta$ from 40° to 70° (i.e. nearly perpendicular to the surface of the truncated cone). Beside, the number of active modules is drastically reduced (24 instead of 144) by having a fixed distribution network per column/subarray. The beam is rotated around the revolution axis basically by means of 24 phase shifters and a set of quasi-Butler matrices. So the 24 SSPAs located before the matrices transmit all and always the same power: this maximizes the DC-to-RF efficiency. The subarray pattern is optimized (via the network

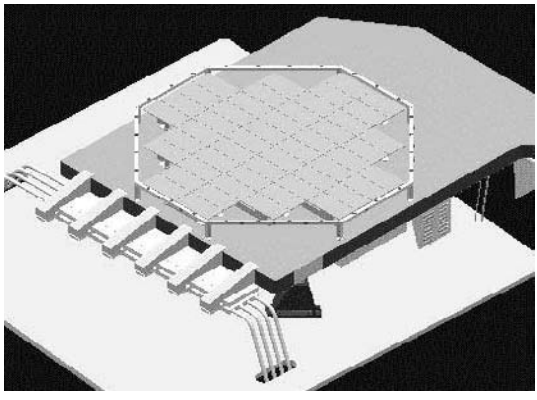

Figure 4: STENTOR Dual-polarised active array – based on planar radiating subarrays (Courtesy of Thales Alenia Space France).

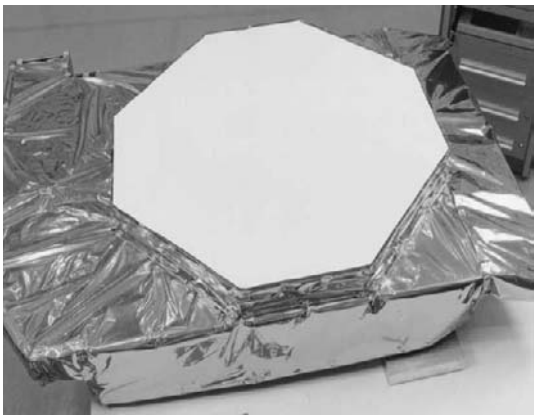

Figure 5: STENTOR active array – Flight Model under test (Courtesy of Thales Alenia Space France).

feeding for the 6 radiating elements) for each mission with reference to the exact template of the gain variation versus $\theta$.

This concept has been developed for various mission applications with a large axi-symmetric scanning range by teams led by Thales Alenia Space France under ESA contract.

*Active (phased) arrays* are mainly implemented as:

- Direct Radiating Arrays in transmission or reception;
- reflectarray;
- lenses;
- hybrid electro/mechanical arrays.

An example of Active Array for Telecommunication is given by the STENTOR program supported by CNES. A Flight Model of a transmitting active array providing 3 beams at Ku band, independently steered over Europe, has been built by Thales Alenia Space France (Figs. 4 and 5). It aimed to demonstrate the capability of new telecom missions:

- either to re-configure a few times the satellite coverage (during a typical 15 year satellite life) in order to match the demand changes: e.g. extension of TV-DBS (Direct Broadcasting from Satellite) over new countries;
- or to provide numerous 'hopping' spot-beams time-multiplexed in coherence with the rate of a TDMA frame.

The main characteristics of the planar dual-pol radiating elements are:

Figure 6: Artists view of Sentinel-1 platform (Courtesy of Astrium and Thales Alenia Space Italy).

- 32 patches subarrays;
- H and V dividers: suspended striplines (loss, 0.6 dB);
- X-pol $> 30$ dB over 1 GHz.

STENTOR has been the victim of a launcher failure.

Another example of active array is given by the SENTINEL–1 program. In the frame of the Global Monitoring for Environment and Security programme (GMES) ESA is undertaking the development of a European Radar Observatory (Sentinel–1) for the continuation of SAR operational applications. The C band SAR antenna is proposed to be an active phased array with wide electronic steering capability along the elevation plane and limited steering along azimuth plane. The radiating aperture is $1.4\,\mathrm{m} \times 10.0\,\mathrm{m}$ and includes $320 + 320$ single channel T/R modules with independent amplitude and phase control. The SAR antenna operates simultaneously in H and V polarization in receiving mode and in H or V polarization in transmitting mode. The antenna is organized in five panels, with the lateral wings foldable (Fig. 6). Thales Alenia Space Italy is responsible of the satellite and SAR instrument is under EADS Astrium GmbH responsibility.

## 5 Active arrays in perspective

Active arrays are a strategic domain and mastering of several technologies is mandatory to comply with users needs over the different frequency ranges. Antenna performance optimization such as gain and isolation are strongly constrained by satellite power and mass budgets. It shall be noted that regarding Power Added Efficiency (PAE) of High Power Amplifier (HPAs), a low efficiency not only impact on the achievable EIRP but also on the power

to be dissipated on the spacecraft. Considering typical values in Ku-band of multicarrier PAE of Travelling Wave Tube Amplifiers – TWTA (50%) and of Solid State Power Amplifiers - SSPA (10–20%), and the major limitations of the satellite thermal control, this justify the large use of passive reflector antennas for space applications.

This situation of SSPA efficiency is expected to improve in the coming years with the appearance of new technologies such as GaN. Generally speaking wide bandgap semiconductor materials (e.g. Gallium Nitride – GaN) have been identified as key disruptive technologies that will have significant impact on SSPA performance capabilities. Particularly, high RF power capabilities, improved efficiency and excellent thermal properties will offer very significant improvements on the power/efficiency capabilities of future SSPAs, currently based on GaAs technology. A further benefit of GaN will be an increased junction temperature compared with current standards with the potential advantage of higher baseplate temperatures and reduced thermal radiators area.

Notwithstanding the promising expectations it has to be noticed that over the last 20 years the improvement in terms of SSPA PAE has never been as quick as anticipated. The situation is a less critical for L and S band applications as more mature technologies with in flight hardware are already available. It is also worth noting that such dissipation and associated thermal problems are largely mitigated in receive antenna.

Active arrays remain an imperative choice when no alternative exist in term of required functionalities as in:

- anti-jamming system;
- multiple beam antenna with beam pointing and steering flexibility (e.g. continuous beam pointing and hopping);
- wide angle field of view;
- antenna with major constraints in term of volume.

The development of multiple beams and reconfigurable active arrays is tightly connected to that of Beam Forming Networks (BFNs). Beamforming networks are complex networks used to precisely control the phase and amplitude of RF energy passing through them, which is conveyed to the radiating elements of an antenna array. BFN configurations vary widely from just a few basic building blocks up to tens of thousands of them depending on system performance requirements. To offer a certain degree of 'smartness' to active arrays the antenna architectures must include advanced reconfigurable beamforming networks which make them capable of various kinds of flexible and real time pattern control:

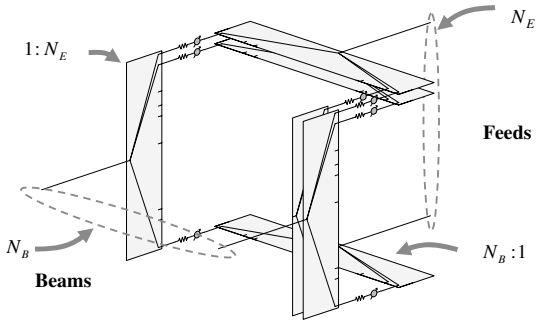


Figure 7: Block diagram of a fully reconfigurable Beam-Forming Network.

- beams can be individually formed, steered and shaped;
- beams can be assigned to individual user;
- interference can be minimized implementing dynamic or adaptive beam-forming.

To allow full reconfigurability, each beam signal must be distributed (Tx case) to all the feeds with different amplitude and phase weights (Fig. 7).

Considering that the complexity of an all analog reconfigurable BFN increases with the number of beams and to take advantage of adaptive beam forming techniques, the possibility to exploit a Digital Beam Forming (DBF) approach has attracted much interest. Such option can be considered an extension of the capabilities of satellite payloads based on digital On-Board Processor (which performs channelisation and routing). Beams bandwidth may be lower than that of the total repeater bandwidth (as in the case of

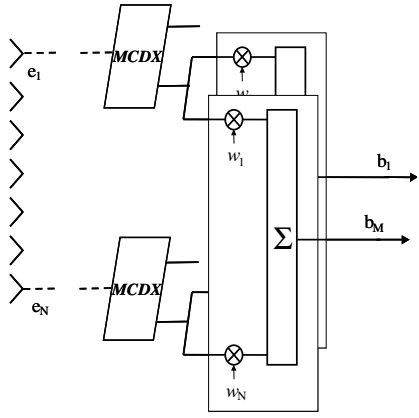


Figure 8: RX Digital Beam-Forming Network (DBFN).

frequency reuse schemes), and this could in principle lead to a complexity saving, by firstly performing demultiplexing of each wideband feed signal into narrower-band signals, and then performing beam synthesis at a lower sampling rate (refer to Fig. 8).

Nowadays DBF is commercially available on several mobile satellites operating at L-band and the INMARSAT 4 processor [1] (EADS Astrium first satellite successfully launched on 11 March 2005) represents the major outcome of ESA funded R&D programmes on DBF. DBF techniques based on Fast-Fourier-Transforms (FFTs) on planar lattices are particularly well suited for periodic active arrays and have been recently implemented, tested and validated in a real-time proof-of-concept demonstrator [2] (Fig. 9).

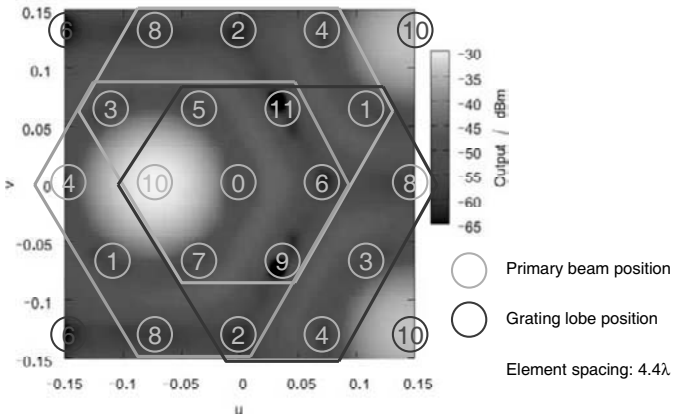


Figure 9: 2-D plot of a beam produced by the 12 pt FFT beamformer. Positions of the other beams are also shown along with three possible (off-centre) coverage regions. (Courtesy of Astrium [2]).

## 6 Array architecture for increased power efficiency

In order to keep under control the cost and the complexity of large direct radiating arrays, it is crucial to reduce the number of active elements and to simplify the beamforming network. Aperiodic arrays with equiamplitude elements represent an interesting solution especially when the array has to generate pencil beams with a limited scanning range. This type of antenna architecture is considered extremely promising for the design of arrays generating a multibeam coverage on the Earth from a geostationary satellite.

Unequally spaced arrays have interesting characteristics and offer several advantages with respect to periodic arrays [3]. Up to now sparse and thinned arrays have been rarely used essentially because of the complexity of their

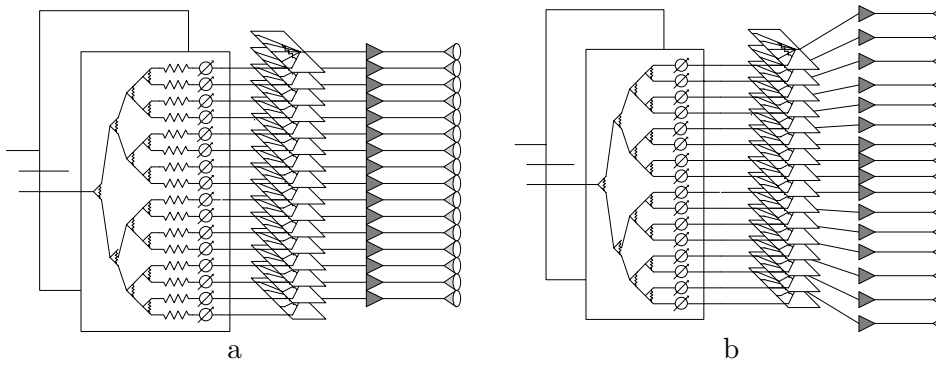


Figure 10: Synoptic of multibeam active direct radiating arrays transmit antenna configurations. (a) Periodic array with amplitude tapering; (b) aperiodic array with density tapering.

analysis and synthesis with a reduced knowledge, as a consequence, of their radiative properties.

Generic block diagrams of active multibeam direct radiating array transmit antennas based on regular and aperiodic lattices are shown in Fig. 10. The two architectures consist of a number of radiating elements and High Power Amplifiers (HPAs), respectively $N$ and $M$ for the two architectures, and $K$ independent beamformers, each with a number of control elements per beamformer equal to the number of radiating elements (amplitude and phase controls can be replaced by phase only controls in a sparse array).

The HPA section and the array design play equally central roles in defining the overall efficiency of a transmit antenna whose final objective is the achievement of a target EIRP on the desired coverage areas. Trade-offs of different solutions should favor high-efficient DC-power to EIRP conversion as well as low complexity, mass, volume and costs. A fair assessment of different design options must consider common radiation pattern requirements such as the ones imposed on broadband multibeam antennas. These antennas adopt frequency reuse to efficiently utilize the available bandwidth but this induces co-frequency/co-polarized beams with strong requirements on Side Lobe Levels to limit beams interferences. A proper design and control of the excitation and/or positioning of the array elements is mandatory.

Recently [4], trade-offs on active DRA architectures based on the two design solutions have been performed on the basis of simplified antenna models comparing:

- periodic array (Fig. 10 (a)) with sidelobe control by means of amplitude tapering with an active section using the same HPA design for all the elements – the HPAs are operated accordingly to the required RF

power for each radiating element with different amplifiers at different output-back-offs (OBO);

- aperiodic array (Fig. 10 (b)) with sidelobe control by means of appropriate element positioning with an active section using the same HPA design for all the elements – all the HPAs are operated at the same working point.

The two architectures consist of a number of radiating elements and High Power Amplifiers (HPAs), respectively $N$ and $M$, and $K$ independent beamformers associated to one beam, each with a number of control elements per beamformer equal to the number of radiating elements (amplitude and phase controls can be replaced by phase only controls in a sparse array).

In an active array, the HPA section and the array design play equally central roles in defining the overall efficiency of the transmit antenna whose final objective is the achievement of a target EIRP on the desired coverage areas. The trade-off should favour high-efficient DC-power to EIRP conversion as well as low complexity, mass, volume and costs.

Multibeam antennas adopt frequency reuse to efficiently utilize the available bandwidth with strong requirements on the Side Lobe Levels to limit beams interferences. A proper design and control of the excitation and/or positioning of the array elements is thus mandatory. For sake of exemplification we present below a trade-off on a simple linear array case comparing the discrete periodic array solution with an equiamplitude aperiodic array, varying the number of elements ($M$). To have a fair assessment of the different design options, a common radiation pattern requirement will be considered to be fulfilled by both the candidate architectures. The pattern requirements will lead to specific amplitude tapering for the periodic array and to a certain density tapering for the equiamplitude aperiodic array.

For the $n$-th HPA we introduce normalized (to saturation) RF and DC power quantities,

$$\text{RF power:} \quad \tilde{P}_n = \frac{P_n}{P_{\text{SAT}}} \in [0,1] \tag{1}$$

$$\text{DC power:} \quad \tilde{W}_n = \frac{W_n}{W_{\text{SAT}}} \in [0,1]. \tag{2}$$

Three major factors must be analysed to determine the overall DC-to-EIRP conversion efficiency:

1. *The RF Power*

   It depends only on the amplitude excitation and can be evaluated adding up power levels relevant to individual radiating elements

$$\tilde{P}_{\mathrm{TOT}} = \sum_{n=1}^{N} \tilde{P}_n. \tag{3}$$

2. *The antenna Gain*

   It is governed by the combination of radiating element patterns, array geometry and amplitude/phase excitations. For the following analyses the antenna gain is simplified to an array directivity evaluation which is based on an analytical closed form formulation [5].

3. *The DC Power Consumption*

   The DC power consumption of the overall antenna system can be determined by summing up all the individual DC power consumptions of each HPA (defined, in turn, by the output-back-off relevant to the element amplitude excitation)

$$\tilde{W}_{\mathrm{TOT}} = \sum_{n=1}^{N} \tilde{W}_n. \tag{4}$$

Subsequent analyses are based on the following hypotheses:

- reference linear aperture constituted by a continuous Taylor distribution [6] ($10\,\lambda$, SLL $= -20\,$dB, $\bar{\mathrm{n}} = 5$);
- discrete periodic array excitation ($d = \lambda/2$) obtained by sampling the reference distribution;
- sparse array designed by means of an improved Doyle technique [7]–[9];

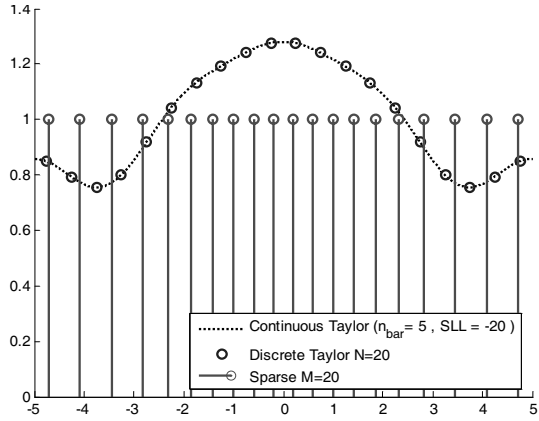


Figure 11: Aperture field distributions; $x$ axis in $d/\lambda$ ($M = 20$; $N = 20$).

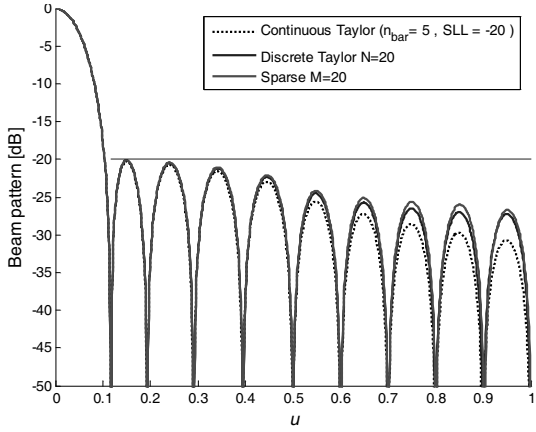


Figure 12: Far-field power radiaton patterns ($M = 20$; $N = 20$).

- upper hemisphere omnidirectional radiation pattern assumed for both discrete and sparse arrays elements;
- antenna gain reduced to array directivity evaluation based on an analytical closed form formulation [5];
- identical normalized HPA saturation power for both periodic and sparse arrays active element amplifiers;
- typical SSPA efficiency assumed for the HPA power consumption evaluation (30% efficiency at saturation).

The design procedure consists in synthesizing the periodic array and the equiamplitude sparse arrays with different number of elements starting from

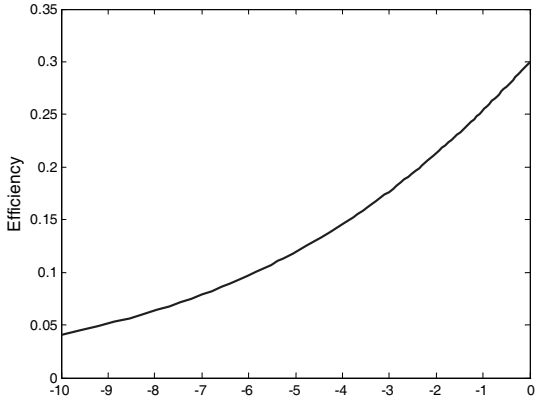


Figure 13: Single amplifier efficiency vs. OBO.

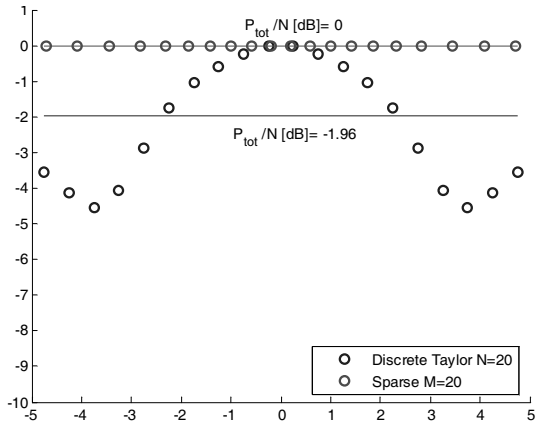


Figure 14: Amplifiers OBO.

the reference continuous Taylor distribution (Fig. 11 refers to the aperture distributions of $N = M = 20$ elements for regular and sparse arrays and Fig. 12 compares the obtained radiation patterns). RF power levels can be evaluated per radiating element from the excitations and, based on the DC-to-RF conversion efficiency (Fig. 13), individual DC power consumption and efficiency can be estimated (see Figs. 14 and 15 in which the continuous horizontal lines refer to the overall antenna DC-to-RF efficiency). It is worth noting that the selected reference tapering law, while being moderately limited in amplitude tapering depth (less than 5 dB peak, about 2 dB average), suffers a drastic loss in DC-to-RF efficiency (from 30% for the sparse array to only 21% for the discrete periodic array with amplitude tapering).

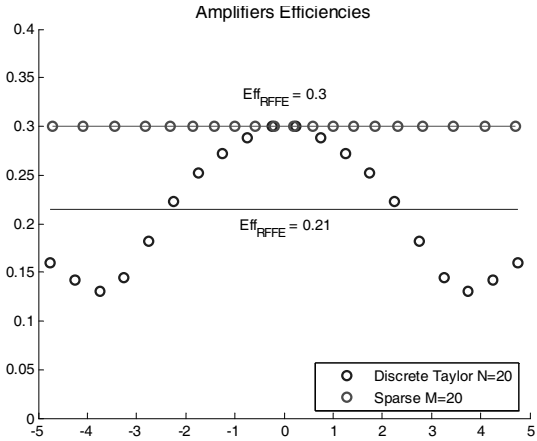


Figure 15: Amplifiers efficiencies vs. OBO.

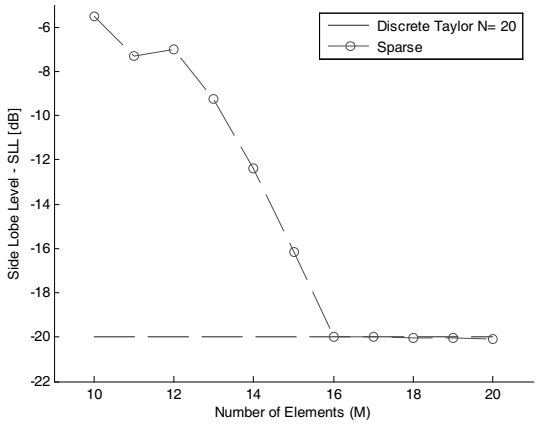


Figure 16: Maximum side lobe level.

A similar synthesis exercise can be repeated decreasing the number of radiating elements ($M$) of the sparse array. Pattern performances gradually degrade with the progressive reduction of the number of elements ($M$) but a 16 element sparse array still fulfils the sidelobe mask at $-20\,\mathrm{dB/max}$ (Fig. 16). Due to the substantial similarity of the synthesized sparse arrays radiation patterns no major directivity degradations are introduced notwithstanding the reduction of elements (Fig. 17).

The most interesting outcome of the analyses can be appreciated comparing DC consumption (Fig. 18) and EIRPs (Fig. 19), both measured relatively to the periodic array. While an active sparse array with a reduced number of elements (e.g. $M = 18$) could be synthesized exhibiting about the same

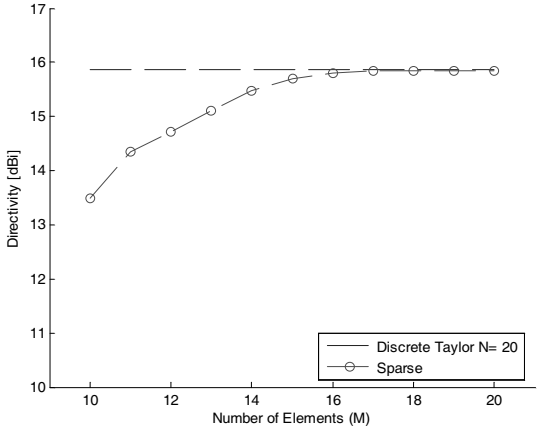


Figure 17: Array directivities.

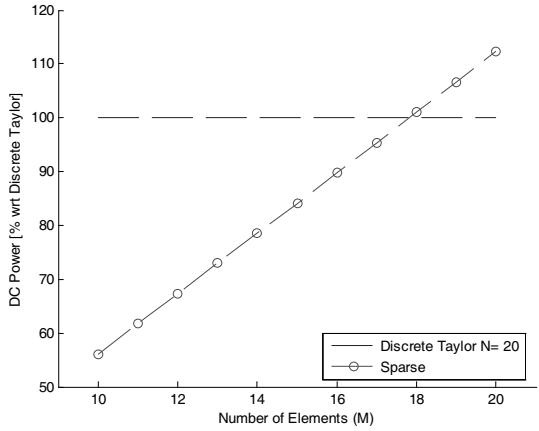


Figure 18: Relative DC power consumption.

DC power consumption of the active discrete periodic array (i.e. $N = 20$), its EIRP capability exceeds the one of the discrete periodic array (e.g. more than 1 dB for $M = 18$ elements).

Similarly, a sparse array with the required radiation performances (e.g. SSL lower than $-20$ dB) can be synthesized with a reduced number of elements (e.g. $M = 16$) with a lower DC power consumption (i.e. an improvement of more than 10 percentage points) still exceeding the EIRP of the discrete periodic array.

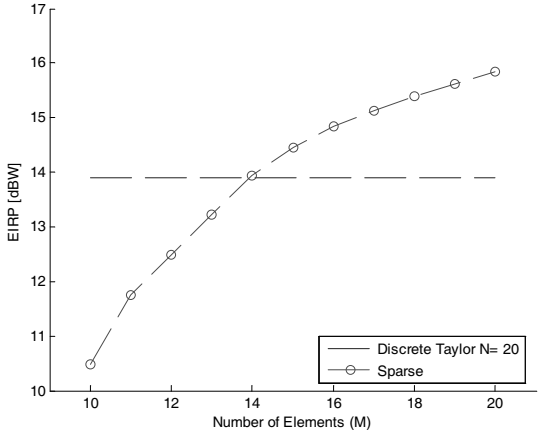


Figure 19: Relative EIRP.

# 7 Conclusions

This paper has presented an overview of the ongoing European activities on phased arrays. In particular, a preliminary assessment of the benefits of active direct radiating arrays based on non regular lattices (i.e. sparse arrays) for multibeam transmit antenna applications has been reported. Notwithstanding some simplifying assumption, the outcomes of the trade-off exercise clearly showed the high potentialities of active aperiodic arrays in terms of reduction of the number of elements, active control elements and amplifiers while improving overall antenna DC-to-EIRP conversion efficiency.

# Bibliography

[1] A. M. Bishop, O. Emam, A. D. Craig, L. Farrugia, R. J. F. Hughes, M. Childerhouse, M. Ali, P. Cornfield, P. Marston, S. Taylor, G. Thomas, D. Schmitt, X. Maufroid, and L. Hili, "The inmarsat 4 digital processor and next generation developments," in *Proc. 23$^{rd}$ AIAA International Communication Satellite Systems Conference (ICSSC)*, Rome, Italy, Sept. 2005.

[2] C. Topping, A. M. Bishop, A. D. Craig, D. M. Howe, J. Hamer, P. Angeletti, and A. Senior, "S-UMTS processor key technolgies demonstrator," in *Proce. 10$^{th}$ International Workshop on Signal Processing for Space*, Rhodes Island, Greece, Oct. 2008.

[3] G. Toso, C. Mangenot, and A. G. Roederer, "Sparse and Thinned Arrays for Multiple Beam Satellite Applications," *29$^{th}$ ESA Antenna Workshop on Multiple Beams and Reconfig. Antennas*, Noordwijk, the Netherlands, April 2007.

[4] G. Toso, P. Angeletti, and C. Mangenot, "Direct radiating array architecture based on non regular lattice," in *Proc. ESA Workshop on Advanced Flexible Telecom Payloads*, Noordwijk, the Netherlands, Nov. 2008.

[5] P. Angeletti, F. Frezza, R. Vescovo, and G. Toso, "On the directivity of planar arrays with $\cos^q \theta$ element patterns," in *30$^{th}$ ESA Antenna Workshop*, Noordwijk, the Netherlands, May 2008.

[6] T. T. Taylor, "Design of line source antennas for narrow beamwidth and low sidelobes," *IEEE Trans. Antennas Propag.*, vol. 3, pp. 16–28, Jan. 1955.

[7] W. Doyle, "On approximating linear array factors," *RAND Corp Mem RM-3530-PR*, February 1963.

[8] M. I. Skolnik, "Chapter 6. Nonuniform Arrays," in *Antenna Theory, Part I*, R. E. Collin and F. Zucker (eds), New York, McGraw-Hill, 1969.

[9] O. M. Bucci, M. D'Urso, T. Isernia, P. Angeletti, and G. Toso, "A new deterministic technique for the design of uniform amplitude sparse arrays," in *30$^{th}$ ESA Antenna Workshop*, Noordwijk, the Netherlands, May 2008.

# Antenna front-ends for mobile satellite terminals: design & realisation

**Rens Baggen**, **Sybille Holzwarth** and **Martin Böttcher**
*IMST, Carl-Friedrich-Gauss Str. 2, D-47475 Kamp-Lintfort, Germany*
*(baggen@imst.de)*

**Abstract**

This article presents an overview of developments at IMST in the area of antenna front-ends for mobile satellite terminals. Such type of antennas has become a key area of interest because of the ever growing multimedia services provided over wireless links and satellites. Various activities in this area have been conducted in the past, and are on-going. Antenna front-ends for mobile platforms are, in general, complex systems because they have to incorporate special features in order to perform beam steering, and at the same time also be cost-effective. The complexity of the antenna systems, developed at IMST, ranges from small arrays with switch-able elements and partially mechanically and electronically steerable arrays (hybrid systems) to fully electronically steerable arrays. This article examines which kind of user requirements for the three basic mobile platforms (land, maritime and aeronautical) exist, and what kind of impact they have on the design of the front-ends. Latter aspect is critical to achieve a cost-effective design. This is illustrated by examples from past and on-going projects in L-, Ku-, and K/Ka-band. Different concepts are presented and key aspects discussed.

## 1 Introduction

Satellite services have been well established for the last decades. A household with a parabolic dish on its balcony or rooftop is a common picture nowadays. The development of the space segment for multimedia satellite services has been - and still is - progressing in a rapid pace in L-band, S-band, Ku-band and the upcoming Ka-band. In the past, the larger part of the consumer market for satellite receivers was focussed on fixed users (households, offices, etc.) and nomadic users (caravans, expeditions) that did not require agile satellite front-ends on the ground. Ku-band and K/Ka-band fixed or nomadic satellite terminals are available on the market and are sold in increasing numbers. However, users demand multimedia access all time at all places, and whether this information originates from wireless

Antennas for Ubiquitous Radio Services in a Wireless Information Society
I.E. Lager and M. Simeoni (Eds.). 
doi:10.3233/978-1-60750-487-0-121

networks on earth or satellites, is not of interest to the end-user. Therefore, an increasing demand for mobile satellite terminals is emerging that requires antenna front-ends capable of tracking one or more satellites (uni-/bidirectional) and provide at the same time sufficient bandwidth. Mobile satellite terminals are therefore a growing commercially interesting market for maritime, aeronautical and land mobile applications, providing multimedia satellite broadcasting services on-the-move. Standard satellite antenna front-ends, available on the market today, track in general the satellite by means of mechanical steering (two- or three-axis steering system, often encountered in L-band) or use a hybrid concept (a mix of mechanical and electronic steering, for example encountered in Ku-band, see Fig. 1), and in general offer only an unidirectional link.

Figure 1: Hybrid rooftop antenna by RaySat Inc. for DBS-reception [1].

The telecommunication market requires however far more cost-effective, yet powerful, and compact solutions. Also, front-ends equipped with mechanically moving parts, are maintenance intensive, often heavy and/or bulky, and sensitive to G-forces. These issues do not make this type of antenna that well suited for automotive (not aesthetic enough, too bulky) or aeronautical applications (too maintenance intensive).

In the last decade, antenna front-ends for mobile satellite terminals have become a key area within IMST. The range of steerable antenna systems, developed by IMST, varies from small arrays with switch-able elements and partially mechanically and electronically steerable arrays (hybrid systems) to fully electronically steerable antenna arrays. The front-ends employ concepts like RF-phase and -amplitude shifters for each element (or a group of elements) also called phased arrays, or the design can be based on Digital Beam Forming (DBF). This technique, in which each array element signal is available directly on a digital level, allows the most flexible and powerful control of the antenna beam (beam forming and tracking). This article

discusses various RF-topologies used for mobile satellite antenna front-ends in L-band, Ku-band and K/Ka band: switch-able antenna beams, classical phased arrays, and DBF-concepts. Architectures for different mobile platforms will be presented. It is intended to give here a global overview and not a detailed technical description. Please note that the applications focused on within this article are all commercial, not military.

First, the requirement profile for mobile platforms will be analysed in detail. In order to achieve a cost-effective design, the global specifications for each type of mobile platform (car, ship, plane, etc.) will be defined. This is a crucial first step in order to achieve a competitive RF-front-end concept. Thereafter, a summary of typical RF-topologies used for steerable antenna arrays is presented, and different concepts will be listed. This is followed by examples on antenna front-ends, developed by IMST (as a whole or in cooperation with partners). Key design aspects will be pointed out for each example. A conclusion will close this article.

## 2 Mobile platform requirements

One can distinguish 3 main types of mobile platforms, namely: land mobile, aeronautical, and maritime. Each of them will now be discussed with respect to:

[**R.1**] Total size/volume,

[**R.2**] Preferred aperture/shape and

[**R.3**] Cost price (please note that the cost prices are listed relative to each other and only serve as an indication, not an absolute value).

### Land mobile

[**R.1**] The size/volume of the antenna strongly depends on the type of land mobile platform. One has to distinguish here between the automotive sector, and trains. The automotive platform has to be subdivided into 'large' platforms like trucks, buses and caravans, and 'standard' platforms such as cars. The first category allows for more available space onto the hull of the vehicle (due to its sheer size). The size restrictions for cars are much more severe. Here, a diameter of the satellite terminal between 20 cm and 30 cm with a height of only several centimetres applies. For trains, the size restriction does not really apply. In near future, it is however expected that the height of the terminal will be restricted due to the fact that more and

more double-decker trains are expected (height restriction due to tunnels). The satellite terminal for internet onboard of the THALYS (European high speed train) is shown in Fig. 2. For sake of comparison, please have a look at the size of the train wagon itself.


a b

Figure 2: Satellite terminal front-end on top of the THALYS train for Internet onboard. (a) General view; (b) detail on the antenna.

**[R.2]** Especially for the normal person car, aesthetics are of outmost importance. For this reason the size restrictions are as listed under **[R.1]**. Such sizes allow for an aesthetic integration of the front-end in the car rooftop. For larger vehicles like trucks and busses, the form factor of the terminals is far more relaxed. The same applies for trains although a more streamlined approach of the antenna front-end would be logical. However, concluding from the THALYS-system depicted in Fig. 2, this seems not be a key issue.

**[R.3]** The cost price for the automotive market is very competitive, not to say aggressive. Add-ons like stereos and GPS-based navigation systems for cars range from a couple of hundreds to a couple of thousand Euros. It is expected that an automotive front-end for mobile satellite reception will have a market introduction price of around €1000 or less. For the 'larger' vehicles like caravan, busses or trains, the cost price can be several thousand Euros or even more.

### Maritime

**[R.1]** The total size/volume of maritime front-ends is normally not that critical, especially because ships are large in size with respect to the satellite terminal size. A mix of mechanically steerable parabolic reflectors, patch arrays (in Ku-band for example) or helical arrays (L-band for example) are available on the market, covered normally with a radome shaped as a half sphere.

[**R.2**] The preferred shape of such front-end aperture is normally determined by the radome as just pointed out. One aspect to consider here is that such antennas should be able to steer the beam below the horizon which normally results into a half sphere shape of the radome extended with a small cylindrical rim.

[**R.3**] Cost prices for such terminals range normally from a couple of thousand Euros to ten of thousands of Euros or more.

**Aeronautical**

[**R.1**] The total size/volume for aeronautical platforms is mainly determined by how much extra fuel the additional front-end will cost. Normally, this is not a critical issue; more important is the fact that the integrity of the hull of the aeroplane is not compromised.

[**R.2**] The shape of the aperture is of importance from the point of aerodynamics. If the front-end (radome included) is sticking out too much from the hull of the plane, the drag can become an important factor and fuel costs become an issue. Whether this is a critical factor, is not clear at the moment, opinions tend to differ on this issue. A factor that plays also a role in this is whether the customers are commercial airlines or private jet owners. The demands of both categories can differ considerably.

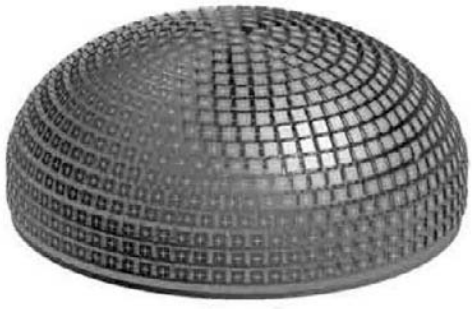

Figure 3: Full electronically steerable array for aeronautical platforms by Space Engineering Spa [2].

[**R.3**] Because this is a high-end market, the cost price of the terminal itself will be quite higher than in case of the land mobile and maritime platforms. Here, other external factors can play also an equal important role such as the time to install such a terminal. The time periods that a plane is not in the air, create costs, so the maintenance/installation time should

be kept as small as possible. Therefore, the time to install such a front-end can becomes a critical issue and also its maintenance. For this reason, completely electronically steerable arrays are preferred for such applications because it is expected that maintenance will be negligible in comparison to mechanical steerable systems. Several opinions go around stating that drag is a less important cost factor than maintenance, and therefore an aeronautical antenna as shown in Fig. 3 is possible. In the case of reducing drag, planar structures are preferred as shown in Fig. 4. They have however also reduced scanning capabilities.

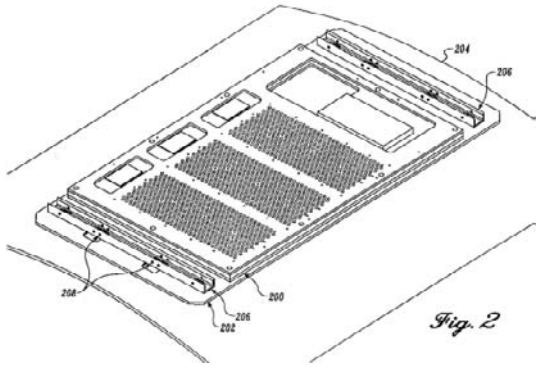


Figure 4: Full electronically steerable array for aeronautical platforms by BOEING [3].

Three other aspects should also be considered when looking at the requirement profiles of mobile satellite front-ends. The services in Ku-band (Rx: 10.7 GHz ÷ 12.75 GHz) in Europe use linear polarised signals. This implies that besides beam pointing, the polarisation also has to be adapted; the polarisation of the array on the mobile platform has to be adjusted towards the polarisation of the incoming satellite signal. This results into a significant increase in system complexity and poses quite some challenges for the antenna design.

Another point is the blockage effect with which land mobile systems have to cope. On land, blockage can be caused by trees, building, bridges, tunnels and similar structures. This becomes quite severe for the higher frequencies as for example Ku-band. In order to establish an adequate data link with the satellite, a Line-of-Sight (LoS) connection is required. This implies that a 100% reliable data connection between land mobile systems and satellites can never be guaranteed under normal user conditions. In order to solve this problem, one requires a dedicated combination of satellite services, front-end terminal and modem (satellite receiver) as proposed in [4].

The last aspect is whether the antennas are receive-only or both transmit/receive. For transmit systems, strict FCC-regulations (Federal Communications Commission) exist that impose quite severe design restrictions on mobile transmit terminals. Also, satellite service providers like Inmarsat have often even more strict regulations imposed on top of the normal requirements.

# 3 Mobile satellite RF front-end design

## 3.1 Summary of typical RF-architectures

The design of phased arrays involves different areas of expertise such as antenna design, feeding networks, beamforming/steering algorithms, signal processing, prototyping and complex measurements. Before several antenna topologies, developed in past and on-going projects at IMST, are described in this section, first some basic RF front-end topologies will be presented. From each of the RF front-ends described, key points will be addressed.

Basically, one can divide steerable antennas in completely mechanically steerable arrays, hybrids (partially mechanically, partial electronically), and fully electronically steerable antennas (phased arrays). The first category usually employs a three-axis system which allows automatic pointing of the antenna beam towards the satellite while moving. This category will not be considered here. The second one, the hybrid, as illustrated in Fig. 5, consists normally of rows of antenna elements that are placed on a turning table and can be steered electronically in only one plane (the elevation). Such a design requires only few RF-components like phase shifters and LNAs as compared to completely electronically steerable concepts. Nevertheless, it requires regular maintenance with respect to the mechanical parts.

One can distinguish two basic concepts for the third category, the fully

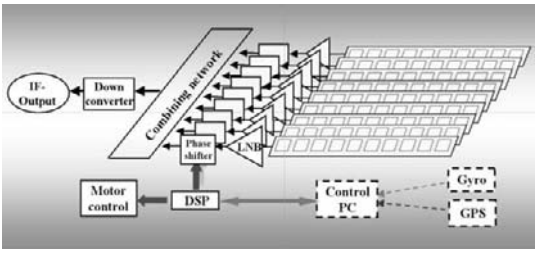


Figure 5: Hybrid RF front-end concept for receive-only terminals.

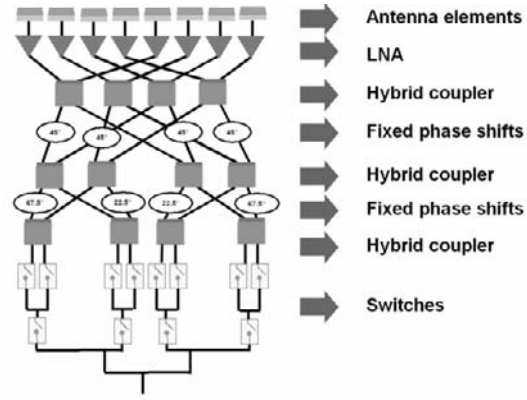


Figure 6: RF front-end topology for a linear 8-element array based on the Butler matrix (Rx-case).

electronically steerable arrays: one based on switch beam networks (see Fig. 6) and the other on phase shifting devices (see Fig. 7). Latter implies that normally each antenna element requires a phase shifting device and LNA. This can result into quite an expensive design when considering large arrays. For switch beam networks, Butler or Blass topologies can be applied [5], for example. A large disadvantage of this concept is that it requires RF-switches that introduce extra losses and increase the overall cost price. One can extend the two-dimensional topology as depicted in Fig. 6 (allowing for scanning in only one plane), to a three-dimensional concept [6].

The concept in Fig. 7 can also be realised digitally which means that each antenna element is equipped with a complete down-/upconverting circuit, and the received/transmitted element signal is digitalised at baseband and directly processed by a digital unit (e.g. a DSP or FPGA). This is not only the most complex system, but also the most flexible one. Because of the fact that the complete beam forming is performed within the DSP-unit,

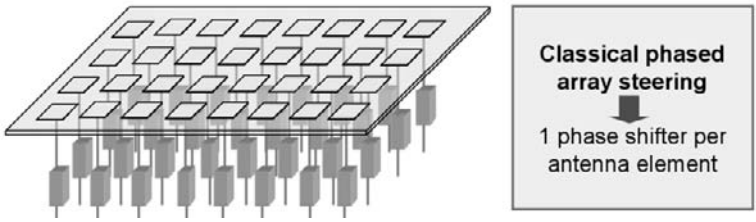


Figure 7: Phased array topology using one phase shifter per antenna element.

all kind of signal processing operations can be performed. This is called Digital Beam Forming [7]. The amount of signals to be processed can however become very high, hence the processing power has to be dramatically increased. Therefore, some concepts consider the combination of RF-phase shifters topologies and distributed digital logic architectures. A conceptual picture is displayed in Fig. 8.

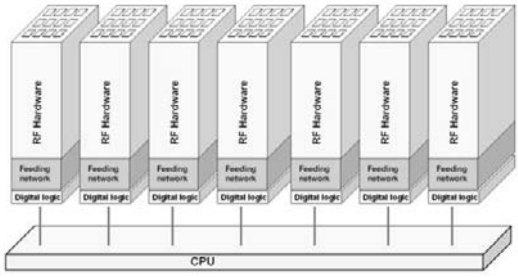


Figure 8: Combination of RF-phase shifting and distributed digital processing units.

### 3.2 Hybrid front-end at L-band

The focus of the project ALCANT (Active Low Cost steering ANTenna) was on the development and prototyping of a transmit/receive array for maritime applications in L-band. This is one of the earliest projects that IMST conducted. At that time, specific requirements for mobile terminals did not exist. Therefore, the specifications for fixed or nomadic terminals were adapted. This still resulted into quite severe requirements:

- Frequency range: $1.5\,\mathrm{GHz} \div 1.7\,\mathrm{GHz}$ (bandwidth 8.5%);
- Polarisation: circularly;
- G/T: $-4\,\mathrm{dB/K}$;
- Scan range: $-10^\circ \div 100^\circ$ in elevation and $360^\circ$ in azimuth;
- Operation mode: Tx and Rx

The G/T requirement (G/T: Figure-of-Merit) was very hard to achieve and required a relatively large aperture. The scan range even enlarged this aperture because scanning below the horizon is required for maritime terminals as pointed out in the previous section. Extensive investigations of conformal antenna array topologies resulted in this case in a solution which is a compromise between size, costs and performance: the hybrid steering concept.

In this case, it implies that the antenna is steered electronically in elevation and mechanically in azimuth. The antenna aperture was designed by the University of Karlsruhe (Germany) with support of IMST which included amongst other, the design and measurement of the antenna elements, and the definition of the array topology. The feeding network topology, Tx/Rx modules included, has been designed and characterised by IMST. The technology demonstrator buildup is shown in Fig. 9 (a).

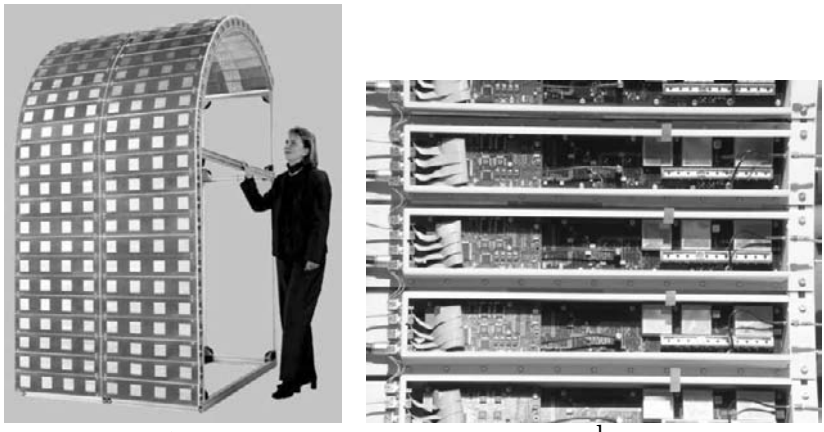

a b

Figure 9: (a) Hybrid maritime Tx/Rx antenna front-end in L-band; (b) Tx/Rx modules at the back of the array aperture, one module for each horizontal row of 4 patches.

The design for steering the beam electronically in elevation is based on a classical phased array approach where RF-amplitude and phase shifters are used. The antenna aperture consists of 256 patches, and each horizontal row of $1 \times 4$ patches has its own RF-phase and -amplitude circuit, as shown in Fig. 9 (b). For a more detailed description is referred to [8]. The project was supported by the German Ministry of Education and Research (BMBF) in the ALCANT-SATCOM project 01AK007G/8.

### 3.3 Phased arrays at L-band

Especially for operating frequencies like L-band where the number of antenna elements is relatively low, 'simple' switching between antenna elements could be an effective way of steering the antenna beam. Such concepts in generally involve only a small number of RF-components but usually require high performance RF-switches [9]. However, the problem that arises for such configurations is that due to strict regulations with respect to the satellite service providers, requirements like gain ripple, for example, can be

too strict for 'simple' switching and combined element patterns have to be used, resulting in a more costly design as we will see in the following part. Two projects in L-band have been conducted focusing on land mobile and maritime platforms.

The first one is called INES (INexpensive Earth Station) and is funded under ESA, ARTES 5. It focussed on land mobile platforms like vans or trucks, for example (Fig. 10). This Tx/Rx front-end was intended for INMARSAT BGAN systems and uses a (limited) phased array approach. It consists of 8 stacked patches (circularly polarised), and uses, besides the element patterns, also 7 antenna beams generated by a combination of paired patches, each pair being the zenith patch and one of the low elevation patches. The antenna has a diameter of approximately 40 cm and a height of 20 cm. For more detailed information please refer to [10, 11].

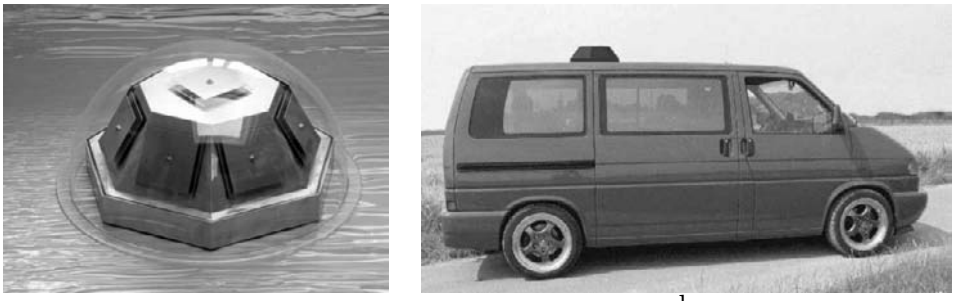

a b

Figure 10: The INES antenna front-end. (a) Demonstrator; (b) artist impression of INES rooftop terminal.

The INES-concept has been used as a basis for the follow-up project IRIS: Innovatives Array mit intelligenter Steuerung, funded by DLR Bonn, Germany (BMWi), FKZ: 50 YB 0707. This terminal is dedicated for maritime platforms and provides a full-duplex L-band satellite connection. The antenna which is based on the phased array principle (i.e. for each antenna element one phase/amplitude shifter) consists of a conformal medium gain phased array of stacked patches. The requirements for this design are again quite challenging: the gain must remain at a level of minimal 12 dBic for a scanning range of maximal 5° below horizon in elevation, while still keeping a good axial ratio. Moreover, the gain variance over the steering range has to be as small as possible, in order to achieve a stable EIRP-level in case of Tx. On the other hand, the number of antenna elements should be as low as possible, in order to be as cost-effective as possible.

Based on these requirements, several aperture shapes were investigated using analytical methods and numerical simulation [12]. The aperture shape

is based on a truncated icosahedron consisting of pentagonal and hexagonal surfaces, each of them equipped with one radiating element as shown in Fig. 11. The hexagons have two different edge lengths, whereas the pentagons have equal edge lengths. Therefore the surface areas of the pentagons and the hexagons have almost the same size. Moreover, the phase centres of all patch elements have similar distance to the centre of the sphere.

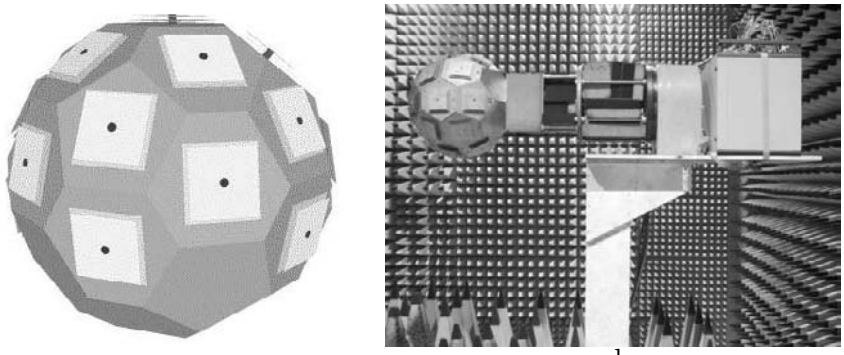

a b

Figure 11: (a) Optimised antenna aperture for the IRIS-terminal; (b) realised prototype in the IMST anechoic chamber.

The antenna pattern measurements have been performed in the anechoic chamber of IMST. In order to minimise the errors in the measurements due to temperature drift, unwanted signals and reflections, the chamber is fully shielded and air-conditioned. During these measurements, the antenna was used in receive mode. A complete three-dimensional antenna pattern has been measured with a roll-over-azimuth positioner as depicted in Fig. 11 (b). Please note that some absorbers present during the measurements, have been removed for making the antenna more visible. All measurements have been performed at far field conditions. The resulting diagrams are depicted in Fig. 12, together with the simulated patterns. The plots in Figs. 12 (c) and 12 (d) clearly show that the antenna can scan below horizon, as required for maritime platforms.

### 3.4 Phased array at Ku-band

Mobile satellite terminals in Ku-band suffer from a major disadvantage: beside the normal beam pointing the polarisation also has to be adjusted because most satellite services in Europe use linear polarised signals. This results in a highly complex design that proofs to be quite a challenge, surely when considering cost-effective realisations. The project NATALIA (New Automotive Tracking Antenna for Low-cost Innovative Applications),

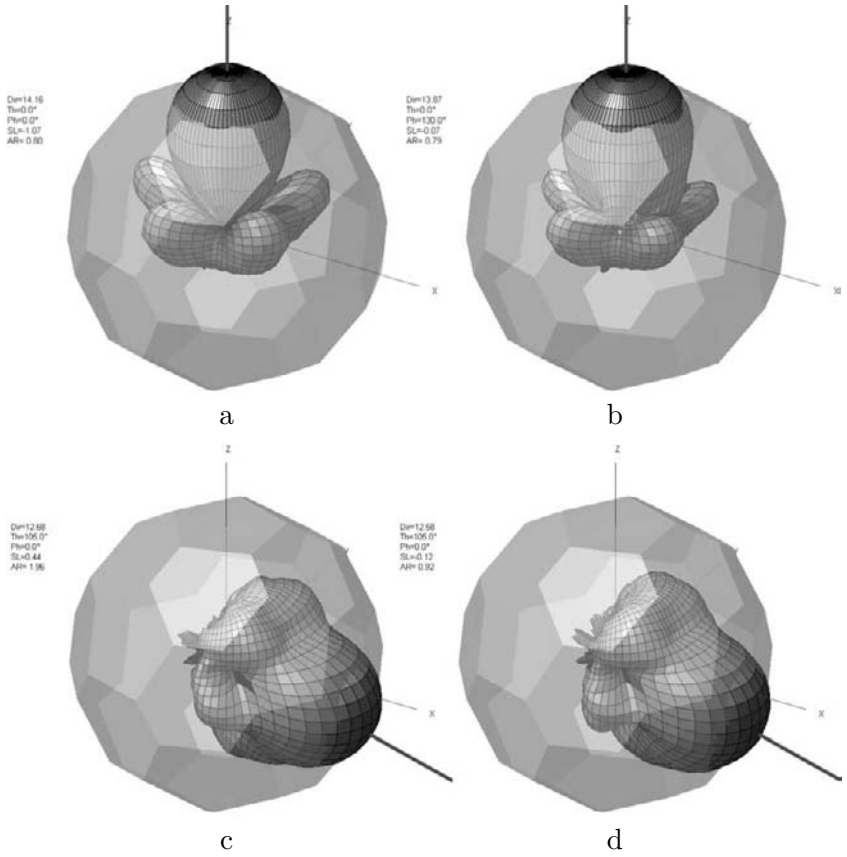


Figure 12: Comparison of simulated and measured radiation patterns pertaining to the antenna aperture for the IRIS-terminal. (a) Simulation results at $\theta = 0°$ (boresight of the antenna); (b) measurements results at $\theta = 0°$; (c) simulation results at $\theta = 110°$ (below horizon); (d) measurement results at $\theta = 110°$.

funded by ESA under ARTES 5, tackles precisely this challenge. Its mission is the development of a cost-effective solution for a compact receive-only tracking antenna front-end for automotive platforms in Ku-band. This antenna is completely electronically steerable.

The concept of the NATALIA antenna is depicted in Fig. 13. The consortium is composed of partners from Switzerland, Luxembourg, and Germany. As one can see in Fig. 13, the complete system consists not only of the antenna front-end envisaged here, but also of a dedicated receiver and dedicated satellite services that have been investigated and developed in a separate ESA-funded project. This aspect is rather important because without latter services and customised receiver, the NATALIA antenna concept

cannot be exploited in a commercial successful way. The services and receiver are based on the blocking/interference scenarios that an automotive terminal experiences. As previously mentioned, a line-of-sight connection between satellite and terminal, required for adequate signal reception, can never be guaranteed during normal operation due to blockage by buildings, trees, bridges, tunnels, trucks, etc [13]. This implies that real-time reception for such applications is actual only possible for a limited time, thus one can at best speak here of near real-time. This problem cannot be solved by changing the antenna design: satellite services and receiver modem can only cope with this major problem by providing multimedia contents on an interleaving basis (repeating it at certain intervals), and by storing received broadcast news in a memory cache that compensates for certain blockage times. This also allows the user to 'customise' the information he wants to hear ('dedicated news').

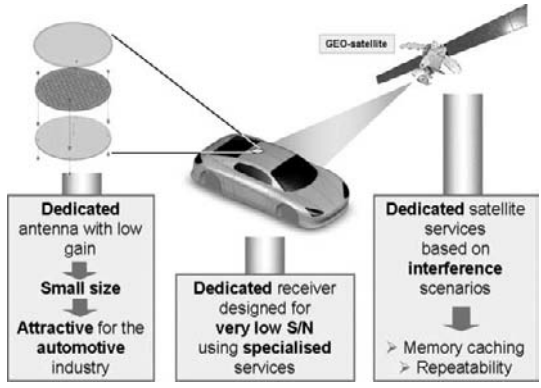


Figure 13: The NATALIA concept.

The NATALIA antenna is a fully electronically steerable, receive-only antenna, linear polarised, and suited for dedicated KU-band broadcast services (10.7 GHz ÷ 12.75 GHz) of providers like SES Astra. The requirement profile is listed below and not only contains the most important electrical parameters but also estimated cost price and physical dimensions:

- Operating frequency: 10.7 GHz ÷ 12.75 GHz;
- Operation: Rx-only;
- Polarisation: linear;
- G/T: greater than −6 dB/K;
- Aperture size: 20 cm in diameter (EU), 30 cm (USA);

- Estimated manufacturing price: less than €1000;
- Scan range: $20° \div 60°$ in elevation from horizon, $0° \div 360°$ in azimuth.

Latter values have been established after elaborate discussions with the car industry and service providers. In order to perform the polarisation adjustment, a special concept has been developed in which the beam pointing and the polarisation adjustment are combined using only two RF-phase shifting elements. More details on this cannot be disclosed at this time. A principal overview of the NATALIA architecture and a view of the antenna aperture are displayed in Fig. 14. The number of antenna elements amounts up to approximately 150. The front-end employs dedicated MMIC components that each combines LNA, phase shifter and the required digital logic to steer the phase shifter of one MMIC. This is the only way to achieve the degree of integration required for such compact automotive terminals. The manufacturing numbers for this type of terminal are expected to be high, so MMIC-components become relatively low in costs (expected production is several millions of MMIC per year).

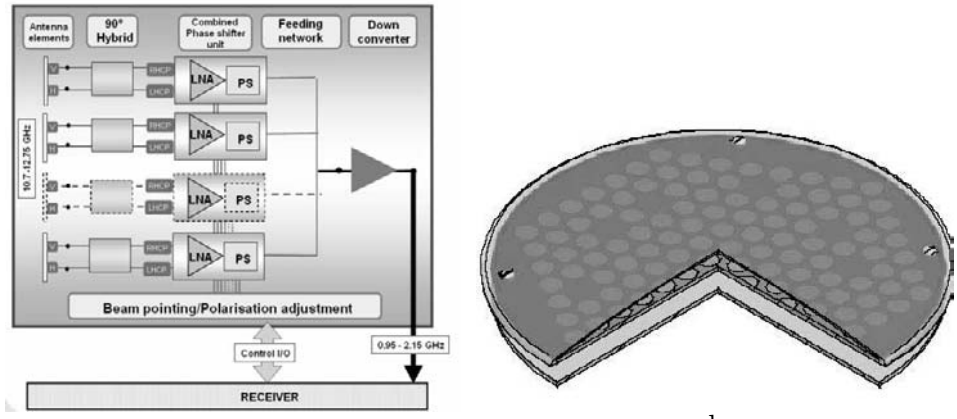


a b

Figure 14: (a) Schematic of the Ku-band automotive Rx-antenna using a combined beam pointing and polarisation adjustment; (b) artist impression of antenna front-end.

The antenna front-end will consist of one core PCB (Printed Circuit Board) with the patches on one side and active components (MMIC) on the other side. A first prototype of this PCB is depicted in Fig. 15. The topside of the PCB where the patches will be mounted upon is shown. One can clearly distinguish the coupling slots, two for each patch. The MMIC and related components will be mounted on the back of this PCB. The design of the PCB has already been optimised for mass production as much as

possible. This in combination with the dedicated MMIC-components should result into a rather cost-effective front-end. More detailed information can be found in [14, 15].

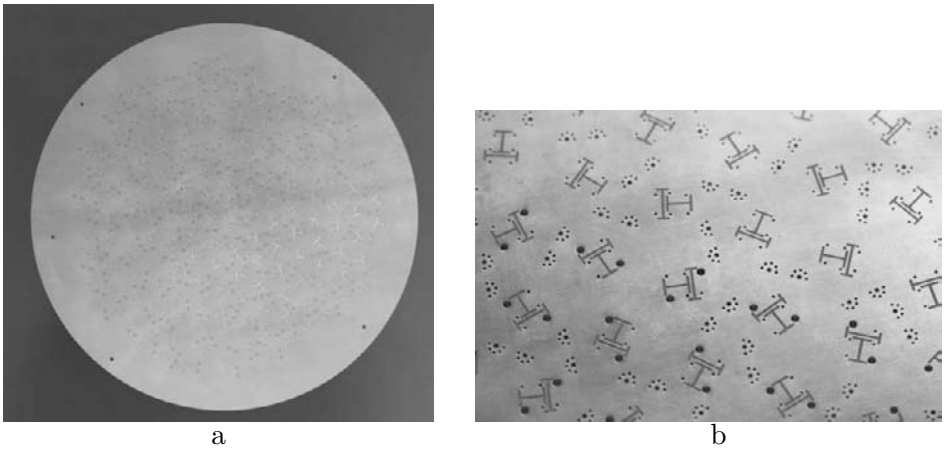

a b

Figure 15: Prototype of the NATALIA-PCB, topside without patches. (a) Overall view; (b) detail of the aperture with the coupling slots.

### 3.5 DBF array at K/Ka-band

The absolute high-end of phased array technology employ DBF architectures. Such technology can be applied for any frequency band but within this subsection the focus is on airborne Ka-band satellite terminals for broadband multimedia services (internet in the sky). The DBF-terminal itself is divided into a separate Tx (30 GHz) and Rx (20 GHz) antenna array. The frequency bands are based on future satellite multimedia applications. Figure 16 shows an $8 \times 8$ patch array that forms the basis for the complete array. The basic element design is based on circularly polarised patches. A key feature of the antenna concept is the modular build-up, which allows adapting the number of elements to different applications and data rates.

The circular polarisation of the patch elements is achieved by using two decoupled feeds and one 90° hybrid ring per element. In addition, the antenna elements are sequentially rotated to further enhance the polarisation behaviour of the array. 64 Antenna elements, with hybrid ring feeds and internal calibration network, are integrated in one complex LTCC (Low-Temperature Co-fired Ceramics) multilayer module (see Fig. 16). Such an $8 \times 8$ building block can be calibrated automatically using an internal calibration receiver. Figure 17 shows the exploded view of one single antenna element as realised in LTCC. The structure consists of 11 layers of FERRO

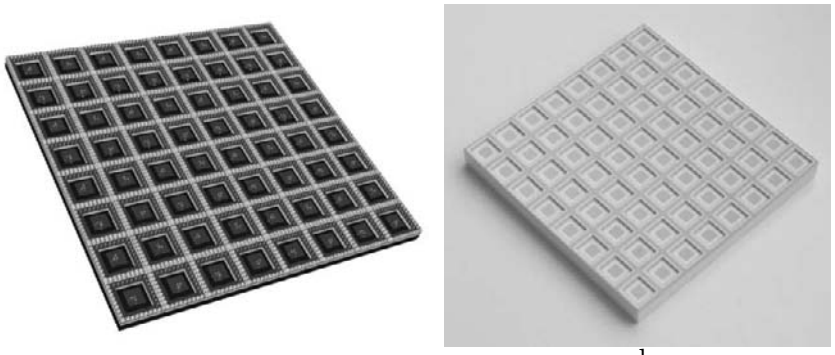

a b

Figure 16: The $8 \times 8$ Tx-array. (a) Simulation model; (b) realised $8 \times 8$ submodule in LTCC.

A6 LTCC-substrates. Four different functional blocks can be identified: the antenna patch with two feeding ports located in a cavity (created by vias), a hybrid ring coupler, the calibration network and the antenna interface (via probe). The functional blocks of the antenna elements and the specific design issues of the array are described in detail in [16, 17, 18].

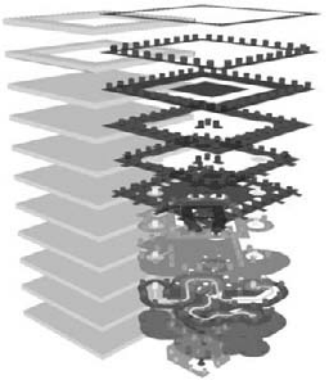

Figure 17: Exploded view of one antenna element.

The measurement results show that the antenna can be pointed in any fixed azimuth-plane within an elevation from boresight of $\pm 60°$ without any scan blindness problems. The side lobe levels are maintained at levels of approximately 13 dB (no amplitude taper applied) and a very good suppression (larger 20 dB) of the cross-polar component can also be observed. The good polarisation performance is the result of several factors: the feeding of the antenna elements using the hybrid ring coupler allows for a very good axial ratio of each single element. In addition, the hybrid ring feeding also attenuates the cross-polar components resulting from coupling effects. Finally, the

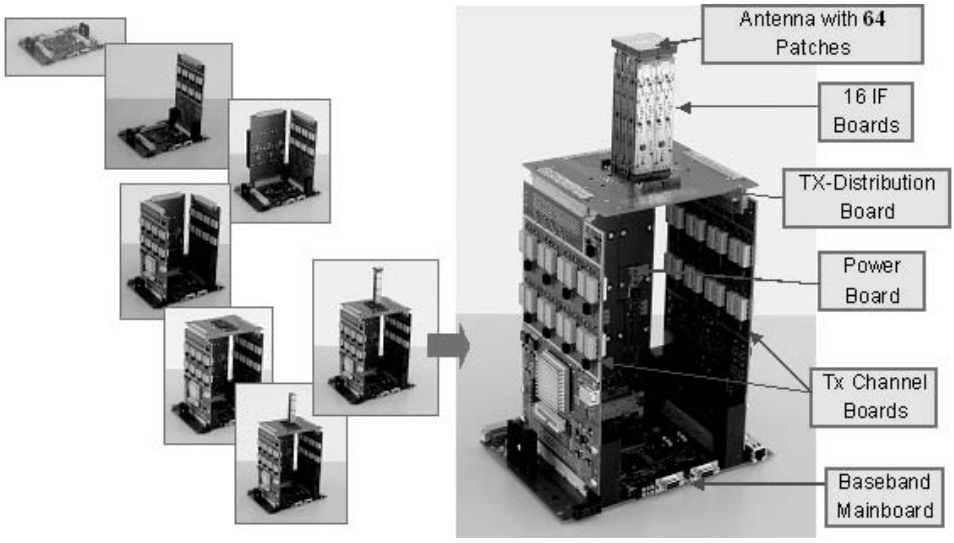


Figure 18: Complete DBF Tx-array with $8 \times 8$ patch array, RF-hardware and the complete digital processing logic.

sequential rotation of the antenna elements improves the axial ratio at the array level. The complete buildup is shown in Fig. 18. This buildup consists of not only the antenna aperture realised in LTCC (Fig. 16) and the up-converting RF-circuitry but also of the complete digital hardware necessary for the controlling of the antenna signals at digital level. Please note that this is an experimental buildup suitable for testing the complete circuitry. For possible industrial applications in future, the digital hardware will be

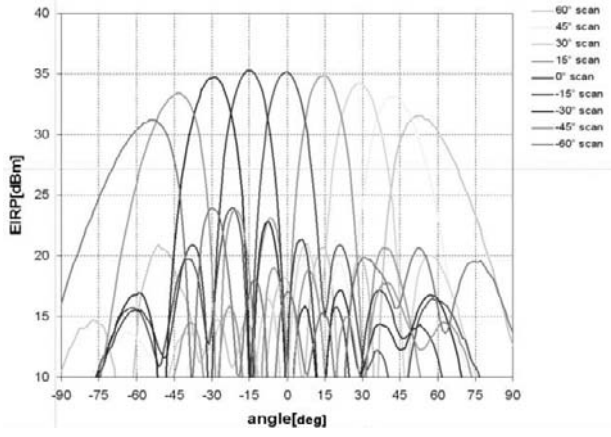


Figure 19: Measured antenna beams for scanning in a fixed azimuth plane.

integrated and only require a fraction of the original volume. An example of the measured far-field patterns is displayed in Fig. 19.

The work described in this subsection is performed within the project SANTANA (I-II-III) and is supported and funded by the German Ministry of Education and Research (BMBF/DLR) under research contracts 50YB0101, 50YB0311 and 50YB0710, in cooperation with the Technical University of Hamburg, DLR and Astrium.

The DBF-architecture presented within this section requires a high degree of integration with respect to the large number of components and a high speed digital processing unit. Especially with respect to the latter unit, the real-time processing of thousands of antenna element signals is not practicable. Therefore, alternative topologies are investigated at IMST that are combinations of DBF-technology and special IF-feeding architectures. The idea behind such topologies is to reduce the number of interconnections between the RF-part and digital logic, thus reducing the number of antenna element signals to be processed (reduction of the computational load).

## 4 Conclusions

An overview of the different user requirements for land mobile, maritime and aeronautical platforms has been presented. It has been shown that such requirements can have a huge impact on the RF-front-end architecture. Several developments at IMST have illustrated the complexness of such front-ends and the challenge to arrive at a cost-effective design. Different antenna front-end topologies have been described for different operating frequencies. Each type of architecture has been discussed and key items have been discussed. It is believed that the mobile satellite front-ends presented in this article will contribute - for a significant part - to the wireless world of tomorrow.

## Bibliography

[1] M. Gatchev, E. Totomanov, V. Boyanov, B. Marinov, I. Slavkov, I. Ivanov, S. Kamenopolsky, and I. Stoyanov, "Low profile mobile scanning phased array antenna system for DBS leception," in *Proc. 1$^{st}$ European Conference on Antennas and Propagation – EuCAP*, Nice, France, November 2006.

[2] A. Catalani, M. Migliorelli, L. Russo, F. di Paolo, G. Toso, "Ku-band fully electronic antenna for aircraft in flight entertainment," in *Proc. 29$^{th}$ ESA Antenna Workshop on Multiple Beams and Reconfigurable Antennas*, Noordwijk, the Netherlands, April 2007.

[3] D. Riemer, D. Harvey, J. McCandless, G. Fitzsimmons, "Low-cost communication phased array antenna," US-Patent Nr. 5886671 by BOEING, March 23, 1999.

[4] G. Jager-Waldau, "Presentation of the project satcom-on-the-move in ND SatCom," in *Proc. 3rd European Conference on Antennas and Propagation – EuCAP*, pp. 487–491, Berlin, Germany, March 2009.

[5] J. Shelton, and K. Kelleher, "Multiple beams from linear arrays," *IRE Trans. on Antennas Propagat.* vol. 9, no. 2, pp. 154–161, March 1961.

[6] L. Baggen, M. Böttcher, and M. Eube, "3D-Butler matrix topologies for phased arrays," in *Proc. ICEAA07*, pp. 531–534, Torino Italy, Sept. 2007.

[7] A. Gustafsson, R. Malmqvist, L. Pettersson, G. Huss, M. Alfredson, S. Lindstrom, I. Ferrer, P. Grahn, S. Leijon, C. Samuelsson, T. Nilsson, A. Pohl, A. Ouacha, B. Carlegrim, S. Hagelin, and R. Erickson, "A very thin and compact smart skin X-band digital beamforming antenna," in *Proc. 1st European Radar Conference – EuRAD*, pp. 313–316, Amsterdam, the Netherlands, October 2004.

[8] D. Löffler, W. Wiesbeck, M. Eube, K. Schad, and E. Ohnmacht, "Low cost conformal phased array antenna using high integrated, SiGe-technology," in *IEEE Antennas Propagat. Symp. Dig.*, pp. 334–337, Boston, USA, July 2001.

[9] N. Karmakar and M. Bialkowski, "A low cost switched beam array antenna for L-band land mobile satellite communications in Australia," in *Proc. IEEE 47th Vehicular Technology Conf. 1997*, pp. 2226-2229, Phoenix, AZ, USA, May 1997.

[10] S. Jellet, M. Bialkowski, and R. Varnes, "An L-band vehicle mounted cylindrical array for satellite communications," in *Proc. IEEE ICCS*, pp. 710–14, Singapore, India, 1994.

[11] M. Böttcher, R. Gieron, M. Eube, P. Siatchoua, M. Geissler, "Electronically steered L-band antenna for mobile applications," in *Proc. 29th ESA Antenna Workshop on Space Antenna Systems and Technologies*, Noordwijk, the Netherlands, June 2005.

[12] M. Geissler, F. Woetze, M. Böttcher, S. Korthoff, A. Lauer, M. Eube, and R. Gieron, "Innovative phased array antenna for maritime satellite communications," in *Proc. 3rd European Conference on Antennas and Propagation – EuCAP*, pp. 735-739, Berlin, Germany, March 2009.

[13] M. Holzbock, O. Lücke, and B. Oeste, "Mobility requirements of landmobile antennas for broadband satellite communication," in *Proc. EMPS 2000*, Bradford, UK, September 2000.

[14] S. Vaccaro and F. Tiezi, "Hybrid phased array antenna for mobile Ku-band DVB-S services," in *Proc. 1st European Conference on Antennas and Propagation – EuCAP*, Nice, France, November 2006.

[15] R. Baggen R, S. Vaccaro, and D. Llorens del Róo, "Design considerations for compact mobile KU-band satellite terminals," in *Proc. 2nd European Conference on Antennas and Propagation – EuCAP*, Edinburgh, UK, November 2007.

[16] A. Dreher, D. Heberling, S. Holzwarth, C. Hunscher, A. F Jacob, N. Niklasch, H. Pawlak, L. Richard, A. Schroth, L. C. Stange, and M. Thiel, "Ka-band DBF terminal concepts for broadband satellite communications," in *Proc. 25th ESA Antenna Workshop on Satellite Antenna Technology*, pp. 95–102, Noordwijk, the Netherlands, September 2002.

[17] A. Geise, A. F. Jacob, K. Kuhlmann, H. Pawlak, R. Gieron, P. Siatchoua, D. Lohmann, S. Holzwarth, O. Litschke, M. V. T. Heckler, L. Greda, A. Dreher, C. Hunscher, "Smart antenna terminals for broadband mobile satellite communications at Ka-band," in *Proc. 2nd International ITG Conference on Antennas – INICA '07*, pp. 199–204, Munich, Germany, March 2007.

[18] S. Holzwarth, O. Litschke, W. Simon, K. Kuhlmann, and A. F. Jacob, "Far field pattern analysis and measurement of a digital beam forming 8×8 antenna array transmitting from 29.5 to 30 GHz," in *Proc. 2nd European Conference on Antennas and Propagation – EuCAP*, Edinburgh, UK, November 2007.

# Receiving array systems for radio astronomy

**Wim A. van Cappellen**
*Netherlands Institute for Radio Astronomy (ASTRON), Dwingeloo, the Netherlands (cappellen@astron.nl)*

**Abstract**

New astronomical science will be enabled by the use of array technology in radio astronomy. Development efforts concentrate on two concepts: aperture arrays and phased array feeds. Key challenges in the front-end development of such systems are the bandwidth, low-noise and stability requirements. A (dense) phased array feed prototype in a 25 m dish of the Westerbork Synthesis Radio Telescope (WSRT) successfully demonstrated the ability to electronically scan the beam about 2 half-power beamwidths in both directions while retaining a high antenna efficiency and low system noise temperature. The final system will lead to a 20× improvement of the WSRT survey speed. The Low Frequency Array (LOFAR) operates in the 15 – 240 MHz band using sparse antenna arrays. The Low-Band Antenna stations (15 – 80 MHz) have a pseudo-random configuration of the antenna elements to smoothen the station beams. Both aperture array and phased array feed technologies are important pathfinders for the next generation radio telescope, the Square Kilometre Array.

## 1 Introduction

Recent developments in antenna array technology are about to cause a paradigm shift for the next generation radio telescopes such as the Square Kilometre Array (SKA) [1]. Given the very small flux density of the signals being observed in radio astronomy, observations require many hours of integration. Present-day telescopes can instantaneously image only a very small fraction of the sky. Enlarging the field of view of the telescope will enable deeper and/or more extended surveys and new scientific projects will come within reach. In this contribution, it is shown that array technology enables new front-end concepts for radio telescopes to significantly increase the survey speed. Challenges and results of array based systems being developed at ASTRON are presented.

Antennas for Ubiquitous Radio Services in a Wireless Information Society
I.E. Lager and M. Simeoni (Eds.). 
doi:10.3233/978-1-60750-487-0-143

## 2 Array concepts

A larger field of view (FoV) can be obtained by forming multiple scanned beams on the sky simultaneously. This paper introduces two possible realizations: aperture arrays and phased array feeds.

An aperture array (AA) is a phased array pointing directly to the sky. Aperture arrays can in principle simultaneously image the entire hemisphere if sufficient beams can be formed in parallel. The systems that are currently being developed have a processing capacity such that the total observed field in a single observation is about thousand times bigger than the "single pixel" beam of horn-fed telescopes with 25 m diameter at one GHz.

A Phased Array Feed (PAF) is a dense array antenna in the focal plane of a reflector telescope. It uses much less antenna elements per square meter of collecting area, but the field of view is much smaller than an aperture array. In practice a total FoV of a few tens of square degrees can be realized at 1 GHz and varies less than a factor two over an octave bandwidth. The FoV is determined by the dish diameter, its focal ratio, the size of the array and the available data transport and processing. Phased Array Feeds are very promising candidates for new telescopes, like the SKA, but also form an interesting upgrade path for existing reflector telescopes.

## 3 Antenna challenges in radio astronomy

The antenna arrays for the AA and PAF systems share the requirement to perform over a very wide frequency band, up to 4:1 (120%). For AA's above 300 MHz and for PAF's dense arrays are considered. The enormous bandwidth requirement and the dense spacing between the elements ($\approx \lambda/2$ at the highest frequency of operation) necessitate the use of strongly coupled array elements, such as tapered slot antennas. It is stressed that in this situation mutual coupling is a desired effect and is the only way to achieve the required bandwidth. But the mutual coupling also complicates the system design and calibration because it introduces a dependency on scan angle of system characteristics like effective area and system temperature.

Modern large radio telescopes use aperture synthesis to provide high resolution images. The rotation of the earth is used to synthesize an aperture with a diameter equal to the largest baseline in the array. For an East-West interferometer, like the Westerbork Synthesis Radio Telescope (WSRT), it takes 12 hours to measure all visibilities to create an image. The images are generated after extensive post-processing, including calibration of instrumental parameters. The possibility to detect very faint radio sources close to

relatively stronger ones (which are present in almost every image) results in a dynamic range between $10^5$ and $10^7$. This requires an extremely accurate calibration and stability of the receiving system over the full 12 hour observation. Stability and/or smoothness over frequency and time of instrumental characteristics, such as the radiation pattern, are critical for a successful calibration. The levels of for example sidelobes and cross- polarization are of minor importance, as long as they are stable. The far sidelobes of a Low Frequency Array (LOFAR) station are up to -11 dB and the sidelobes near the main lobe vary between -15 and -20 dB.

The observed sources in radio astronomy are very weak and hence the sensitivity ($G/T_{sys}$ or $A_e/T_{sys}$) of a radio telescope is of key importance. Traditional horn fed reflector systems use cryogenically cooled receivers to minimize the receiver noise contribution. In array systems cooling is not feasible and room temperature low noise amplifiers are used. Table 1 gives an overview of the noise budget of the APERTIF phased array feed system [2]. It is a major challenge to design the antenna and Low Noise Amplifier (LNA) such that the sensitivity is maximized over the wide frequency range and scan angle. But also the antenna losses cannot be neglected. An antenna efficiency of 98% (resulting in a 6 K noise contribution) already increases the system noise temperature by $> 10\%$. This pushes the antenna design towards metal only structures because dielectrics are lossy and/or expensive.

Table 1: System noise temperature budget of the APERTIF Phased Array Feed.

| | Noise contribution |
|---|---|
| Antenna losses | 6 K |
| LNA + second stage | 28 K |
| Noise coupling | 8 K |
| Spillover | 10 K |
| Sky noise | 3 K |
| **Total** | **55 K** |

The modeling and design of the above receiving systems is a major challenge, especially the electromagnetic modeling of strongly coupled, large arrays of tapered slot antennas and the optimization of the sensitivity and beam patterns over frequency and scan angle. For this purpose a dedicated tool has been developed at ASTRON. It combines an enhanced MoM simulation with a circuit modeling tool [3, 4]. It has successfully demonstrated to accurately model the patterns and noise temperature of AA and PAF systems [5].

# 4 Experimental results

ASTRON is developing several PAF and AA based systems. This section presents experimental results demonstrating the unique features and challenges of array systems.

a

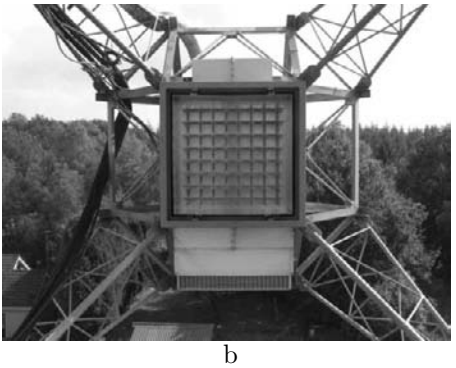

b

c

Figure 1: (a) The 25 m WSRT dish in which the PAF prototype is installed, (b) The phased array feed installed in the focus cabin, (c) Detail of the $8\times7\times2$ Vivaldi array showing the metal tapered slot elements and microstrip feeding-lines on low-loss dielectric substrate.

## 4.1 APERTIF

APERTIF ("APERture Tile In Focus") is a PAF system that is being developed for the Westerbork Synthesis Radio Telescope (WSRT) to increase its survey speed with a factor $\approx 20$ [6]. APERTIF will operate in the frequency range from 1000 to 1750 MHz, with an instantaneous bandwidth of 300 MHz, a system temperature of 55 K and an aperture efficiency of 75%. The goal is to have 37 beams on the sky constituting an effective FoV of 8

square degrees (compared to single beam of $\approx 0.3\,\mathrm{deg}^2$ with the current horn feed at 1400 MHz). An additional advantage of this technique is that a PAF allows optimizing the radiation pattern in terms of sensitivity, sidelobes and polarization characteristics.

To demonstrate the feasibility of the PAF concept a prototype has been installed in one of the 25m WSRT dishes (see Fig. 1). The array consists of 112 ($8 \times 7 \times 2$) tapered slot Vivaldi elements at a pitch of 10 cm ($\lambda/2$ at 1500 MHz). This pitch is the sweet spot for maximizing the aperture efficiency [7]. Low noise amplifiers are connected to all 112 elements, but only 60 are connected to a receiver and digitizer. Signals from the individual elements are weighted and combined to digitally form a compound beam. The results in this paper have been obtained with weights that maximize the sensitivity. Eventually, an alternative weighting can lower the effects of instrumental polarization at the cost of sensitivity. The all-digital beam former allows to simultaneously form multiple compound beams at different locations on the sky.

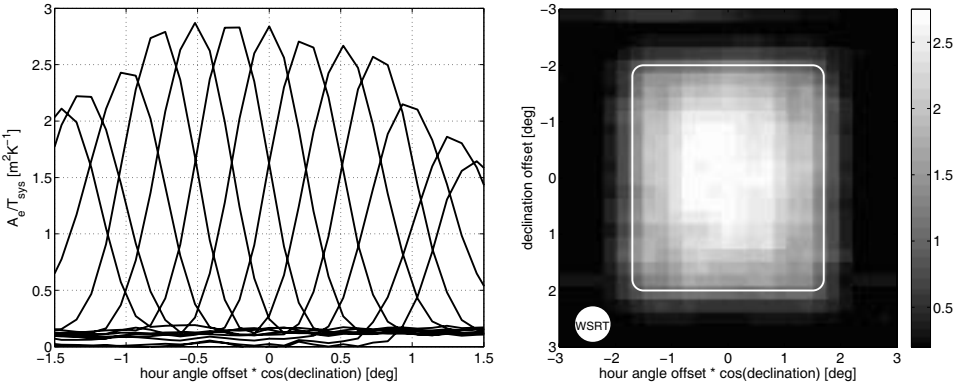


a b

Figure 2: (a) Measured compound beam sensitivity; (b) the sensitivity on the sky of the WSRT dish fitted with a PAF. The white rectangle denotes the half-power contour. For comparison, the field of view of the "old" WSRT system is also shown.

The characterization of the demonstrator concentrated on the beam properties (sensitivity, pattern) and imaging capability of the system [8]. Figure 2.a shows the measured sensitivity of a series of compound beams. Each beam combines all 56 horizontally polarized elements of the phased array feed. The beams overlap at their -0.7 dB points to demonstrate the ability to form highly overlapping beams with high sensitivity in a deep dish. In the final APERTIF system the beams will overlap at half power.

For comparison, the current horn fed system only has one such beam. Figure 2.b shows the measured sensitivity [$m^2/K$] over the field of view of the telescope. Each pixel represents the sensitivity of a compound beam formed in that particular direction. These measured sensitivities agree very well with the modeled ones [5].

## 4.2 LOFAR

The Low Frequency Array (LOFAR) [9] is a large distributed aperture array radio telescope with its core in the North of The Netherlands. LOFAR operates in the 15–240 MHz range. It uses two types of antennas: The Low Band Antenna (LBA) from 15 to 80 MHz and the High Band Antenna (HBA) from 120 to 240 MHz. The Low Band Antenna consists of an inverted V-shaped dipole above a $3 \times 3$ meter metal ground plane (Fig. 3).

Figure 3: LOFAR Low Band Antennas in a pseudo-random sparse configuration.

For the LBA stations, each consisting of 96 antennas, trade-offs between dense versus sparse and regular versus irregular configurations have been made [10]. The results are summarized in Table 2. Given these considerations, the antennas in the LOFAR LBA stations are placed in a pseudo-random and exponentially space tapered configuration. The diameter of a station is approximately 81 m. The primary motivation of this configuration is the smoothness of both the station beam and the average element beam. The resulting strong variations of the individual element beams will challenge the station calibration techniques.

Apart from the regular beamformed observations, a LOFAR LBA station also has the capability to measure a full correlation matrix between all

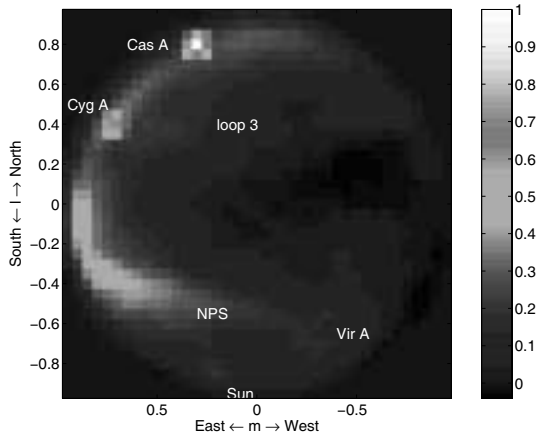


Figure 4: LOFAR LBA instantaneous all-sky image.

elements of the array (for a single frequency channel at a time). From this information an instantaneous image of the entire sky can be generated. Figure 4 shows an example in which the galactic plane (the milky-way) is visible at the Eastern horizon. Also other strong radio sources like Cassiopeia A, Cygnus A, Virgo A and the Sun are indicated.

Table 2: Summary of array characteristics.

| | | **Regular** | **Irregular** |
|---|---|---|---|
| | Sidelobes | Lowered by gain taper | Lowered by space taper |
| **Dense** | Grating lobes | No | |
| | Receiver temp. | Lower, smooth (angle, freq.) | |
| | Effective area | Constant over frequency, smooth over angle | |
| | Element patterns | Depend on position | |
| | Beamwidth | Large | |
| **Sparse** | Grating lobes | Few high ones | Many low ones |
| | Receiver temp. | Higher, not smooth (angle, freq.) | Higher, smooth (angle, freq.) |
| | Effective area | Steep decrease with wavelength | Steep decrease with wavelength |
| | | Not smooth (angle, freq.) | Smooth (angle, freq.) |
| | Element patterns | Constant for most elements | Depend on position |
| | Beamwidth | Smaller | |

### 4.3 EMBRACE

The EMBRACE project [11] entails a phased array technology demonstrator in the 500–1500 MHz band. It demonstrates functionality and low cost technology suitable for building large phased array stations for the SKA. The front-end consists of a dense array of Vivaldi elements. A 144 $m^2$ array is currently being built at the WSRT (see Fig. 5) and a 100 $m^2$ array will be built at the Nançay observatory in France.

Figure 5: The EMBRACE tapered slot antenna array.

## 5 Summary

New astronomical science will be enabled by the use of array technology in radio astronomy. Key challenges in the front-end development of such systems are the bandwidth, low-noise and stability requirements. Several activities, like LOFAR, APERTIF and EMBRACE, aim to demonstrate the feasibility and competitiveness of these systems for the Square Kilometre Array (SKA).

## Bibliography

[1] A. van Ardenne, J. D. Bregman, W. A. van Cappellen, G. W. Kant, and J. G. Bij de Vaate, "Extending the field of view with phased array techniques: Results of European SKA lesearch," *Proceedings of the IEEE*, vol. 97, no. 8, pp. 1531–1542, Aug. 2009.

[2] J. G. Bij de Vaate, L. Bakker, E. E. M. Woestenburg, R. H. Witvers, G. W. Kant, and W. A. van Cappellen, "Low cost low noise phased-array feeding systems for SKA pathfinders," in *Proc. ANTEM 2009*, Banff, Canada, Feb. 2009.

[3] R. Maaskant, R. Mittra, and A. Tijhuis, "Fast analysis of large antenna arrays using the characteristic basis function method and the adaptive cross approximation algorithm," *IEEE Trans. Antennas Propag.*, vol. 56, no. 11, pp. 3440–3451, Nov. 2008.

[4] R. Maaskant, D. J. Bekers, M. J. Arts, W. A. van Cappellen, and M. V. Ivashina, "Evaluation of the radiation efficiency and the noise temperature of low-loss antennas," *IEEE Antennas Wireless Propag. Lett.*, vol. 8, pp. 1166–1170, 2009.

[5] M. V. Ivashina, O. A. Iupikov, R. Maaskant, W. A. van Cappellen, L. Bakker, and T. A. Oosterloo, "Off-axis beam performance of focal plane arrays for the Westerbork Synthesis Radio Telescope – Initial results of a prototype system," in *IEEE Antennas Propagat. Symp. Dig.*, Charleston, SC, June 2009.

[6] M. A. W. Verheijen, T. A. Oosterloo, W. A. van Cappellen, L. Bakker, M. V. Ivashina, and J. M. van der Hulst, "APERTIF, a focal plane array for the WSRT," in *The Evolution of Galaxies through the Neutral Hydrogen Window*, R. Minchin and E. Momjian (editors), *AIP Conference Proceedings*, vol. 1035, Melville, New York 2008.

[7] M. V. Ivashina, M. Ng Mou Kehn, and P.-S. Kildal, "Optimal number of elements and element spacing of wide-band focal plane arrays for a new generation radio telescope," in *Proc. 2nd European Conference on Antennas and Propagation – EuCAP*, Edinburgh, UK, Nov. 2007.

[8] W. A. van Cappellen, L. Bakker, and T. A. Oosterloo, "Experimental results of a 112 element phased array feed for the Westerbork Synthesis Radio Telescope," in *IEEE Antennas Propagat. Symp. Dig.*, Charleston, SC, June 2009.

[9] M. de Vos, A. W. Gunst, and R. Nijboer, "The LOFAR Telescope: system architecture and signal processing," *Proceedings of the IEEE, Special Issue 'Advances in Radio Telescopes"*, Jacob W. M. Baars (editor) vol. 97, no. 8, pp. 1431–1437, August 2009.

[10] W. A. van Cappellen, S. J. Wijnholds, and J. D. Bregman, "Sparse antenna array configurations in large aperture synthesis radio telescopes," in *Proc. 3rd European Radar Conference – EuRAD*, pp. 76–79, Manchester, UK, Sept. 2006.

[11] A. van Ardenne, P. N. Wilkinson, P. N. Patel, and J. G. Bij de Vaate, "Electronic multi-beam radio astronomy concept: EMBRACE a demonstrator for the European SKA program," *Experimental Astronomy*, special issue on SKA, vol. 17, pp. 65–77, 2004.

# Puzzling radiators – functionality enhancement by means of shared aperture antennas

**Ioan E. Lager**[†], **Massimiliano Simeoni**[†], **Cristian I. Coman**[‡], **Christian Trampuz**[†], **Leo P. Ligthart**[†] and **Piet van Genderen**[†]

[†]*International Research Centre for Telecommunications and Radar (IRCTR), Faculty of Electrical Engineering, Mathematics and Computer Science, Delft University of Technology, 2628 CD Delft, the Netherlands (e-mail: I.E.Lager@tudelft.nl).*

[‡]*NATO Consultation, Command and Control Agency (NC3A), Surveillance & Reconnaissance Resource Centre, 2597 AK The Hague, the Netherlands.*

**Abstract**

The present account reports on the shared aperture antenna concept as an instrument aimed at enhancing the functionality of antenna systems. Non-uniform array antennas implementing, in a concurrent manner, different functionalities are deployed on a common physical area. This concept is adopted to assemble multi-frequency, multi-channel and multi-polarization antenna systems. These applications are illustrated by physical implementations. The advantages introduced by the advocated approach and the challenges that it poses are discussed.

## 1 Introduction

Modern ubiquitous radio services need to reduce, as much as possible, the number of antennas needed to support them. The reduction of the number of antennas reduces the size, the complexity and the cost of the terminals, these aspects being crucial for massively deployed systems. One way to achieve the sought reduction of the number of antennas is to integrate them in multi-functional compounds. The multi-functionality of the antenna systems can be achieved in two ways:

- time sharing (time multiplexing) – the antenna resources are able to perform various tasks and are employed sequentially to implement the different functionalities at distinct time slots;
- aperture sharing (aperture segmentation) – separate radiators (or set

Antennas for Ubiquitous Radio Services in a Wireless Information Society
I.E. Lager and M. Simeoni (Eds.). 
doi:10.3233/978-1-60750-487-0-153

of radiators) are concurrently employed for performing the required functionalities.

While the former approach requires antenna elements able to implement various functionalities (this possibly implying a complication in the design of the elements themselves), the latter relies on the use of *specialized* radiators to be used only for specific applications.

The aperture sharing approach clearly introduces the advantage of enabling multi-functionality reducing the pressure on the intrinsic complexity of the employed radiating elements. The emphasis, as it will become evident in the remainder of this account, is on the architecture of the aperture hosting the different radiating elements. The shared aperture antenna can be seen as an array-antenna in which each functionality is associated with a specific subarray.

In principle, the aperture sharing approach can be implemented by placing on the relevant aperture either identical or different radiators. The former choice allows a (possibly dynamic) reconfiguration of the aperture. However, the various tasks to be accomplished are often associated with frequency bands that are spread over a wide frequency range and, possibly, with different polarizations of the radiated field. This suggests that, more often than not, the antenna elements need to be of different varieties.

A rather intuitive manner of implementing the aperture sharing concept is by deploying next to each other a number of compact subarrays [1], p. 206. Consequently, each subarray is confined to a small area, thus providing but limited angular resolution (wide radiation beams). To tackle this problem, the radiators composing the various subarrays may be spread over the entire available area, in an interleaved manner. This solution is conceptually simple, but it results in severe limitations as far as scanning range, polarization, and the ratio between the frequency bands pertaining to the subarrays are concerned and poses serious challenges to the design of shared aperture, multi-functional array antennas. To start with, each subarray should be *sparse*, in the sense that it occupies oly a part of the aperture in order to leave enough room to accommodate other subarrays (hence other functionalities). Secondly, the strategies to share the aperture between different subarrays need to be sought for.

In the present account, the shared aperture approach is advocated as an instrument to achieving multi-functional (array) antenna systems. Firstly, the preparatory studies on sparse array antennas are briefly reiterated. Secondly, the shared aperture concept is introduced and then applied to three specific cases of multi-functional antennas: one operating at different frequency bands, one implementing the different functions (transmit and re-

ceive) of a radar antenna and one achieving polarization agility, combined with beam scanning, by using differently polarized subarrays. The examples presented are supported by experimental prototypes whose manufacturing and testing related issues are also discussed.

## 2 Shared aperture array antennas

### 2.1 Sparse arrays – the precursors

The use of sparse subarrays can facilitate the task of interleaving two (or more) subarrays on a common aperture. At the same time, each subarray needs to be able to perform the task associated with it. This clearly calls for design techniques that can yield sparse arrays offering controlled radiation characteristics.

Usually, a distinction is made between two kinds of sparse arrays: thinned arrays and non-uniform arrays. Thinned arrays are antenna architectures obtained by eliminating (thinning down) some elements of a fully populated array antenna that is commonly deployed on a uniform spatial grid. Non-uniform arrays are antenna architectures composed of individual radiating elements located at arbitrary positions in space.

The problem of designing sparse arrays (thinned or non-uniform) [2] is at the center of an intense research activity in the international community and has been addressed at the International Research Centre for Telecommunications and Radar (IRCTR) by using both a stochastic approach [3] and deterministic techniques [4].

The former approach is based on the Genetic Algorithm (GA) optimization technique and yields non-uniform sparse array configurations. Once the number of radiators composing the array has been fixed, their positions (along a linear direction) are optimized such that to satisfy the requirements formulated in terms of the angular width of the main radiation beam and on the maximum level of the side-lobes. It is worth stressing the fact that this approach does not guarantee a successful design, a thorough formulation of the design requirements is instrumental to yield satisfactory results. This approach has been successfully adopted in [5] for designing array antennas for narrow-beam, wide-angle scanning applications.

The technique described in [4] relies on the correlation properties of the so-called Cyclic Difference Sets (CDS), sets of numbers extensively used in the realm of communication technology and cryptography [6]. When compared with the stochastic methods, the CDS-based combinatorial design approach offers the advantage of an *a priori* knowledge of the average level

of the radiation in the side lobe region. Moreover, the combinatorial methods are also superior to stochastic ones as concerns the computation time demands. In view of the advantages that it introduces, the combinatorial CDS-based design technique has been extensively adopted at IRCTR for designing thinned sparse arrays, a brief description of its fundamentals being hereafter provided.

By definition, a $(V, K, \Lambda)$ difference set is a set of $K$ unique integers $D = d_0, d_1, \ldots, d_{K-1}$, with $0 \leq d_i \leq (V-1)$, such that for any integer $1 \leq a \leq (V-1)$

$$(d_i - d_j)(\mathrm{mod}\, V) = \alpha, \quad \text{for } i \neq j, \tag{1}$$

has exactly $\Lambda$ solution pairs $\{d_i, d_j\}$ from the set $D$, with "mod" standing for the "modulo" operation. From a difference set $D$ having the parameters $(V, K, \Lambda)$, one can construct a sequence of ones and zeros

$$A_D(i) = \begin{cases} 1 & \text{if } i \in D \\ 0 & \text{if } i \notin D \end{cases}, \tag{2}$$

with $i = 0, 1, \cdots, V-1$.

The $A_D$ sequence exhibits some remarkable properties. The autocorrelation function of an infinite vector obtained by periodically repeating $A_D$ is a *two-valued* function [4]. Similarly, the spectrum of the Discrete Fourier Transform (DFT) of the sequence $A_D$ derived from a CDS $(V, K, \Lambda)$, by taking $V$ points in the DFT, exhibits one maximum, only, that has a level related to $K$, whereas all the other spectral components have an identical, low value (related to $\Lambda$). Note that, due to the fact that the radiation pattern of an (array) antenna is associated to the DFT of the aperture's current distribution, this property is of high relevance in the field of (array) antenna studies. These properties can be exploited for thinning down a fully populated linear array antenna based on a fixed, linear, uniform lattice. By placing the elements in a linear, thinned array at the positions of the ones in $A_D$, the antenna radiation pattern preserves the beamwidth of the full array (consisting of $V$ uniformly distributed radiators) whereas the side-lobes level is approximately constant, oscillating for an approximately half thinned down array around $1/(2K)$ of the main beam's level [4].

A planar, thinned array of dimensions $V_x$ and $V_y$ can be obtained from the difference set $D$ with parameters $(V, K, \Lambda)$ by defining the matrix of ones and zeros:

$$M_D\left[i(\mathrm{mod}\ V_x), i(\mathrm{mod}\ V_y)\right] = \begin{cases} 1 & \text{if } i \in D \\ 0 & \text{if } i \notin D \end{cases}, \tag{3}$$

with $i = 0, 1, \cdots, V-1$ and $V_x V_y = V$. Using one set from the elements of matrix $M_D$ (ones or zeros) to deploy the radiators in the sparse configuration,

the radiation pattern of the thinned array has a beamwidth similar to the one of the full planar array, whereas the side lobe level is approximately constant and low.

Another placement strategy for designing non-uniform, linear array antennas was introduced in [7] where the effectiveness of the grid-search strategy for the assembling of large, non-uniform, linear arrays was demonstrated by solving some problems in the realm of pattern shaping. In [7], since the complete set of radiation parameters corresponding to a large sample of linear arrays are readily available, an inspection directly indicated what the feasible design requirements are for a given number of elements and an available physical area. This result could be achieved by exploiting a highly effective computational engine evaluating the beam-widths and the peak side lobe level (PSLL) values for the full range of acceptable inter-element spacings[1] and for a wide range of array element numbers.

The potentiality for achieving dynamically reconfigurable radiation patterns by means of thinned sparse arrays was investigated in [8]. In particular, the drop in the antenna gain experienced when the main beam of a phased-array antenna is steered away from the broadside direction (commonly known as *scan loss*) was compensated by applying a different degree of thinning to a uniform linear array antenna.

## 2.2 The shared aperture antenna concept

As indicated in Section 1, sharing the physical area of the antenna aperture between different subarrays implementing the different functionalities of a complex antenna system introduces various advantages, the most notable one being the possibility of concurrently performing multiple tasks.

The solution of interleaving on a common aperture (see Fig. 1 for a graphical exemplification of this concept) was firstly advocated in [9].

The design of an antenna systems based on this concept relies on the proper design of the individual subarrays (see Section 2.1) and on the strategies needed to interleave them. The latter aspect has also been an object of investigation at IRCTR over the last few years and will be briefly discussed in Section 2.3.

[1] A lower limit of the inter-element distances amounting to $\lambda/2$ allows for accommodating physical radiators while an upper limit of $\lambda$ implies that no grating lobes are generated in the case of a broadside radiation.

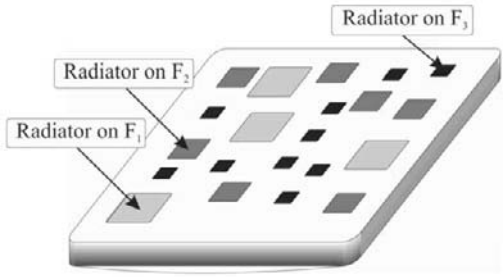


Figure 1: Illustrative for the shared aperture antenna concept: different sets of radiators (*subarrays*) implement different fucntionalities.

## 2.3 Shared aperture antenna design

A number of issues need to be addressed in designing a shared aperture antenna. Firstly, the constituent subarrays need to be designed to satisfy their relevant requirements. Secondly, a strategy for collocating them on the common aperture needs being identified. At this stage, it is crucial avoiding any physical overlapping between the elements of the individual subarrays. Finally, optimal use of the available aperture surface has to be ensured.

In the case of designing the subarrays by means of the technique in [4], yet another interesting feature of the CDS sequences can be exploited. Referring to the notation introduced in Section 2.1, one can note that the set $D^* = [0, V-1] \setminus D$ (referred to as the complementary of $D$) is also a difference set with parameters $(V, V-K, V-2K+\Lambda)$. By using the CDS $D$ and its complementary $D^*$ it is possible to design two sparse arrays, which are naturally interleaved [4]. The resulting shared aperture will then be composed of two subarrays having similar radiation patterns, non overlapping elements and completely covering the aperture area. This approach has been extensively used to design shared aperture antennas at IRCTR (see the examples in Section 3) and, as detailed in [10], can be extended to design antennas consisting of multiple interleaved CDS-based subarrays.

Another way of addressing the issues related to the design of a shared aperture antenna is resorting to statistical methods, an example of this approach being reported in [11]. There, the elements of a uniform, fully populated array are randomly partitioned in two sub-sets, each consisting of half of the total elements. The two resulting subarrays are naturally interleaved, not overlapping and completely filling the available aperture area. Moreover, the arrangement of the subarray radiators across the aperture is homogeneous, consequently each subarray exhibits a main radiation beamwidth virtually equivalent to that of the initial complete array. The extension of this techniques to the design of shared aperture antennas consisting

of more than two subarrays is straightforward. Naturally, the reliability of this approach relies on statistical considerations and is guaranteed only for large arrays.

An important aspect to be considered when designing array antennas is the level of mutual interaction occurring between the elementary radiators. The performance of array antennas, in particular the scanning capabilities of phased-array antennas, are strongly influenced by the mutual couplings between the elements of the array. Effects such as scan blindness (the gain drop observed as the antenna beam is steered from the broadside direction) and (large) variations of the individual antenna input impedances with the scanning angle variations are induced by strong mutual interactions between the antenna elements. This problem is partially mitigated in the case of sparse arrays since the average distance between the elements of an array antenna is generally larger than in the case of fully populated arrays. Moreover, in the case of shared aperture antennas, neighboring elements are in some cases belonging to different subarrays, hence implementing different functionalities (e.g., different frequencies, different polarizations, etc.), therefore less prone to interact with each other. Despite this, the problem of the mutual interaction between the individual elements of shared aperture antennas has been investigated, both theoretically and experimentally, with [12] and [13] yielding accurate prediction methods and effective technical solutions for mutual coupling mitigation.

## 2.4 Implementation related aspects

As stated in Section 1, in order to properly address the demand for ubiquitous radio services, the relevant antennas need to be minimized in their number and, possibly, integrated in multi-functional units. This is, however, not sufficient. The complex multi-functional antenna units need also being low-cost. Addressing this desideratum has a direct impact on the choice for the manufacturing technology to be employed for the production of the antenna (systems). It is obvious that the selected manufacturing technology must allow a facile and accurately reproducible production of both individual radiators and antenna arrays. As a consequence a design methodology, referred to as *technology driven design* [14], has been identified at IRCTR and consistently enforced for the production of the concept demonstrators reported in this account.

This design methodology is based on the preeminence of a beforehand chosen manufacturing technology. This choice is justified by the fact that when the mass-production of antenna (systems) is aimed at, it seems convenient to base the design process on a specified, fully mastered manufacturing

technology. Confining the design methodology to the frame of a given technology has other favorable effects, as well. For example, the designer has the guarantee that the designed product can be actually constructed. Furthermore, the manufactured product has good prospects to perform very similarly with the designed one. On the other hand, such a design approach may also lead to some limitations. In this respect, a traditional performance driven design assumes a maximum freedom during the design phase, with the consequence of maximizing the chances to implement the desired functionality. On the contrary, when a technology is imposed from the very beginning, some habitual antenna design procedures could become immaterial, that may impede on the features of the end product. Nevertheless, this 'limitation' may stimulate the engineers to explore alternative solutions that will, in turn, lead to higher quality radiators. An exemplification of this concept is reported in [5], where the lithographic etching of microstrip laminates was selected as driving technology for the antenna design. The design resulted in an inexpensive, highly integrated and easily reproducible antenna module.

## 2.5 Validation and measurements

In general, the validation of theoretical concepts by means of practical experiments is the ultimate tool for proving their correctness. This is particularly true for the concepts hereby advocated. In view of the complexity of some of the designs resulting from the application of the shared aperture concept, an experimental validation phase has been consistently resorted to. This was made possible by the availability of the DUCAT (Delft University Chamber for Antenna Test) facility, an electromagnetic anechoic chamber optimized for measurements in the X-band.

Demonstrators have been produced for any of the antenna systems described in Section 3. Moreover, various array antennas, meant to be experimental platforms to investigate different array architectures, have been designed and manufactured. One of these test antennas consisting of a uniform array of identical radiators that are individually accessible by means of coaxial connectors and deployed over a uniform, rectangular lattice is shown in Fig. 2.

The shared aperture concept has been repeatedly validated at IRCTR by means of laboratory experiments. Figure 3 shows a view of a typical test set-up where two interleaved subarrays are fed by means of coaxial cables connected to two power dividing networks. The input ports of the power dividers represent the access points of the two subarrays.

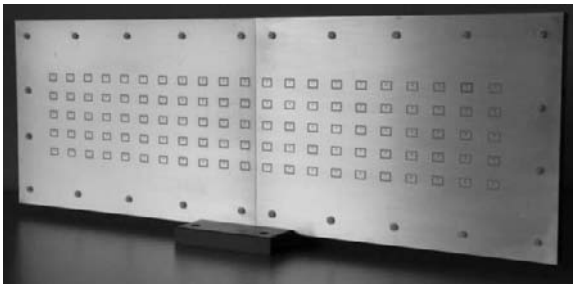

Figure 2: A uniform array antenna used for experimenting various shared aperture configurations.

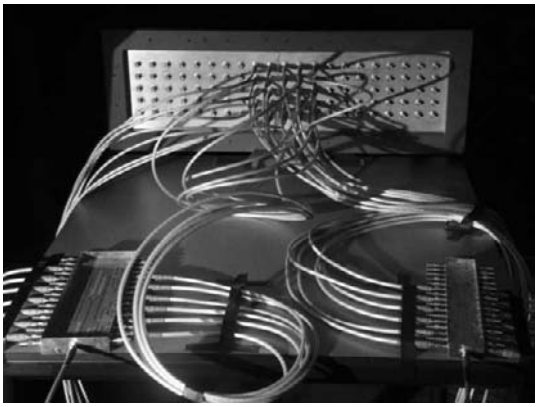

Figure 3: A test set-up for validating the shared aperture concept.

Since most of the array antennas designed to demonstrate the potentiality of the shared aperture concept turn out to be rather large (when compared to the operational wavelength), their direct far-field characterization is not feasible in the DUCAT facility. This limitation was circumvented in two alternative ways: (1) by performing near-field measurements and subsequently a near-to-far field transformation; (2) by implementing an innovative processing technique enabling far-field characterization of large array antennas in small anechoic chambers. The former technique was made possible by the near-field scanner integrated in DUCAT. The latter technique, described in [15], relies on the observation that the constituent elements of the arrays are small enough to be individually measured under far-field conditions. Subsequently, their radiation patterns can be properly combined by following an algorithm resulting from some geometrical considerations. This technique has enabled the far-field characterization of array antennas having physical dimensions largely exceeding the maximum size of an antenna directly characterizable in the anechoic chamber at hand.

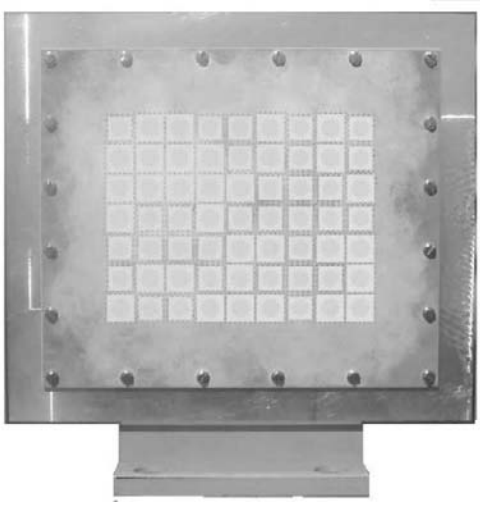

Figure 4: Shared aperture array antenna accommodating two types of elements operating between $8.0 \div 8.5\,\mathrm{GHz}$ and $8.5 \div 9.5\,\mathrm{GHz}$, respectively. The placement uses a deterministic CDS-based strategy.

# 3 Applications of the shared aperture concept

## 3.1 Multi-frequency arrays

The shared aperture concept has been firstly applied to the design of wide-band array antennas. In the work reported in [9], [16] and [17] the antenna aperture is divided in two subarrays by means of the combinatorial CDS-based technique described in Sections 2.1 and 2.3. The elements composing the two subarrays are designed to operate at two adjacent frequency bands. The sub-arrays are hereafter referred to as $\mathrm{SA_H}$ and $\mathrm{SA_L}$, where the indices "H" and "L" designate the higher ($8.5 \div 9.5\,\mathrm{GHz}$) and the lower ($8.0 \div 8.5\,\mathrm{GHz}$) frequency bands, respectively. Since, as discussed in Section 2.3, the radiation patterns of the two subarrays are very similar, the interleaving of them yields a collective array operating over a frequency range which is the sum of the two sub-bands provided by the subarrays.

A physical implementation of the design is displayed in Fig. 4 where the elements belonging to the different subarrays are distinguishable in view of their physical size. This shared aperture antenna was manufactured in microstrip technology using Rogers© RO 4003 laminate boards.

The experimental investigations were performed in the DUCAT facility. The radiation characteristics of the sparse array antennas (not shown here for brevity) were evaluated by firstly measuring the individual patterns of

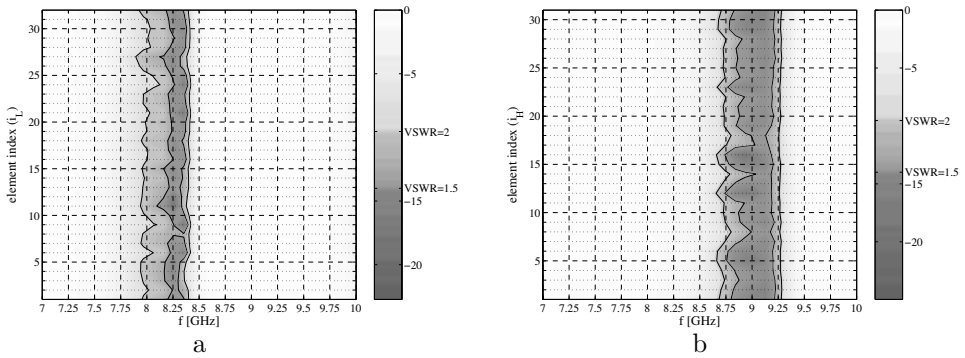


a b

Figure 5: The frequency dependence of the active reflection coefficient for each elementary radiator in the two subarrays; the solid contours indicate the levels corresponding to VSWR=2 and VSWR=1.5, respectively. (a) Sub-array $SA_H$; (b) sub-array $SA_L$.

the elementary radiators. The sub-array radiation patterns were then calculated by summing up (possibly with suitable phase shifts) these measured data. The frequency behavior of the reflection coefficients measured at the individual array elements are depicted in Fig. 5(a) and (b) for the two subarrays, separately. These plots clearly illustrate the fact that the two subarrays efficiently cover the designated sub-bands.

## 3.2 Multi-function arrays

The use of the shared aperture concept for the design of the transmit (Tx) and receive (Rx) antennas equipping a frequency-modulated, continuous-wave (FMCW) radar was proposed in [18]. By relying, again, on the properties of the CDS-based design techniques, it was possible to design virtually collocated array antennas featuring highly similar radiation patterns. These features are particularly attractive for the FMCW radar application since they enable a very good alignment between the transmit and receive radiation patterns and can, by exploiting the so-called 'correlation effect' [18], diminish the overall system phase noise.

In a subsequent work [19] this concept was refined by combining the classical CDS-based design with a so-called 'trimming' strategy. Since the cited work focuses on an FMCW radar application, *two-way* front-end parameters, defined with respect to the product Tx-Rx radiation patterns, are applicable. With the goal of reducing the side-lobes level in the two-way radiation pattern, the reduction of the number of rows or columns (array trimming) of the individual subarrays has the effect of shifting the angular

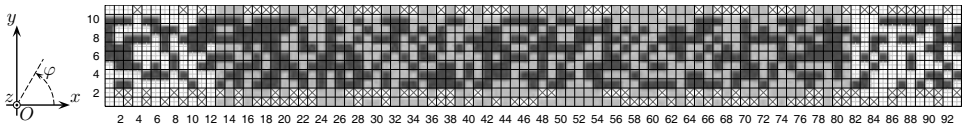


Figure 6: The radiating aperture's architecture after trimming. The dark squares correspond to the Tx sub-array and the light ones to the Rx sub-array. The crosses indicate the switched off elements in the Tx sub-array and the pluses the switched off elements in the Rx one.

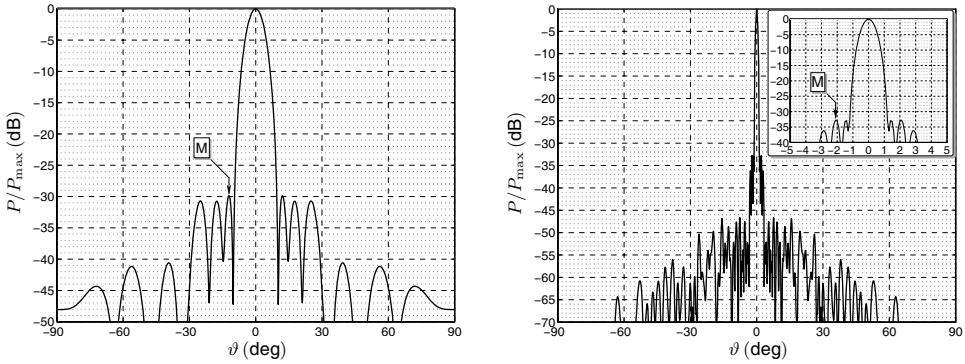


Figure 7: The normalized, two-way radiation pattern referring to the antenna architecture depicted in Fig. 6. (a) The pattern in the $x = 0$ plane; (b) the pattern in the $y = 0$ plane. The inset depicts a zoom-in on the main beam.

position of the relevant radiation pattern nulls. This procedure eventually results in lowering the two-way radiation pattern side lobe level. The architecture of a shared aperture antenna implementing this concept is depicted in Fig. 6. The two-way radiation patterns are shown in Fig. 7(a) and (b), the design strategy reducing the peak side lobe level by approximately 6 dB.

An alternative approach was presented in [20]. The sharing of the antenna aperture between the Tx and Rx functions of an integrated antenna module for FMCW radar was deigned by means of a statistical approach. More specifically, in [20] the antenna aperture was first randomnly subdivided in two (Tx and Rx) subarrays. Subsequently, the complete aperture was divided in concentric areas, each of which being designated to have a given element density that mimicks a specific illumination tapering function selected to satisfy the design requirements formulated in terms of main beam width and side lobe level. The actual element distribution was then obtained

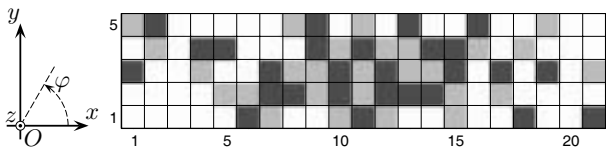


Figure 8: Shared aperture thinned array architecture for FM-CW radar. The dark gray squares correspond to the transmit sub-array, the light gray boxes to the receive one and the white squares to the eliminated elements.

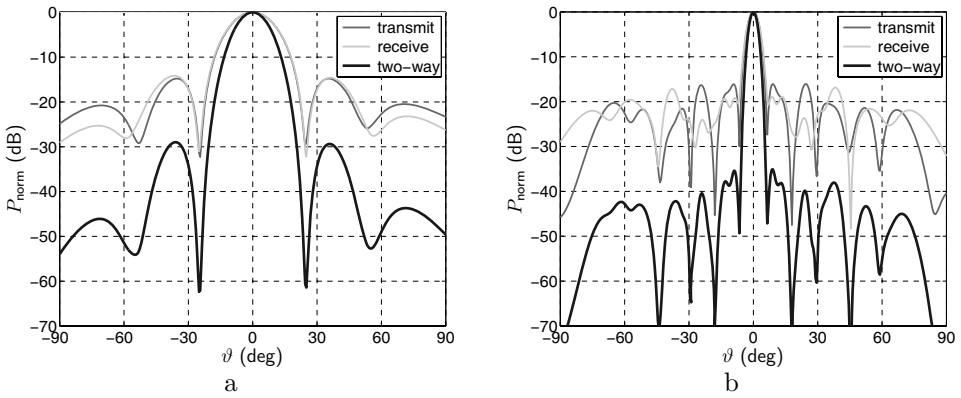


Figure 9: The normalized radiation patterns referring to the antenna architecture depicted in Fig. 8. (a) The patterns in the $x = 0$ plane; (b) the patterns in the $y = 0$ plane.

by thinning down the array, such to reach the desired element density in each area of the total aperture. This procedure was performed for both the Tx and the Rx subarrays. One array architecture resulting from this design procedure is shown in Fig. 8. The corresponding normalized radiation patterns evaluated at two cut-planes ($x = 0$ and $y = 0$ planes) are shown in Fig. 9(a) and (b), respectively.

### 3.3 Multi-polarization arrays

In [21] and [22] the shared aperture concept was applied to the design of planar array antennas offering the possibility of dynamically adjusting the polarization properties of the radiated waves, even in conjunction with beam steering. The proposed method relies on interleaving two subarrays with orthogonal, linear polarizations. Each subarray is responsible for providing one of the two mutually orthogonal components needed to achieve any desired polarization state. In [21] it was proved that, by dynamically controlling the amplitude and the phase of the signals fed to the subarrays, arbitrary polar-

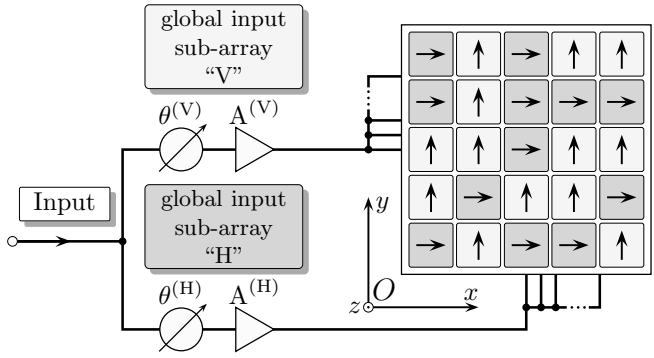


Figure 10: Array antenna system composed of two interleaved sparse arrays and the pertaining phase and amplitude control circuitry required for achieving polarization agility. The phase shifters (one per radiator) required for steering the antenna beam are not shown.

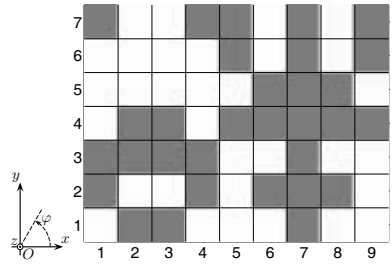


Figure 11: Architecture of the CDS 9 × 7-based array. The dark squares indicate the elements of the 'H' sub-array (consisting of $N^{(\mathrm{H})} = 31$ elements) and the light ones the elements of the 'V' sub-array (consisting of $N^{(\mathrm{V})} = 32$ elements). The total number of radiating elements is $N = 63$.

izations can be achieved. Subsequently [22] demonstrated that the stability of the polarization state can be maintained during beam scanning, as well. A graphical representation of this concept is depicted in Fig. 10.

A CDS-based architecture designed to demonstrate the advocated concept is displayed in Fig. 11. The complete array consists of 63 radiating elements subdivided in two subarrays. Figure 12(a) and (b) shows the variation of the radiated field ellipticity in the planes $\vartheta = 30°$ and $\varphi = 45°$, respectively, when the main radiation beam is pointing in the direction $(\vartheta, \varphi) = (30°, 45°)$ and a right handed circular polarized field is prescribed. The elementary radiator is a microstrip patch embedded in a dielectric filled metallic cavity which is radiating through a rectangular slot. In order to estimate the effects of the mutual electromagnetic coupling between the in-

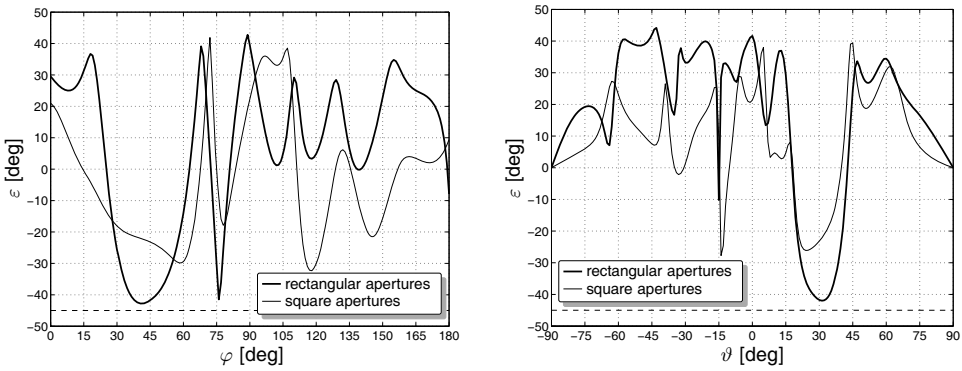


Figure 12: Variation of the total field's ellipticity $\varepsilon$ in the case of the CDS $9\times 7$-based architecture, using rectangular or square radiating apertures. The dashed line corresponds to the required $\varepsilon = -45^\circ$ ellipticity. (a) Variation in the $\{\vartheta = 30^\circ\}$ plane; (b) Variation in the $\{\varphi = 45^\circ\}$ plane.

dividual radiating elements on the antenna performance, two different slot shapes were considered: (1) rectangular apertures, the cross-section dimensions of the radiating slots being: $a \times b = 12$ mm $\times$ 6 mm; (2) square apertures, the cross-section dimensions of the radiating slots being: $a \times b = 12$ mm $\times$ 12 mm. Naturally, the mutual coupling is stronger in the case of using square apertures. The stronger coupling results in a stronger excitation of the higher-order modes that can radiate waves with a different polarization than that ascribed to the relevant subarray. This, in turn, generates a degradation of the polarization state of the overall radiated field. This effect can be easily observed in Fig. 12.

An experimental prototype of the antenna sketched in Fig. 11 is currently under assembly, a picture of the radiating end being shown in Fig. 13.

## 4 Conclusions

The shared aperture concept for multi-functional array antenna design was introduced, described and justified. This concept was found to be a powerful instrument for designing integrated, multi-functional antenna modules that show the potentiality of becoming a basic constituent of future generations of ubiquitous radio systems. Several techniques for the design of shared aperture antennas have been discussed and their application to the implementation of multi-functional antenna modules has been illustrated by practical examples. The technological issues related to the production of massively deployable multi-functional antenna modules have been briefly

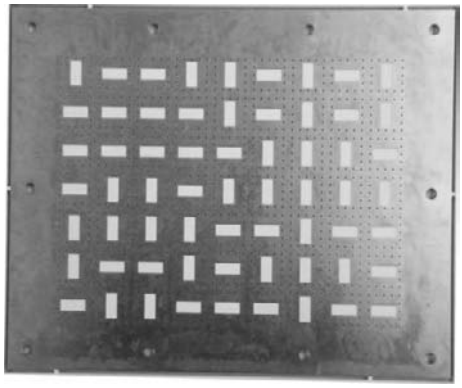

Figure 13: Shared aperture array antenna accommodating two types of elements radiating horizontal and vertical polarized waves, respectively. The placement uses a deterministic CDS strategy.

addressed together with the relevant testing related aspects.

## 5 Acknowledgement

The authors would like to acknowledge A. G. Roederer for many interesting discussions concerning the polarization-agile array antennas and various other topics. A special thank goes to the IRCTR technical staff consisting of P. J. Aubry, J. H. Zijderveld, P. Hakkaart and W. F. van der Zwan for the instrumental support in the experimental validation of the concepts hereby illustrated. The support of the Electronic and Mechanical Support Division (Dienst Elektronische en Mechanische Ontwikkeling, DEMO) of the Faculty of Electrical Engineering, Mathematics and Computer Science (Faculteit Elektrotechniek, Wiskunde en Informatica, EWI) and in particular of M. van der Wel and B. Bakker is gratefully acknowledged.

## Bibliography

[1] N. Fourikis, *Phased Array-Based Systems and Applications.* New York: Wiley, 1996.

[2] C. I. Coman, I. E. Lager, and L. P. Ligthart, "Sparse array antennas," *Workshop EuMC WS 5. Multifunction Radar Front End Design and Management*, pp. 19–22, Munich, Germany, October 2003.

[3] C. I. Coman, I. E. Lager, and L. P. Ligthart, "Optimization of linear sparse array antennas consisting of electromagnetically coupled apertures," in *Proc.* $1^{st}$ *Eu-*

*ropean Radar Conference – EuRAD*, pp. 301–304, Amsterdam, the Netherlands, October 2004.

[4] D. G. Leeper, "Isophoric arrays - massively thinned phased arrays with well-controlled sidelobes," *IEEE Trans. Antennas Propag.*, vol. 47, no. 12, pp. 1825–1835, Dec. 1999.

[5] M. Simeoni, C. I. Coman, and I. E. Lager, "Cost-effective array antennas for narrow-beam, wide-angle scanning applications," in *Proc. 36$^{th}$ European Microwave Conference – EuMC*, pp. 1790–1793, Manchester, UK, Sept. 2006.

[6] S. W. Golomb and G. Gong, *Signal Design for Good Correlation: For Wireless Communication, Cryptography, and Radar*, Cambridge: Cambridge University Press, 2005.

[7] J. H. Dickhof, C. I. Coman, I. E. Lager, and M. Simeoni, "Pattern synthesis of linear, sparse array antennas," in *Proc. 3$^{rd}$ European Radar Conference – EuRAD*, pp. 84–87, Manchester, UK, Sept. 2006.

[8] M. Simeoni, J. H. Dickhof, and I. E. Lager, "Investigation of the potential for reconfigurability of the non-uniform, linear array antennas," in *Proc.* 29$^{th}$ *ESA Antenna Workshop on Multiple Beams and Reconfigurable Antennas*, Noordwijk, The Netherlands, April 2007.

[9] C. I. Coman, I. E. Lager and L. P. Ligthart, "Multifunction antennas – the interleaved sparse sub-arrays approach," in *Proc. 36$^{th}$ European Microwave Conference – EuMC*, pp. 1794–1797, Manchester, UK, Sept. 2006.

[10] C. I. Coman, I. E. Lager, and L. P. Ligthart, "A deterministic solution to the problem of interleaving multiple sparse array antennas," in *Proc. 2$^{nd}$ European Radar Conference – EuRAD*, pp. 243–246, Paris, France, October 2005.

[11] C. Trampuz, M. Simeoni, I. E. Lager, and L. P. Ligthart, "Low sidelobe interleaved transmit-receive antennas for FMCW radar applications," in *IEEE Antennas Propagat. Symp. Dig.*, Charleston, USA, June 2009.

[12] M. J. Mehta, I. E. Lager, "Two-dimensional interpolation for the numerical estimation of the mutual coupling in large antenna arrays", in *Proc.1$^{st}$ European Conference on Antennas and Propagation – EuCAP*, Nice, France, November 2005.

[13] I. E. Lager, M. Simeoni, "Experimental investigation of the mutual coupling reduction by means of cavity enclosure of patch antennas," in *Proc.1$^{st}$ European Conference on Antennas and Propagation – EuCAP*, Nice, France, November 2005.

[14] I. E. Lager, M. Simeoni, and L. P. Ligthart, "Technological antenna design – an instrument for the mass-production of antenna systems," in *Proc.* 11$^{th}$ *Int. Symp. on Antenna Technology and Applied Electromagnetics*, pp. 44–45, Saint-Malo, France, June 2005.

[15] M. Simeoni, I. E. Lager, C. I. Coman, "Measurement of electrically large array antennas in small anechoic chambers," *IEEE Antennas Propag. Mag.*, vol. 49, No. 2, pp. 100–106, April 2007.

[16] C. I. Coman, I. E. Lager, and L. P. Ligthart, "The design of shared aperture antennas consisting of differently sized elements," *IEEE Trans. Antennas Propag.*, vol. 54, no. 2, pp. 376–383, Feb. 2006.

[17] C. I. Coman, *Shared Aperture Array Antennas Composed of Differently Sized Elements Arranged in Sparse Sub-arrays*, dissertation, Delft University of Technology, January, 2006.

[18] C. Trampuz, M. Simeoni, I. E. Lager, L. P. Ligthart, "Complementarity based design of antenna systems for FMCW radar," in *Proc.* $5^{th}$ *European Radar Conference – EuRAD*, pp. 216–219, Amsterdam, the Netherlands, October 2008.

[19] I. E. Lager, C. Trampuz, M. Simeoni, and L. P. Ligthart, "Interleaved array antennas for FMCW radar applications," *IEEE Trans. Antennas Propag.*, vol. 57, no. 8, pp. 2486–2490, Aug. 2009.

[20] C. Trampuz, I. E. Lager, M. Simeoni, L. P. Ligthart, "Channel crosstalk analysis in interleaved array antennas for FMCW radar," in *Proc.* $39^{th}$ *European Microwave Conference – EuMC*, pp. 1345–1348, Rome, Italy, October 2009.

[21] M. Simeoni, I. E. Lager, and C. I. Coman, "Interleaving sparse arrays: a new way to polarization-agile array antennas?," in *IEEE Antennas Propagat. Symp. Dig.*, pp. 3145–3148, Honolulu, USA, June 2007.

[22] M. Simeoni, I. E. Lager, C. I. Coman, and A. G. Roederer, "Implementation of polarization agility in planar phased-array antennas by means of interleaved subarrays," *Radio Science*, vol. 44, RS5013, October 2009.

This page intentionally left blank

This page intentionally left blank